The Dissertation Committee for John Arthur Breier Jr.

certifies that this is the approved version of the following dissertation:

Quantifying Groundwater Discharge to Texas Coastal Bend Estuaries

Committee:

Henrietta N. Edmonds, Supervisor

Paul Montagna

John Sharp Jr.

Tamara Pease

Dong-Ha Min

Quantifying Groundwater Discharge to Texas Coastal Bend Estuaries

by

John Arthur Breier Jr., B.S.M.E.

Dissertation

Presented to the Faculty of the Graduate School of

The University of Texas at Austin

in Partial Fulfillment

of the Requirements

for the Degree of

Doctor of Philosophy

The University of Texas at Austin

May 2006

To Crystal and my parents John and Barbara who got me through this.

Acknowledgments

The time series of salinity, water level, rain, evaporation, and river flow used in this study were collected by several organizations and individuals including Tony Amos at The University of Texas Marine Science Institute, staff and researchers at the Conrad Blucher Institute for Surveying and Science, the National Weather Service, and the United States Geological Survey. I would also like to thank Billy Moore and Matt Charette for their advice and help with processing my Ra samples; Marc Russell, Scott Applebaum, and Joel Stevens for assistance in the field; and Markus Lagmanson and Advanced Geosciences for use of their equipment. This project was made possible by funding from the Texas Water Development Board, The University of Texas at Austin Environmental Science Institute, Texas Sea Grant, and The Geological Society of America.

JOHN ARTHUR BREIER JR.

The University of Texas at Austin

May 2006

Quantifying Groundwater Discharge to Texas Coastal Bend Estuaries

Publication No. ______________________

John Arthur Breier Jr., Ph.D.
The University of Texas at Austin, 2006

Supervisor: Henrietta N. Edmonds

Recent studies have provided evidence that submarine groundwater discharge is a significant source of water and dissolved nutrients to the coastal ocean. The chemical implications of these studies are especially important because, relative to surface water, groundwater is typically enriched in many compounds including nitrogen bearing nutrients. Therefore by affecting the supply and relative proportions of essential nutrients, direct groundwater discharge has the potential to influence phytoplankton populations and estuarine ecosystems as a whole. Another potential submarine discharge that may occur in the shallow restricted waters of the Texas coast is leakage of oil-field brine. Such leakage also has important ecological implications similar in some ways to groundwater discharge. The studies in this dissertation concern improving the methods and techniques used in measuring submarine discharges. Using the Texas Coastal Bend as a study area I have: 1) conducted a detailed evaluation of submarine discharges to Nueces Bay and 2) compared indications of submarine discharge between Nueces, Baffin, and Copano Bays. These investigations use a combination of geochemical and geophysical techniques. The geochemical methods are based primarily on measurements of naturally-occurring dissolved Ra isotopes in samples of bay, river, ocean, and groundwater. The geophysical methods employ electrical resistivity profiling to look for evidence of groundwater movement within the bay bottom sediments. Results show that dissolved radium concentrations within Nueces Bay are among the highest observed in coastal estuaries. Geochemical analysis and geophysical surveys indicate that both groundwater and leakage of oil-field brine are potential submarine inputs. Samples from Nueces, Copano, and Baffin Bays show that the seasonal increase in dissolved ^{226}Ra activity for Nueces Bay is substantially larger than that of the other two bays. This increase is not readily explained by either evaporation or riverine supply. These results clearly suggest that the Ra supply to Nueces Bay is unusually large. For Nueces Bay, the most relevant differences between the three bays that might account for this are 1) the proportionally larger salt marsh and 2) the higher density of petroleum wells and pipelines. Though submarine groundwater discharge is not to be ruled out, leakage of oil-field brine is strongly indicated.

Contents

List of Tables

List of Figures

Chapter 1

Direct Groundwater Discharge to the Coastal Ocean

Direct groundwater discharge to the coastal ocean occurs as submarine seeps and occasionally springs. These discharges occur most frequently along or near the shoreline but are also known to occur quite far offshore (*Karpen et al.*, 2004). These discharges are largely unseen and difficult to quantify. Consequently, this submarine component of the hydrologic cycle has historically received little attention. However, recent concerns about coastal water quality have prompted increased interest in characterizing and quantifying this submarine groundwater discharge (SGD) and its biogeochemical implications (*Moore*, 1999) (Figure 1.1). Numerous studies based on direct and indirect measurements have now provided evidence that the exchange of water between coastal sediments and surface waters can be a substantial fraction of surface freshwater inflow (e.g., *Basu et al.*, 2001; *Bugna et al.*, 1996; *Cable et al.*, 1996; *Charette and Buesseler*, 2004; *Charette et al.*, 2001, 2003; *Gramling et al.*, 2003; *Kelly and Moran*, 2002; *Laroche et al.*, 1997; *Moore*, 1997; *Scott and Moran*, 2001; *Sewell*, 1982).

Johannes (1980) was one of the first researchers to discuss groundwater as a potential pathway for nutrients to coastal estuaries. Because groundwater is often enriched in natural and anthropogenic nutrients (*Kreitler and Jones*, 1975), SGD may be ecologically important even where discharge rates are small compared to surface inputs (*Burnett et al.*, 2002). If SGD does represent an important control on estuarine salinity and chemical cycling particularly nutrients then it is reasonable to expect that SGD dynamics and distribution may also affect ecosystem processes (*Johannes*, 1980). Two widely expressed concerns are that 1) anthropogenic increases in groundwater NO_3^- concentrations are partially responsible for the increasing eutrophication of coastal waters (e.g., *Johannes*, 1980; *Laroche et al.*, 1997; *Valiela et al.*, 1992) and 2) fluctuations in SGD rates or water quality are related to the initiation of nuisance algal blooms (*Laroche et al.*, 1997; *Sewell*, 1982).

Perhaps the most widely discussed hypothesis related to SGD is that changes in the associated nutrient flux may initiate algal blooms. There is some indirect evidence for this. A statistical review by *Laroche et al.* (1997) of 11 years worth of Long Island (NY) well water levels, coastal salinities, nutrient levels, and cell counts of *Aureococcus anophagefferens* indicated that brown tide bloom intensity was inversely related to well water levels and directly related to coastal salinities. *Laroche et al.* (1997) hypothesized that drops in SGD caused a decrease in the ratio of DIN to DON making *A. anophagefferens* more competitive and contributing to bloom initiation. However subsequent efforts to examine the actual delivery of nutrients by SGD have been unsuccessful. The three papers reviewed by the author that specifically looked for a spatial relationship between SGD and water column nutrient concentrations found no significant correlation (*Charette et al.*, 2001; *Nowicki et al.*, 1999; *Rutkowski et al.*, 1999). It is likely that this is partially due to the rapid and intense biologic cycling of dissolved nutrients but it is also a reflection of the current limitations and real challenge of identifying and quantifying the actual fluid discharge itself.

Most studies have relied on chemical tracers or direct spot measurements of seepage to estimate SGD. Natural chemical tracers of SGD such as Ra isotopes, Rn, and CH_4 can be used in a mixing model to estimate SGD to large areas (*Cable et al.*, 1996; *Charette et al.*, 2001). Alternatively, point discharge measurements collected with seepage meters (Figure 1.2) can be spatially averaged to estimate SGD (*Cable et al.*, 1997b). While both approaches have their merits they typically result in large uncertainties. They are also difficult to relate because estimates from chemical tracers cannot pinpoint localized discharges while estimates from seepage meters can miss significant discharges altogether. Finally, unless coupled with supplemental measurements both approaches lack the specificity to distinguish between different kinds of submarine discharge (e.g., groundwater advection, seawater recirculation, oil-field brines).

One goal of this dissertation has been to develop a more robust approach to quantifying SGD using 1) a combination of regional, local, and small scale investigations; 2) novel applications of supplemental measurements such as sediment resistivity profiling and chemical tracers of oil-field brine; and 3) natural experiments examining changes in bay Ra activities in response to seasonal freshwater flushing and along precipitation gradients. The other goal of this dissertation was to quantify SGD to Texas Coastal Bend bays and estuaries which are hydrologically distinct from previous areas where SGD has been investigated. The hypotheses tested are:

Principal: The Ra activity of Texas Bend bays and estuaries is partially attributable to SGD.

Secondary: The spatial distribution of SGD within these bays is heterogeneous and increases towards the shoreline.

Secondary: The Ra activity of Texas Bend bays and estuaries is partially attributable to leakage of oil-field brine from submerged petroleum wells and pipelines.

1.1 Quantifying Submarine Groundwater Discharge

Submarine groundwater discharge (SGD) is a mixture of both fresh advecting groundwater (AGW) and saline recirculated seawater (RSW) (*Moore*, 1999).[1] There are three basic approaches to quantifying these fluxes including hydrogeologic modeling, direct seepage measurements, and chemical tracer measurements coupled with mixing models (*Burnett et al.*, 2002; *Oberdorfer*, 2003). These methods do not all measure the same components of SGD and are not necessarily directly comparable. Hydrogeologic modeling has typically been used to estimate the AGW component of SGD. More recently, variable density groundwater transport algorithms have been used to include both AGW and RSW components (*Oberdorfer*, 2003). Seepage meters are used in relatively small areas where SGD is already known to occur. Seepage meter measurements reflect total SGD; if discharge salinity is also measured then the RSW and AGW components can be also be estimated. Chemical tracers are the most common approach because they can be used to estimate SGD to large areas. Chemical tracer estimates generally reflect some combination of RSW and AGW discharge depending on the specific tracer. Table 1.1 lists the papers reviewed for this study and the methods they employed.

Estimates of SGD are theoretically possible if the nearshore hydraulic gradient and sediment permeability are well known (*Weight and Sonderegger*, 2000). In practice obtaining the necessary data in other than the first few meters of sediment requires extensive drilling, geophysical surveying, or extrapolation of sparse data. *Langevin* (2001) used the USGS SEAWAT variable density groundwater transport code to model total SGD to Biscayne Bay Florida with mixed results. Both a regional 3D and local-scale 2D vertical models were developed assuming steady state conditions and homogeneous aquifer char-

[1] In this dissertation salinity (S) is reported using the Practical Salinity Scale of 1978 (PSS78). This salinity scale is based on the ratio of two conductivities and is therefore dimensionless (*Pilson*, 1998). However this scale is considered functionally equivalent to salinities expressed in mass based concentration units (e.g., g/kg or ‰) such that S=34.75 (mean ocean salinity) is equivalent to 34.75 g/kg or 34.75‰.

acteristics. While the variable density transport code was capable of estimating both the AGW and RSW components of SGD the accuracy of the estimates are difficult to evaluate. The models did not accurately simulate the groundwater salinities beneath Biscayne Bay as observed in monitoring wells, and seepage meter measurements were unsuccessful, so independent discharge estimates are unavailable. Additionally surface aquifer recharge rate and the terrestrial boundary groundwater flux must be estimated and the aquifer hydraulic parameters adjusted to calibrate the model water table elevations to monitoring well water levels (*Langevin*, 2001). Similar boundary conditions and calibrations are necessary in most if not all hydrogeologic models and introduce considerable uncertainty in their results.

SGD can be directly measured at the sediment/water interface using a seepage meter (Figure 1.2) (e.g., *Burnett et al.*, 2002; *Cable et al.*, 1997a,b; *Michael et al.*, 2003) which collects seepage through a small area of the sediment. Seepage meters are labor intensive and have an inherent bias which underestimates discharge due to the increased hydraulic friction associated with the meter (*Cable et al.*, 1997a). Further, because SGD is frequently heterogeneous, seepage meter results exhibit large variability (*Michael et al.*, 2003) and only limited extrapolation of results to larger areas is possible.

Chemical tracers provide an integrated spatial signal allowing quantification of SGD throughout entire bay systems (e.g., *Cable et al.*, 1996; *Charette et al.*, 2001; *Corbett et al.*, 2000; *Hussain et al.*, 1999; *Kelly and Moran*, 2002; *Krest and Harvey*, 2003; *Krest et al.*, 1999; *Rama and Moore*, 1996; *Schwartz*, 2003; *Scott and Moran*, 2001). The ideal chemical tracer of SGD is a dissolved constituent that 1) exhibits a substantial enrichment in groundwater relative to other potential source waters (e.g., seawater, river water, rain, and runoff) and 2) behaves conservatively within the coastal zone (*Charette et al.*, 2001). Radon, radium, and methane are the tracers most commonly used. Radion-222 is perhaps closest to the ideal, because it is highly enriched in groundwater, as a noble gas exhibits very conservative behavior, and is relatively straightforward to measure (*Cable et al.*, 1996). Its interpretation is complicated slightly by the need to account for gas exchange. $^{226}\mathrm{Ra}$, $^{228}\mathrm{Ra}$, $^{224}\mathrm{Ra}$, and $^{223}\mathrm{Ra}$ are also powerful tracers of SGD because they behave conservatively in brackish and marine waters and are enriched in groundwater (*Krest et al.*, 1999). They also provide a means of estimating bay residence time and tidal transport which are essential to properly modeling Ra mixing within a study area (*Charette et al.*, 2001). Methane is a product of anaerobic decay and is found in high concentrations in anoxic groundwaters with sufficient organic matter for methanogenesis (*Bugna et al.*, 1996). Methane concentrations in groundwater range from 0.1 to 6300 μM, river water contains 0.0048 to 5.0 μM (*Bugna et al.*, 1996), and seawater has a concentration of 0.002 μM (*Kehew*, 2000). Methane however is subject to microbial uptake and production and is not strictly conservative. It is usually used in conjunction with other tracers because it is relatively easy to analyze (e.g., *Cable et al.*, 1996, 1997a; *Swarzenski et al.*, 2001).

The studies in this dissertation rely on Ra isotopes as chemical tracers of SGD. The four naturally occurring Ra isotopes are members of the three long lived radioactive decay chains and are each the daughter nuclides of Th isotopes (Figure 1.3). While Th readily adsorbs to particles Ra is much more soluble. As salinity (S) increases Ra partitions into the dissolved phase; at S$>$5 Ra desorption is nearly complete (*Krest et al.*, 1999). Brackish groundwater has the highest Ra activities typically found in surface and near surface waters due to the presence of Th in the aquifer matrix. In surface waters what little Th is produced by decay of the traces of dissolved U is scavenged by particles and transported to the sediments. Consequently there is little Ra production in surface water and the open ocean has low Ra activities (*Krest et al.*, 1999). On the other hand, Ra is also very high in oil-field brine (produced water). In the recent past oil-field brine was routinely discharged to surface waters. That discharge has stopped but leakage of oil-field brine from submerged petroleum pipelines and wells could still be contributing substantial Ra in certain areas such as the Texas Coastal Bend.

1.2 Study Area: Coastal Bend of Texas

The Texas Coastal Bend is distinct from most areas in which SGD has been investigated. Tidal range is small or the order of 15-30 cm. It is semi-arid. Annual evaporation typically exceeds precipitation which is seasonal and driven by summer thunderstorms, tropical storms, hurricanes. Topographically the area is relatively flat but reaches elevations >100 m at the western extremes of the watersheds. The coastal plain is slightly elevated (10 m) above sealevel and the major river valleys.

1.2.1 Nitrogen Budgets, Groundwater, and Ecology

In many areas the dissolved nutrient concentrations of groundwater are significantly higher than those of regional surface waters. This can occur naturally as infiltrating water leaches nutrients from decaying organic matter within the overlying soil. Agricultural activities and septic systems also contribute significant amounts of nutrients, notably NO_3^-, to groundwater (*Sewell*, 1982). Since nitrogen is often a limiting nutrient in coastal waters, increases in the nitrogen concentrations of discharging groundwater can have ecological consequences and is thought to be a potential contributor to the eutrophication of some coastal waters (*Johannes*, 1980).

The Texas Coastal Bend has experienced problems associated with eutrophication, specifically loss of seagrass and blooms of harmful algae such as the Texas brown tide *Aureoumbra lagunensis* (*Buskey et al.*, 1998). *Brock* (2001), after attempting to develop a detailed N budget for Nueces Bay, noted that for each of the four years examined the N exported from the bay was greater (>30%) than the estimated N input. *Brock* (2001) concluded a partial explanation may be supply from SGD. Nueces Bay NO_3^- concentrations average 4.6 (max. 23) μM (*Pennock et al.*, 1999) which is relatively high for surface waters. In contrast, wells in the agricultural areas of Nueces and San Patricio counties have been found to have NO_3^- concentrations as high as 22-30 μM and several have concentrations greater than 60 μM (*Texas Water Development Board*, 2005a) — some of the highest groundwater NO_3^- levels within the state of Texas (*Hudak*, 2000).

1.2.2 Hydrogeology

The Texas coastal plain is the result of Cenozoic sedimentation from fluvial, deltaic, and marginal marine environments. During the Pleistocene, the frequent rise and fall of the sea level resulted in shifts of the shoreline accompanied by erosion and redeposition of sediments (*Tunnel*, 2002). During this time the coastal rivers changed their course and depositional patterns in response to climatic shifts which has resulted in a layered stratigraphy of modern and paleo-river alluvium (e.g., *Abdullah*, 1995). The result is an interfingering of beds and lenses of silt, clay, sand, and gravel with a potential range in hydraulic conductivity of over ten orders of magnitude (10^{-2} to 10^{-11} m sec^{-1}). This type of depositional environment is thought to form a network of subsurface conduits from the most permeable facies (*Chapelle*, 1997) creating a heterogeneous aquifer and controlling the groundwater flowpath (*Bersezio et al.*, 1999).

Geologic units in the area known to contain fresh to slightly saline water are, in order of decreasing age: the Goliad Sand, Lissie Formation, Beaumont Clay, barrier island deposits, South Texas eolian deposits, and river alluvium (*Ryder*, 1996; *Shafer*, 1968). The most productive portions of these units are the Chicot aquifer in the Beaumont Clay and Lissie Formations and the Evangeline aquifer in the Goliad Sand (Figure 1.4). The deposits are a series of clastic wedges that thicken and tilt southeastward to the Gulf of Mexico (*Ry-*

der, 1996). Erosion of the uplifted landward portions of the clastic wedges allows recharge in the exposed permeable sands north and west of San Patricio and Nueces counties. In addition the Chicot aquifer receives diffuse recharge in areas where the Beaumont clay is absent and the sands beneath are exposed.

Groundwater in the region is present in both unconfined (water table) and confined (artesian) aquifers (*Shafer*, 1968). A review of Texas Water Development Board (TWDB) well records finds numerous entries such as "well formerly artesian" and "no longer operating due to increased total dissolved solids" which illustrates how the hydrostatic pressure in the confined aquifers of the region has decreased during the period of record (1920-2002) (*Texas Water Development Board*, 2005a). Today shallow wells in the unconfined aquifer often have total dissolved solids >1000 mg/l and are unsuitable for human consumption; instead the water is used for agriculture and livestock. The deeper confined aquifers in the region are used by municipalities such as Kingsville. Industrial activities rely on both the unconfined and confined aquifers. Corpus Christi and most other local municipalities receive their water from surface reservoirs on the Nueces River.

In unconfined or phreatic aquifers the waterlevel and thereby the hydraulic gradient is generally found to follow the topography (*Freeze and Cherry*, 1979). An examination of records in the TWDB database (*Texas Water Development Board*, 2005a) shows that this also holds true in the Coastal Bend region. Figure 1.5 was created by the author in order to evaluate the potential for SGD in the Coastal Bend and as an aid for study site selection. The figure is an approximation of the regional water table surface in the unconfined aquifer and was created by spatially interpolating 2000-2002 waterlevel records from nine counties. The color gradient and contour lines both show the watertable elevation in feet above mean sea level. Figure 1.5 shows that the regional watertable does in fact mirror the surface topography. This is apparent if you compare the water table surface, which is based solely on well water levels, to the stream system, which is directly related to surface topography. The area surrounding Baffin Bay is a notable exception. This part of the region has seen long term groundwater withdrawal and as a result the water table has been drawn down over 30 m below the land surface (*Shafer*, 1968). In the rest of the area, groundwater moves towards the bays and lower river reaches of the Nueces, Mission, and Aransas Rivers. This analysis suggests that Nueces and Mission Bays have a greater potential for SGD (note the zero contour crosses into each of these bays) than Baffin Bay even apart from their differences in annual precipitation.

1.2.3 Terrestrial Springs

Brune (1981) documented the springs of Texas during the 70's and 80's including the Coastal Bend. Springs were historically important sources of water for native Americans, European explorers, and early settlers. There were at least eight named springs in the area: Round Lake, Mission, Hynes, Dismero, Ojo de Agua (a Spanish colloquialism for a spring), Malaquite, and Santa Gertrudis. These springs have all declined or failed due to changes in land cover and groundwater pumping. Ephemeral seeps still occur however and were documented by Brune in the 1970s. While collecting groundwater samples I have also seen ponds and pools at the base of bluffs along the shoreline and Nueces River valley such as Hazel Bazemore park and McGloins Bluff that also appear to be fed by groundwater seepage. The presence of terrestrial springs suggests that SGD does in fact still occur at least ephemerally.

1.2.4 Uranium Deposits

Major deposits of uranium are present in Eocene or younger formations which outcrop inland of the bay system and are thought to be associated with volcanic ash in the

Catahoula formation of Miocene age (*Cech et al.*, 1988). Uranium mining in the region was extensive, peaking in the early 1970s. Because ^{238}U is the progenitor of $^{226}\mathrm{Ra}$ the location of these U deposits could potentially influence the activity of $^{226}\mathrm{Ra}$ in the deepest groundwaters. $^{228}\mathrm{Ra}$ on the other hand is controlled by the amount of thorium in the aquifer solids. To evaluate the mobility of U in the Nueces River watershed *Brandenberger et al.* (2004) measured dissolved U concentrations in the surface waters of Lake Corpus Christi, local groundwaters, and a livestock pond that borders an area with U mine tailings; they found no evidence of U enrichment due to mining operations beyond the local scale. Lake Corpus Christi dissolved U concentrations were approximately 1 ug L^{-1} (322 dpm m^{-3}) with particulate concentrations nearly an order of magnitude less; the livestock pond dissolved concentrations were similar but the particulate concentrations were as much as 3 ug L^{-1} (965 dpm m^{-3}). Of the 16 groundwater samples, one was nearly 40 ug L^{-1} (12,900 dpm m^{-3}), two were approximately 15 ug L^{-1} (4830 dpm m^{-3}), and seven were between 2 and 7 ug L^{-1} (2250 to 643 dpm m^{-3}).

1.3 Study Design

My research has been conducted along two complimentary lines: 1) a detailed study of submarine fluid discharge to Nueces Bay and 2) a regional comparison of SGD tracers in Copano, Nueces, and Baffin Bays. In the first case, my approach has been to use a series of progressively more refined studies to identify areas of submarine discharge within Nueces Bay, starting at the regional level, down to the bay scale, and finally to specific subregions of the bay where discharge indications are strongest. In the second case, Copano, Nueces, and Baffin Bays represent a natural experiment in that they differ in river supply, water table elevation, net precipitation, and submerged petroleum infrastructure. Comparing Ra concentrations in these bays over an annual wet dry cycle offered the possibility of identifying bay characteristics relevant to Ra supply and SGD.

Chapter 2 of this dissertation concerns the initial 2002–2003 field season which focused on Nueces Bay. The results provided evidence of a substantial submarine input of dissolved $^{226}\mathrm{Ra}$ to Nueces Bay. Chapter 3 concerns a synoptic geophysical and geochemical survey I conducted to further investigate the occurrence and spatial distribution of submarine discharges of water to the head of Nueces Bay. The survey was conducted in the 12 km^2 head of Nueces Bay where previous dissolved Ra measurements (Chapter 2) suggested a significant submarine groundwater discharge. Chapter 4 covers the final 2004–2005 field season and compares the Ra activities of Copano Bay, Nueces Bay, and Baffin Bay at three periods during their seasonal flushing cycles. These results show that the seasonal increase in dissolved ^{226}Ra activity for Nueces Bay is substantially larger than for either Copano Bay or Baffin Bay. Though submarine groundwater discharge is not ruled out it cannot completely account for the high Ra flux indicated by the study results. The dissolved Ra activity of the majority of groundwater samples was less than Ra activities frequently observed in the bays. Even using groundwater activities at the upper end of those measured would still require an unrealistically high groundwater flux compared to 1) global estimates of AGW/surface water ratios and 2) the combined flow from the known subaerial springs in the greater Corpus Christi area (*Brune*, 1981). Therefore I conclude that SGD supplies only a portion of the ^{226}Ra imbalance. Leakage of oil-field brine could potentially account for a large portion of the ^{226}Ra imbalance because oil-field brine Ra activities are substantially higher than those of groundwater. Since the distribution of petroleum wells is in general agreement with the differences in Ra activities between Nueces, Baffin, and Copano Bays I conclude that leakage of oil-field brine is a significant source of Ra to Nueces Bay.

Table 1.1: Submarine groundwater discharge studies.

Study Site	Technique	Reference
Big Bend Region, Fl	Rn and CH_4	*Cable et al.* (1996)
Florida Bay	Rn and CH_4	*Corbett et al.* (2000)
Big Bend Region, Fl	seepage meters	*Burnett et al.* (2002)
Chesapeake Bay	Rn and Ra	*Hussain et al.* (1999)
Coastal salt ponds, RI	Ra isotopes	*Scott and Moran* (2001)
Crescent Beach, Fl	Rn, Ra, Ba, CH_4, seepage meters	*Swarzenski et al.* (2001)
Delaware River and Bay Estuary	Rn	*Schwartz* (2003)
Everglades, Fl	Ra isotopes	*Krest and Harvey* (2003)
Ganges Brahmaputra River, Bangladesh	Ra isotopes and Ba	*Moore* (1997)
Mississippi Delta	Ra isotopes	*Krest et al.* (1999)
North Inlet Salt Marsh, NC	Ra isotopes	*Rama and Moore* (1996)
Pettaquamscutt estuary, RI	Ra isotopes	*Kelly and Moran* (2002)
Waquoit Bay, Mass.	Ra isotopes	*Charette et al.* (2001)
Waquoit Bay, Mass.	seepage meters	*Michael et al.* (2003)

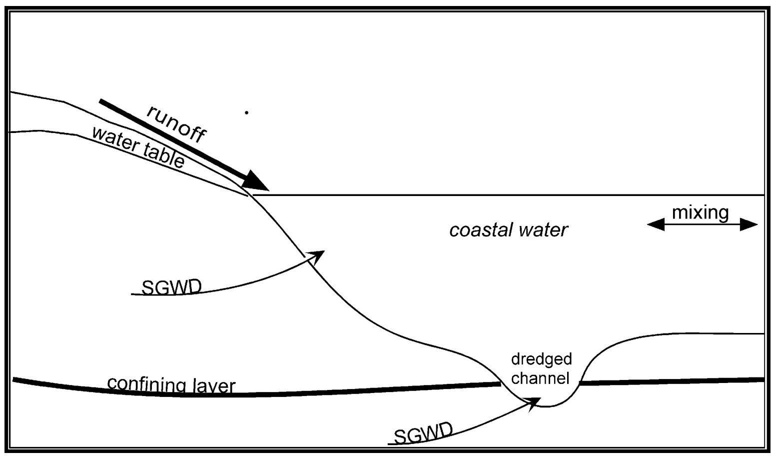

Figure 1.1: SGD from unconfined aquifers occurs at the sediment water interface and is controlled by the height of the water table above sealevel and the permeability of coastal sediments. Discharge from confined aquifers may occur at locations where the confining layer is absent or disrupted. This can occur naturally along fault lines (there is a fault line just south of Nueces Bay) and it can also occur where human activities such as channel dredging have breached the confining layer.

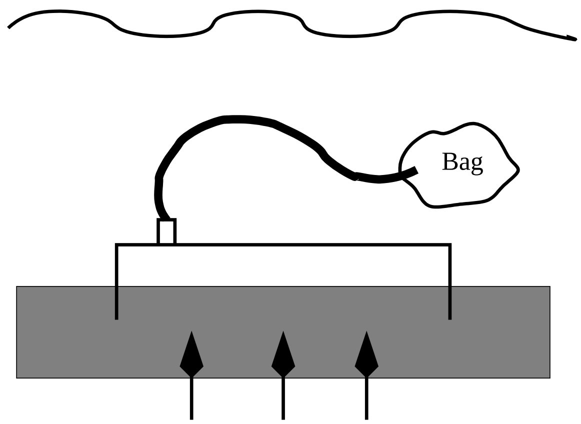

Figure 1.2: Seepage meters are often made from 55 gallon drums cut in two. The seepage meter is inserted into the bay sediment with a hose and bag attached. The bag is initially partially filled with water. The change in water volume or weight in a given time is used to calculate SGD (*Weight and Sonderegger*, 2000).

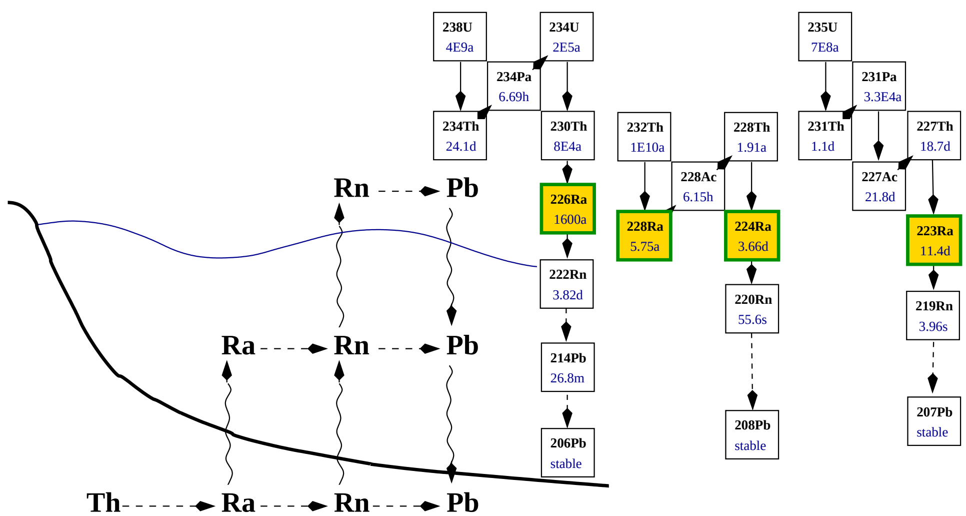

Figure 1.3: The portions of the three naturally occurring radioactive decay chains in which Ra isotopes are present. The half-life of each isotope is reported directly below its identity.

Era	System	Series	Stratigraphic Unit	Lithology	Hydrogeologic Unit
Cenozoic	Quarternary	Holocene	Alluvium	Sand, silt, and clay	Chicot Aquifer
		Pliestocene	Beaumont Formation Willis Sand		
	Tertiary	Pliocene	Goliad Sand		Evangeline Aquifer
		Miocene	Fleming Formation	Clay, silt, and sand	Burkeville Confining Unit

Figure 1.4: This simplified stratigraphic depiction of the Gulf Coast aquifer system shows the Chicot and Evangeline aquifers in relation to the stratigraphy (*Ryder*, 1996).

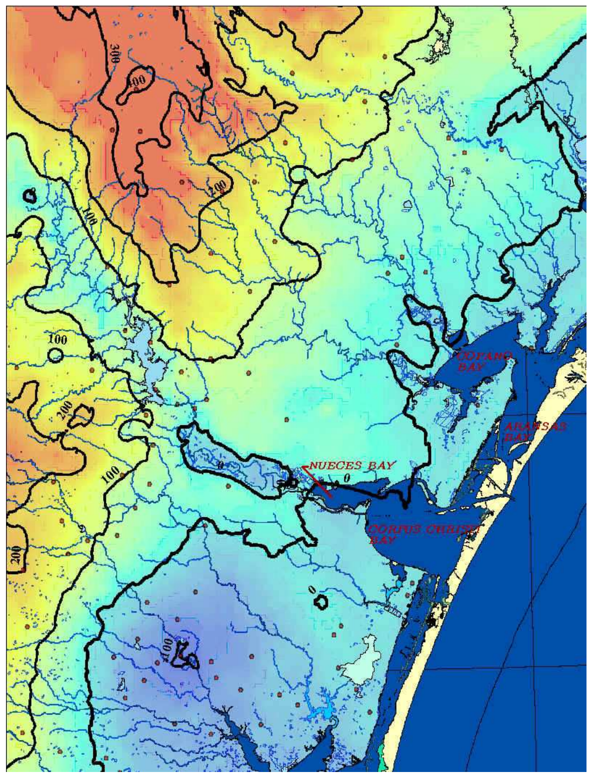

Figure 1.5: This groundwater equipotential map was created as a preliminary aid in selecting study areas for this project. The map is based on well data from the TWDB groundwater database for the year 2000 (*Texas Water Development Board*, 2005a). The contours are based on a spherical krige interpolation of water levels in feet above mean sea level taken from the wells shown on the map (grey circles). The contour interval is 100 ft (30.5 m). The ground coloration also reflects water levels, starting with red at 400 ft (122 m) and ranging to blue at -100 ft (-30.5 m).

Chapter 2

High ^{226}Ra and ^{228}Ra activities in Nueces Bay, Texas indicate large submarine saline discharges

2.1 Abstract

Submarine groundwater discharge (SGD) to Nueces Bay (Texas) was investigated using naturally occurring Ra isotopes. The dissolved Ra activities of Nueces Bay are among the highest observed in coastal estuaries; as great as 2600 dpm m^{-3} for ^{228}Ra and 1000 dpm m^{-3} for ^{226}Ra. A combination of salt and Ra mass balances demonstrates that river discharge and bay bottom sediments cannot supply the Ra needed to balance tidal export. In the case of ^{226}Ra there is an additional source required of $218 \times 10^6 \pm 105\%$ dpm day^{-1} that is 9 times the maximum supply from bay bottom sediments and 50 times the Ra supplied by the Nueces River. Only a portion of this large flux can be supplied by SGD, based on the maximum measured Ra activity of local groundwater (703$\pm 7\%$ dpm m^{-3} ^{226}Ra). The

large size of the Ra flux suggests a fluid of much higher Ra activity such as oil-field brine. The numerous submerged petroleum wells and pipelines in Nueces Bay make leakage of oil-field brine a potential source of Ra to Nueces Bay. In either case, fluxes of brackish groundwater or oil-field brine would represent substantial salt loads, particularly during periods of low river inflow, and should be considered when determining the freshwater inflow requirements for Nueces Bay and similar estuaries. These submarine fluxes may also contribute significant amounts of nitrogen to the bay on the order of 19 million g N yr^{-1} if the discharge is entirely brackish groundwater and 132 million g N yr^{-1} if it is largely oil-field brine leakage.

2.2 Introduction

The exchange of water and dissolved constituents between coastal aquifers and surface waters can be important components of coastal hydrologic and geochemical cycles (*Burnett et al.*, 2003; *Moore*, 1997). In many areas, this water flux has been estimated to be a significant fraction of surface water (e.g., river) inflow (e.g., *Moore*, 1996). This suggests there is also a significant flux of those chemical species that are enriched in aquifer porewaters. Quantifying these fluxes and establishing clear connections with the physical processes that produce them is challenging (*Burnett et al.*, 2003). Moreover the variety and variability of the processes that contribute to such fluxes can complicate interpretation of data that may either target one process or reflect several at once. Specifically, water flux through sediments may be driven by a combination of processes including groundwater advection, sealevel change due to astronomical and wind-driven tides, and density driven free convection (*Bokuniewicz*, 1992; *Moore*, 1999; *Simmons et al.*, 1991). The resulting water flux is a mixture of terrestrial advecting groundwater (AGW) and recirculated seawater (RSW) often collectively referred to as submarine groundwater discharge (SGD).

Recent studies of coastal water bodies have demonstrated significant excesses of dissolved Ra above the inventory supported by surface water supply and diffusion from sediments (e.g., *Burnett et al.*, 2002; *Charette and Buesseler*, 2004; *Charette et al.*, 2001, 2003; *Hancock et al.*, 2000; *Kelly and Moran*, 2002; *Krest et al.*, 1999; *Moore*, 1996; *Rama and Moore*, 1996; *Scott and Moran*, 2001; *Veeh et al.*, 1995). These excesses have been attributed to supply from SGD. Similarly, this study uses naturally occurring Ra (^{226}Ra and ^{228}Ra) and salinity budgets to look for excess dissolved Ra in Nueces Bay, Texas. For Nueces Bay, there are two potential submarine sources of dissolved Ra: SGD and leakage of oil-field brine (formation water) from submerged petroleum wells and pipelines.

The original intent was to apply traditional mass balance calculations to assess seasonal variations in SGD to Nueces Bay. The dramatic change in bay salinity that occurred during the study period necessitated a change in approach, and also offered an opportunity to constrain some of the poorly known components of the bay water balance (i.e., tidal mixing) necessary to construct the Ra budget. Time series hydrographic data, for the period of the bay's recovery from flood conditions, were used to constrain tidal mixing and to construct a Ra budget for the May 2003 sampling period when the bay again approached steady state conditions. The imbalance between the ^{226}Ra supplied by the river and bay bottom sediments and the ^{226}Ra exported by tidal exchange is taken as evidence of additional submarine Ra sources such as SGD discharge and/or leakage of oil-field brine from submerged petroleum wells and pipelines.

2.3 Materials and Methods

2.3.1 Study Area

Nueces Bay (75 km^2 and 0.7 m deep on average) is a secondary bay within the Corpus Christi Bay system of Texas (Figure 2.1). This bay experiences dramatic annual swings in salinity driven by a strong wet/dry net precipitation cycle that features high summertime evaporation and periods of intense precipitation during the late summer and fall. Hypersaline conditions in the summer are common, particularly in the salt marsh at the head of Nueces Bay where sediment porewater salinities are typically between 35 and 80 and can reach as high as 320 (*Dunton et al.*, 2004). The mean daily tidal range for the Corpus Christi Bay system is 15 cm (*Diener*, 1975). Groundwater in the region is present in both confined and unconfined aquifers in a layered stratigraphy of interfingered silt, clay, sand, and gravel beds (*Shafer*, 1968).

This study of SGD to Nueces Bay is pertinent and timely for several reasons. Nueces Bay and the salt marsh at its head are highly productive and ecologically important to the region, but aspects of its nitrogen budget remain uncertain. An attempt by *Brock* (2001) to develop a balanced nitrogen budget for Nueces Bay was unable to account for 30% of the exported nitrogen using known nitrogen inputs. Two possible reasons cited for this imbalance were an underestimate of nitrogen fixation and an unaccounted for contribution from SGD. In addition, dense and persistent blooms of the Texas brown tide *Aureoumbra lagunensis* (*Buskey et al.*, 1998) in recent decades have prompted the question of whether changes in freshwater inflow relative to SGD may play a role in bloom initiation. Finally, local municipalities are increasingly turning to groundwater desalinization to supplement existing surface water supplies and the impacts of such proposals can only be evaluated if the natural system is understood.

2.3.2 Sample Collection

Surface water samples (75 L) for dissolved Ra analysis were collected from Nueces Bay during April (n=19) and July 2002 (n=20) and on 19 and 27 May 2003 (each n=10) (Table 2.1, Figure 2.2). Sample stations were reoccupied during successive surveys to within

20 m of the April 2002 sample locations. The April 2002 sampling was conducted during a prolonged dry period while July 2002 was during a period of heavy precipitation and flooding. May 2003 sampling occurred at the end of a transition between wet and dry conditions. The May 2003 sample stations were collected during both spring and neap tides at a subset of the April and July 2002 stations. Samples were also collected from the Nueces River and river plume (n=12) and from regional water wells (n=14) to assess the Ra contribution of these waters to Nueces Bay (Figure 2.1). Samples were collected by submersible pump, filtered to 1 μm through polypropylene cartridge filters, and stored in 25 L polyethylene bottles. Water temperature and salinity were determined using a YSI Model 6000 Sonde (April & July, 2002), a SeaBird Electronics SeaCat CTD profiler (May 19, 2003), a Guildline Autosal salinometer (May 27, 2003; no temperature data), and a YSI Model 30 Sonde (groundwater samples).

Freshwater (salinity <1) samples (75 L) were collected as grab samples during December 2002 (n=3) from the Nueces River (Table 2.2). In order to evaluate the contribution of Ra desorption from riverine sediments to the bay, the Nueces River plume within the bay was sampled in April 2004 (n=9) across the S=0 to 12 salinity gradient (Table 2.2). Filters were retained in order to determine particulate Ra activity; only one of these samples (Table 2.2: sample 5) contained Ra above detection limits.

Groundwater samples (75 L) were collected from wells equipped either with downhole pumps or windmills, or using a portable pump (Table 2.3, Figure 2.3). The wells had either been flowing for an extended period immediately prior to sampling or were allowed to purge before samples were collected. The wells ranged in depth from 3 to 84 m. Wells W1-W10 were used for either irrigation or watering livestock and salinities were 3 or less. Wells W11-W14 were monitoring wells and salinities were 3.2 to 8.9.

Samples (100 L) were also collected from the Gulf of Mexico in September 2002, aboard the R/V *Longhorn* along a transect starting from just offshore of Aransas Pass to a point approximately 160 km from shore (Table 2.4). Surface water samples (n=5) along this transect were collected using the ship seawater collection system.

2.3.3 Radium Activity Measurements

Radium was quantitatively extracted from water samples and co-precipitated with $BaSO_4$ following the procedure outlined by *Rutgers van der Loeff and Moore* (1999). Radium was extracted onto MnO_2 impregnated acrylic fiber at <1 L min^{-1}, the fiber rinsed with deionized water, and the Ra leached from the fiber using 500 mL of 6 N HCl in a Soxhlet apparatus. Radium was co-precipitated with $BaSO_4$ by adding 10 mL of saturated $BaNO_3$ and 25 mL of 7 N H_2SO_4 to the heated extraction solution. The precipitate was allowed to settle overnight after which the fluid was decanted and the precipitate rinsed with 6N HCl and transferred to polystyrene counting vials.

The ^{228}Ra and ^{226}Ra activities of the precipitates were determined by gamma counting the daughter nuclides ^{228}Ac and ^{214}Pb on a high purity germanium well detector (*Moore*, 1984). The precipitates were aged at least 15 days prior to gamma counting to allow the ingrowth of the daughter nuclides. Decay counts for ^{228}Ac and ^{214}Pb were determined from their 911 and 351 keV gamma emmissions, respectively. The 1σ counting error is reported for each measurement and was typically 5-10% or less. Measured activities were decay-corrected to time of sample collection using:

$$\mathrm{dpm}/\left(100\,\mathrm{m}^3\right) = \left(\mathrm{cpm}/\left(C_{eff}\;E_{eff}\;Br\;V\right)\right)\;e^{\lambda\,t_{coll}}\;\left(1000\,\mathrm{L}/\mathrm{m}^3\right) \tag{2.1}$$

where C_{eff} is the combined collection and counting efficiency, E_{eff} is the manganese fiber extraction efficiency, Br is the branching ratio, V is the sample volume in liters, λ is the radioactive decay constant, and t_{coll} is elapsed time between sample collection and activity measurement. In most studies, Mn fibers prepared in this way are assumed to quantitatively extract Ra from water samples at flow rates of $<$1-2 L min^{-1}. Extraction efficiency in this study was verified to be $>$95% by using two MnO_2 columns in series for several samples and determining the relative amounts adsorbed to the primary and secondary columns. A combined collection and counting efficiency for the gamma detector was determined by preparing two solutions of known ^{228}Ra and ^{226}Ra activity from standards and precipitating, collecting, and counting these standards in the same way as the samples.

The 1 and 5 μm polypropylene cartridge filters from the Nueces River plume samples were dried and ashed at 500°C, the ash collected and weighed, and 1 g of the 1 μm and 2 g of the 5 μm ash were packed into counting vials and sealed with epoxy. The samples were then aged at least 15 days and counted in the same way as the dissolved Ra samples.

2.3.4 Time Series Hydrographic and Meteorological Data

In order to construct water and salinity balances for Nueces Bay, time series measurements of Nueces Bay salinity, water temperature, and water height (Division of Nearshore Research, 2003), Aransas Pass salinity and water temperature, Nueces River salinity, temperature, and discharge (Division of Nearshore Research, 2003; U.S. Geological Survey, 2005), and regional precipitation and evaporation (National Atmospheric and Oceanic Administration, 2003) were compiled for 2002 and 2003 (Figure 2.4). Hourly measurements of Nueces Bay and Nueces River salinity and water temperature are recorded by Hydrolab H20 Multiparameter Water Quality Data Transmitters at Texas Coastal Ocean Observation Network (TCOON) stations SALT05, SALT03 and SALT01 operated and maintained by the Division of Nearshore Research at Texas A&M University Corpus Christi. Hourly measurements of water height are recorded at TCOON stations 011 within Nueces Bay and 008 on the shoreline of Corpus Christi Bay 4 km south of the mouth of Nueces Bay (Figure 2.2).

Daily records of maximum, minimum, and mean salinity and water temperature at Aransas Pass are recorded by an Endeco model 1152 sonde continuously deployed from the The University of Texas Marine Science Institute (UTMSI) pier lab. Nueces River mean daily volumetric discharge is recorded at the first USGS stream gauge upstream of Nueces Bay. Daily precipitation is recorded at eight National Weather Service affiliated stations in the region. Daily evaporation is recorded by Class A evaporation pans at a National Weather Service affiliated station near Lake Corpus Christi and at UTMSI. The locations of these recording stations are indicated in Figures 2.1 and 2.2.

Salinity, water temperature, and water height data used to estimate bay volume were smoothed by low pass filtering in the frequency domain to remove signal components with periods less than 17 days. Flood and ebb tide mean heights and frequency were determined by cataloging the change in water height between the inflection points in the unfiltered water height series. Bay volume (Figure 2.4d) was calculated by adding Nueces Bay mean depth to the fluctuations in water height relative to mean sea level recorded at TCOON stations 008 and 011 and multiplying by Nueces Bay mean surface area. Bay evaporation was estimated as 30% of pan evaporation to account for enhanced evaporation from pans relative to the bay (*Fetter*, 1994). Direct net precipitation to Nueces Bay (Figure 2.4c) was estimated by spatially averaging available evaporation and precipitation records to the center of Nueces Bay (Figure 2.2: station 8) and multiplying by the bay surface area to estimate the volumetric rate.

2.4 Results and Discussion

For Nueces Bay, the most significant differences in bay salinity and Ra activities between the sample periods are clearly associated with the flooding of the Nueces River in the summer and fall of 2002 (Table 2.1, Figure 2.5). The low salinity and Ra activities in

July 2002 result from a nearly complete flushing of the bay by Nueces River flood waters which first peaked a week prior to sample collection and which reduced bay salinity from 30 to <1 in 15 days. During peak river discharge the bay water residence time with respect to Nueces River inflow reached a minimum of approximately 1 day. The Nueces River flooded twice more in subsequent months repeatedly flushing the bay to salinities <1.

On 13 November 2002, the salinity recorder at TCOON SALT01 began a steady rise that continued into the summer of 2003 (Figure 2.4a). During this recovery period river discharge was relatively constant (Figure 2.4d) and the mean bay water residence time with respect to Nueces River inflow increased to 60 days. The rise in salinity that began on 13 November 2002 reached its maximum just after the 27 May 2003 sample period and remained relatively stable until July 2003 (Figure 2.4a). Similarly, bay Ra activity (Figure 2.5), river discharge, direct net precipitation, and bay volume (Figure 2.4) were all relatively stable during May 2003.

The analysis and discussion focuses on May 2003 because this period best approximates steady state hydrologic conditions for Nueces Bay during this study. Taken together the 19 and 27 May 2003 mean bay ^{228}Ra and ^{226}Ra dissolved activities were $1553\times10^6\pm24\%$ and $664\times10^6\pm32\%$ dpm m^{-3} respectively. The mean bay salinity was 24 ± 2. Including the 10 days prior to 19 May 2003 through to 27 May 2003, the mean daily river discharge was $19.7\times10^3\pm5\%$ m^3, the ebb tidal prism was $9.40\times10^6\pm11\%$ m^3, the flood tidal prism was $9.71\times10^6\pm11\%$ m^3, and the mean bay volume was $57.8\times10^6\pm11\%$ m^3.

2.4.1 Nueces Bay Salt and Radium Balances

Using the May 2003 results, I demonstrate below that Nueces Bay, like many other coastal water bodies, exhibits a substantial excess of dissolved Ra. This analysis uses mixing models for salt, ^{228}Ra, and ^{226}Ra which are all based on the bay water balance (Figure 2.6a):

$$V_f - V_i = \sum_{n=i}^{f}(FT - ET + R + (P - E) + SGD)_n \tag{2.2}$$

where f and i are the final and initial days of a time period, V is the bay volume, FT is the flood tidal prism, ET is the ebb tidal prism, R is the river discharge, P is direct precipitation, E is direct evaporation, and SGD is the potential submarine groudwater discharge or oil-field brine leakage. Though evaporation and precipitation are important water fluxes for Nueces Bay, they are negligible fluxes of salt and Ra and therefore do not appear in the following salt and Ra balances. However these water fluxes do indirectly effect the bay salt and Ra concentrations by influencing the ebb and flood tidal volumes. In the following analysis the bay water level record is used to determine the ebb and flood tidal volumes. This implicitly accounts for the effects of evaporation and precipitation. Evaporation and precipitation data (Figure 2.4c) are presented for reference.

Nueces Bay tidal mixing efficiency was determined using a bay salt balance (Figure 2.6b):

$$(\bar{s}_B V)_f - (\bar{s}_B V)_i = \sum_{n=i}^{f}(\gamma \bar{s}_{FT} FT - \gamma \bar{s}_{ET} ET + \bar{s}_R R + \bar{s}_{SGD} SGD)_n \tag{2.3}$$

where $\bar{s}_B$ is the mean bay salt concentration, γ is the tidal mixing efficiency, $\bar{s}_{FT}$ and $\bar{s}_{ET}$ are the flood and ebb tide salt concentrations, $\bar{s}_R$ is the river salt concentration, and $\bar{s}_{SGD}$ is the unknown SGD or oil-field brine salt concentration. Neglecting the effects of SGD or oil-field brine leakage on bay salinity, Equation 2.3 can be solved for γ based on the water height, salinity, temperature, and river discharge time series. For this purpose the salinities of Nueces Bay, Aransas Pass, and the Nueces River were converted to mass of dissolved salt per unit volume (specific salt mass) using:

$$\bar{s} = S\ \rho_{sw}\,(S,T)\ \ (\mathrm{kg}/1000\ \mathrm{g}) \tag{2.4}$$

where $\bar{s}$ is the dissolved salt mass per unit volume (kg m^{-3}), S is salinity (g kg^{-1}), and ρ_{sw} is the density of seawater (kg m^{-3}) which is a function of S, salinity, and T, temperature (*Millero and Poisson*, 1981). Using data for the period of 13 November 2002 to 27 May 2003, the calculated mixing efficiency was 0.08±0.02 which is within the range of 0.05 to 0.15 for previous estimates of Corpus Christi Bay (*Brock*, 2001; *Smith*, 1985; *Solis and Powell*, 1999).

Neglecting radioactive decay, balances for both ^{228}Ra and ^{226}Ra are based on (Figure 2.6c):

$$\begin{aligned}(Ra_B V)_f \quad - \quad & (Ra_B V)_i = \sum_{n=i}^{f} (\gamma Ra_{FT} FT - \gamma Ra_{ET} ET \\ + \quad & Ra_R + Ra_{SED} A + Ra_{SGD} SGD)_n \end{aligned} \tag{2.5}$$

where Ra_B is the mean bay Ra activity, Ra_{FT} is the radium activity of the flood tide, Ra_{ET} is the radium activity of the ebb tide, Ra_R is the total dissolved plus desorbable Ra activity supplied by the river, Ra_{SED} is the diffusive supply from bay bottom sediments, A is the area of the bay, Ra_{SGD} is the radium activity of SGD and/or oil-field brine. Radioactive decay can be neglected because the half-lives of ^{228}Ra and ^{226}Ra are significantly longer than the water residence time of Nueces Bay.

At steady state and neglecting the unknown SGD and oil-field brine contributions Equation 2.5 becomes:

$$0 = \gamma Ra_{FT} FT - \gamma Ra_{ET} ET + Ra_R R + Ra_{SED} A \tag{2.6}$$

which is the basis of this analysis. It states that if SGD and oil-field brine leakage are absent the Ra exported by tidal mixing should balance river and bottom sediment supply. This can be independently assessed for ^{228}Ra and ^{226}Ra.

In the following analysis where parameters and their uncertainties (Table 2.5) are estimated, the most conservative values (i.e., values that would minimize any Ra contribution from sources such as SGD) were used. The analysis begins by evaluating each of the terms in Equation 2.6.

Tidal exchange

The Ra activities of the ebb tide are assumed to be the combined 19 and 27 May 2003 bay means; 1553±24% and 664±32% dpm m^{-3} for ^{228}Ra and ^{226}Ra respectively. The Ra activity of the flood tide is assumed to be the mean of the two May 2003 samples collected at station 1 nearest the mouth of Nueces Bay (Figure 2.2); 1000±3% and 339±8% dpm m^{-3} for ^{228}Ra and ^{226}Ra. Based on the mixing efficiency of 0.08±0.02 and mean daily flood and ebb tidal prisms of $9.71 \times 10^6 \pm 11\%$ and $9.40 \times 10^6 \pm 11\%$ m^3 day^{-1} the net tidal export is $411 \times 10^6 \pm 117\%$ dpm day^{-1} of ^{228}Ra and $248 \times 10^6 \pm 91\%$ dpm day^{-1} of ^{226}Ra. The associated uncertainties are large because the difference between the flood and ebb tide fluxes is approximately the same magnitude as their absolute uncertainties. The uncertainty in these numbers dominates the uncertainties in the remaining analysis.

River inputs

The total riverine Ra contribution includes the dissolved flux and also desorbable Ra associated with suspended particulate material. Experiments have shown that the ratio of particulate adsorbed Ra to dissolved Ra is inversely related to salinity (*Webster et al.*, 1995). Therefore as river particulate material mixes with higher salinity water a greater portion of adsorbed Ra will be released into solution. *Krest et al.* (1999) determined that for Mississippi River sediments desorption was essentially complete at a salinity of 5 and that only 10-40% of the total particulate activity is desorbable.

The most conservative estimate of the riverine dissolved Ra activity comes from the July 2002 Nueces Bay samples. These samples were essentially river flood waters with slightly greater activities than the three upstream Nueces River samples collected late that year. The mean ^{228}Ra and ^{226}Ra activities for July 2002 were 222±16% and 186±12% dpm m^{-3} (Table 2.1).

The desorbable Ra activity can be estimated from the Nueces River collected in April 2004 plume samples (Table 2.2: samples 4-12). The initial increase in ^{226}Ra activity between salinities of 0.3 to 4.4 is a barely discernible 30 dpm m^{-3} (Figure 2.7). Assuming for simplicity that this is due to desorption alone (and not also including benthic diffusion or advection of Ra), then the increase is consistent with a release of 43% of the 70 dpm m^{-3} ^{226}Ra particulate activity measured (Table 2.2: samples 5-5μm, and 5-1μm). In comparison, the initial increase in ^{228}Ra activity is 166 dpm m^{-3} which is more than double the total measured particulate ^{228}Ra activity of 84 dpm m^{-3} and suggests that particle desorption is not the sole source of ^{228}Ra for these samples. The most reasonable estimates of the desorbable Ra input are 30±50% dpm m^{-3} for ^{226}Ra and 36±50% dpm m^{-3} for ^{228}Ra; based on the observed ^{226}Ra desorption and the measured particulate ^{228}Ra/^{226}Ra ratio of 1.2±0.2. The 50% uncertainty limits on these estimates are based on the possible desorption of up to 65% of the total particulate activity. Therefore the total effective river Ra activities for ^{228}Ra and ^{226}Ra are 258±15% and 216±12% dpm m^{-3} respectively. Based on the May 2003 mean daily river discharge of $19.7 \times 10^3 \pm 5\%$ m^3 day^{-1}, the total riverine contributions are $5.08 \times 10^6 \pm 16\%$ dpm day^{-1} for ^{228}Ra and $4.25 \times 10^6 \pm 13\%$ dpm day^{-1} for ^{226}Ra.

A more reasonable estimate of the desorbable Ra input is 30±50% dpm m^{-3} for ^{226}Ra and 36±50% dpm m^{-3} for ^{228}Ra, based on the observed ^{226}Ra desorption and the measured particulate ^{228}Ra/^{226}Ra ratio of 1.2±0.2. The 50% uncertainty limits on these estimates are based on the possible desorption of up to 65% of the total particulate activity. Therefore the total effective river Ra activity for ^{228}Ra and ^{226}Ra are 258±21% and 216±17% dpm m^{-3}. Based on the mean daily river discharge of $19.7 \times 10^3 \pm 5\%$ m^3 day^{-1} during May 2003 the total river Ra contributions for ^{228}Ra and ^{226}Ra are $5.08 \times 10^6 \pm 22\%$ and $4.25 \times 10^6 \pm 18\%$ dpm day^{-1}.

Supply from Bay Bottom Sediments

Though Ra desorbs from suspended particles in brackish water, the parent thorium isotopes do not. Therefore by diffusion alone, sediments deposited within the bay remain a small but perpetual source of regenerated Ra until they are buried to a depth sufficient for radioactive decay to occur before diffusion to the surface (*Rama and Moore*, 1996). In addition to simple diffusion the processes of sediment compaction, bioturbation, and sediment resuspension are also important in the supply of Ra from bay bottom sediment porewaters. Similar studies have estimated diffusive fluxes based on the Th distribution in sediment cores (e.g., *Charette et al.*, 2001). For Nueces Bay, it would be difficult to make such an estimate from a reasonable number of sediment cores considering the bay size (75 km^2) and the potential variability in sediment type, porosity, and porewater Ra concentrations created by the relatively frequent major post depositional disturbances (i.e., tropical storms and episodic flooding). Moreover it would be difficult to assess either the uncertainty or the relative conservatism of such an estimate. Since sedimentary fluxes are greater in proportion and absolute value for ^{228}Ra than for ^{226}Ra, I instead make the initial, conservative assumption that all of the excess ^{228}Ra implied by the mass balance evaluation is attributable to a sedimentary source. Due to its slower regeneration rate the ^{226}Ra bay bottom sediment supply is then 1/16 of the ^{228}Ra supply (*Krest et al.*, 1999).

The ^{228}Ra bay bottom sediment supply thus calculated from Equation 2.6 is $723 \times 10^6 \pm 117\%$ dpm day^{-1}. The ^{226}Ra bay bottom sediment supply is then $45.2 \times 10^6 \pm 117\%$ dpm day^{-1}. This is equivalent to a ^{226}Ra sediment flux of 6.0×10^{-5} dpm cm^{-2} day^{-1}, which is 4 to 15 times greater than estimates of diffusive supply for Mississippi shelf and Waquoit Bay sediments (*Charette et al.*, 2001; *Krest et al.*, 1999). Though this approach overestimates the supply of ^{226}Ra from bay bottom sediments it does place a clear and conservative upper limit on this term. It is worth noting that even if the Ra supply from bay bottom sediments were entirely neglected, the calculated ^{226}Ra excess would only increase by 11% because the bay bottom sediment Ra flux is minor in comparison to the tidal Ra fluxes.

Evidence of a submarine Ra source

Based on the analysis above, an additional $218 \times 10^6 \pm 105\%$ dpm day^{-1} of ^{226}Ra is needed to satisfy the Nueces Bay ^{226}Ra balance. This is strong evidence of an additional submarine Ra source. The high absolute Ra activities of Nueces Bay, particularly at the head of the bay (e.g., Figure 2.2 station 16), lend qualitative support to this inference. Nueces Bay Ra activities are among the highest yet observed in coastal waters (Figure 2.8). The maximum observed ^{226}Ra activity in Nueces Bay was 1000±78 dpm m^{-3}, similar to the Bay of Bengal maximum ^{226}Ra activity of 1140 dpm m^{-3} (*Moore*, 1997). In other coastal waters reported ^{226}Ra activities are typically $<$600 dpm m^{-3} (e.g., Spencer Gulf Australia; the waters of Amazon shelf; North Inlet, South Carolina; Waquoit Bay, Massachusetts; and Pettaquamscutt River estuary, Rhode Island) (*Charette et al.*, 2001; *Kelly and Moran*, 2002; *Moore et al.*, 1995; *Rama and Moore*, 1996; *Veeh et al.*, 1995). The substantial

^{226}Ra imbalance and high absolute Ra activities of Nueces Bay suggests the presence of significant SGD and/or leakage of oil-field brine from submerged petroleum pipelines and wells.

SGD may account for a portion of the ^{226}Ra imbalance. However, the highest ^{226}Ra activity in groundwater measured during this study was 703±7% dpm m^{-3} (less than the activity of some Nueces Bay samples). This brackish (S=8.9) groundwater (Table 2.3: W12, Figure 2.2) was collected from a 4 m deep well located only 30 m from the Nueces River. Wells W11, W13, and W14 located in the same area, have similar Ra activities, and are also brackish. If these activities are representative of SGD then a water flux of 311,000±103% m^3 day^{-1} would be required to supply the needed ^{226}Ra. Considering that up to 90% (*Burnett et al.*, 2003) of this SGD flux may be recirculated seawater (RSW), the minimum required terrestrial advecting groundwater (AGW) portion would be 31,100 m^3 day^{-1} or 160% of the mean daily Nueces River discharge during May 2003 (U.S. Geological Survey, 2005). This is high compared to previous estimates of AGW in other regions which are between 0.3% and 16% of river discharge. Further, the combined flow from the known ephemeral subaerial springs in the greater Corpus Christi area is only 1000 m^3 day^{-1} (*Brune*, 1981). Therefore I conclude that either the Ra activity of SGD is higher than any groundwater sampled in this study or SGD can account for only a portion of the observed ^{226}Ra imbalance.

The other potential source of dissolved Ra is oil-field brine leakage. Decades of oil production and the numerous submerged petroleum wells and pipelines in Nueces Bay make this a distinct possibility. The highest dissolved ^{226}Ra activity measured in local produced water samples (n=6) was 34,700 dpm m^{-3} (*Kraemer and Reid*, 1984). Produced water leakage of 6,290 m^3 day^{-1} (32% of the Nueces River discharge) could supply all of the needed ^{226}Ra.

At this stage there is insufficient evidence to definitively conclude that either brackish groundwater discharge or leakage of oil-field brine is occurring or which of these fluxes is more prevalent. However either of these inputs would represent significant salt and nutrient loadings to the bay. This would be especially true during dry periods when river inputs are low, particularly in the case of oil-field brine leakage which would not change seasonally. For groundwater the regional mean nitrate concentration is 1.7 mg L^{-1} N as NO_3^- (*Texas Water Development Board*, 2005a).[1] Assuming that 1) this is representative of brackish groundwater discharge, 2) nitrate is the dominate dissolved inorganic nitrogen species in brackish groundwater discharge, and 3) the submarine Ra input is entirely due to an advecting groundwater discharge of 31,100 m^3 day^{-1}, then the associated nitrogen input would be 19 million g N yr^{-1}. For Gulf of Mexico oil-field brines measured by *Veil et al.* (2005), ammonium is the dominate form of dissolved inorganic nitrogen and the mean concentration is 57.5 mg L^{-1} N as NH_4^+. Assuming 1) this is representative of oil-field brine leakage to Nueces Bay and 2) the submarine Ra input is entirely due to an oil-field brine input of 6,290 m^3 day^{-1} then the associated nitrogen input would be 132 million g N yr^{-1}. These inputs are less than estimates of nitrogen loading to Nueces Bay from wastewater (400-1500 million g N yr^{-1})(*Brock*, 2001) but they are not trivial. Additional work is necessary to fully understand the chemical implications of these potential water fluxes.

2.5 Conclusions

Using the combination of salt, ^{228}Ra, and ^{226}Ra balances provides strong evidence of a large submarine source of dissolved Ra to Nueces Bay. This $218 \times 10^6 \pm 103\%$ dpm day^{-1} supply of ^{226}Ra is 9 times the daily supply from bay bottom sediments and 50 times

[1] Based on 778 NO_3^- measurements made during the period of record from 1931 to 2005 (*Texas Water Development Board*, 2005a). The samples were collected from 308 wells in the following counties: Aransas, Atascosa, Bee, Brooks, Calhoun, De Witt, Duval, Goliad, Jim Wells, Kennedy, Kleberg, Live Oak, McMullen, Nueces, Refugio, San Patricio, and Victoria.

the Ra supplied by the Nueces River. This Ra is most likely being supplied by some combination of SGD and leakage of oil-field brine with a combined water flux greater that may be greater than that of the Nueces River. Additional methods are necessary in order to evaluate and quantify the relative contributions of SGD discharge and oil-field brine leakage. One approach, the subject of Chapter 3, is to conduct high density synoptic surveys of bay bottom sediment resistivity, surface salinity, and Ra isotopes at the head of Nueces Bay where the Ra activities reported in this chapter were generally highest. Another approach, the subject of Chapter 4, is to compare the dissolved Ra inventories of Nueces Bay with those of two neighboring bays that differ in hydrology, industrial activity (including oil and gas production) and land use.

The steady state mixing model approach used in this study, while providing a useful way to make general assessments, also produces large uncertainties due to natural variability, measurement accuracy, and the necessity of making indirect estimates of some processes. In this study the large overall uncertainty is primarily attributable to the fact that the difference between the ebb and flood tide Ra flux is comparable to the absolute uncertainty in these quantities. For bays like Nueces Bay that experience dramatic changes in salinity and in SGD tracers like Ra, the overall uncertainty could be greatly reduced by 1) basing a mass balance on the change of a SGD tracer between the beginning and end of a seasonal flushing event while 2) regularly monitoring the SGD tracer at the tidal inlet. This would increase overall certainty by reducing the uncertainty associated with tidal exchange and include another large but more certain term in the balance: the temporal change of the SGD tracer.

Table 2.1: Nueces Bay temperature, salinity, and dissolved radium activity.

Station	Collected	Temperature* (Celsius)	Salinity*	^{228}Ra	^{226}Ra (dpm m^{-3})	^{228}Ra/^{226}Ra
1	27 Apr 02	26.31	33.67	980±72	280±21	3.49±0.36
2	27 Apr 02	26.04	34.67	1,230±93	335±33	3.67±0.39
3	27 Apr 02	25.59	33.67	1,020±75	286±29	3.58±0.37
4	27 Apr 02	25.96	34.25	1,300±100	329±27	3.95±0.45
5	27 Apr 02	26.40	34.36	1,570±120	452±34	3.47±0.37
6	27 Apr 02	26.25	34.81	1,510±120	435±36	3.47±0.40
7	27 Apr 02	26.06	34.61	1,640±130	450±37	3.64±0.42
8	27 Apr 02	26.66	35.12	1,720±130	455±34	3.78±0.40
9	27 Apr 02	26.89	34.80	1,720±140	458±38	3.76±0.44
10	27 Apr 02	26.86	35.48	1,950±160	583±48	3.33±0.39
11	29 Apr 02	26.67	35.54	1,960±150	509±38	3.85±0.41
12	29 Apr 02	26.02	36.14	1,500±120	501±40	3.00±0.34
13	29 Apr 02	26.66	34.54	1,870±160	488±43	3.83±0.47
14	29 Apr 02	26.88	35.65	1,730±130	456±34	3.78±0.40
15	29 Apr 02	26.82	31.34	1,870±150	529±43	3.53±0.41
16	29 Apr 02	26.86	37.93	2,600±210	665±56	3.91±0.46
17	29 Apr 02	27.10	35.42	1,450±120	401±34	3.61±0.43
18	29 Apr 02	27.09	36.29	1,760±130	456±35	3.85±0.41
19	29 Apr 02	27.12	35.70	2,060±170	491±42	4.19±0.50
4	24 Jul 02	32.49	1.24	244±25	192±16	1.27±0.17
13	24 Jul 02	30.88	0.36	226±20	191±15	1.18±0.14
14	24 Jul 02	31.45	0.59	194±18	182±14	1.07±0.13
15	24 Jul 02	30.48	0.36	241±21	178±14	1.35±0.16
17	24 Jul 02	30.18	0.34	192±22	162±14	1.19±0.17
18	24 Jul 02	29.60	0.42	213±17	190±14	1.12±0.12
19	24 Jul 02	32.56	0.29	219±19	201±16	1.09±0.13
20	24 Jul 02	30.03	0.29	216±17	201±15	1.07±0.12
21	24 Jul 02	31.30	0.33	259±24	191±16	1.35±0.17

* Temperature and salinity were determined using a YSI Model 6000 Sonde except where noted.

Table 2.1: Continued.

Station	Collected	Temperature (Celsius)	Salinity	^{228}Ra (dpm m^{-3})	^{226}Ra	^{228}Ra/^{226}Ra
1	25 Jul 02	29.53	0.36	201±17	174±13	1.15±0.13
2	25 Jul 02	29.59	0.40	150±15	138±11	1.09±0.14
3	25 Jul 02	30.04	0.56	221±21	185±15	1.20±0.15
5	25 Jul 02	29.83	0.90	318±31	247±20	1.29±0.17
6	25 Jul 02	30.19	0.40	235±20	194±15	1.21±0.14
7	25 Jul 02	31.77	1.25	221±21	169±14	1.31±0.16
8	25 Jul 02	31.08	0.32	188±20	158±14	1.18±0.16
9	25 Jul 02	31.51	0.60	195±22	184±16	1.06±0.15
10	25 Jul 02	31.65	0.90	271±24	206±16	1.32±0.16
11	25 Jul 02	30.72	0.35	204±19	182±15	1.12±0.14
12	25 Jul 02	31.43	1.60	235±20	186±15	1.27±0.15
1	19 May 03	29.08†	27.070†	1,030±76	366±27	2.81±0.29
4	19 May 03	30.31†	20.998†	1,320±110	497±39	2.65±0.30
8	19 May 03	28.64†	25.858†	1,210±92	498±37	2.43±0.26
9	19 May 03	31.11†	21.183†	1,290±100	486±37	2.65±0.29
10	19 May 03	29.66†	20.910†	1,270±100	541±40	2.34±0.25
13	19 May 03	30.37†	19.878†	1,520±110	700±52	2.17±0.23
16	19 May 03	28.74†	25.754†	2,230±180	1,000±78	2.23±0.25
17	19 May 03	29.99†	22.855†	1,820±140	855±63	2.13±0.22
18	19 May 03	29.20†	25.610†	1,590±130	821±62	1.94±0.21
21	19 May 03	29.47†	24.600†	1,720±130	830±61	2.07±0.22
1	27 May 03	-	27.847‡	975±75	312±24	3.12±0.34
4	27 May 03	-	27.869‡	1,130±90	381±29	2.97±0.32
8	27 May 03	-	27.849‡	1,460±110	610±46	2.39±0.26
9	27 May 03	-	27.868‡	1,390±100	520±38	2.67±0.28
10	27 May 03	-	27.831‡	1,400±110	592±44	2.37±0.25
13	27 May 03	-	27.852‡	1,580±120	696±53	2.27±0.25
16	27 May 03	-	27.859‡	1,950±150	831±62	2.34±0.25
17	27 May 03	-	27.871‡	2,000±150	870±62	2.31±0.24
18	27 May 03	-	27.851‡	2,180±160	964±70	2.26±0.23
21	27 May 03	-	27.836‡	1,990±150	915±67	2.18±0.23

† Temperature and salinity determined by a SeaBird Electronics SeaCat CTD profiler.

‡ Salinity determined by a Guildline Autosal salinometer.

Table 2.2: Salinity and radium activities in the Nueces River and river plume.

Sample	Collected	Salinity*	^{228}Ra	^{226}Ra	^{228}Ra/^{226}Ra
			(dpm m^{-3})		
1	12 Dec 03	0.7†	187±16	117±9	1.60±0.19
2	12 Dec 03	0.7†	148±12	137±10	1.08±0.12
3	12 Dec 03	0.7†	165±14	107±8	1.54±0.17
4	9 Apr 04	0.30	231±18	177±13	1.31±0.14
5	9 Apr 04	1.02	291±22	176±13	1.65±0.18
5-5μm ††	9 Apr 04	1.02	62±7	52±4	1.2±0.2
5-1μm ††	9 Apr 04	1.02	22±5	18±2	1.2±0.2
6	9 Apr 04	2.16	357±27	220±16	1.62±0.17
7	16 Apr 04	3.28	387±29	199±15	1.94±0.21
8	16 Apr 04	4.42	396±30	206±15	1.93±0.20
9	9 Apr 04	6.70	655±49	337±25	1.94±0.20
10	16 Apr 04	8.63	546±41	257±19	2.12±0.22
11	9 Apr 04	10.22	834±62	388±28	2.15±0.22
12	16 Apr 04	12.76	648±48	252±19	2.57±0.27

* Salinity was determined using a YSI Model 6000 Sonde.

† Salinity recorded at TCOON station SALT05.

†† Activity of suspended particulate material filtered from sample expressed as dpm m^{-3}.

Table 2.3: Dissolved radium activity in regional groundwater.

Sample	Collected	Salinity*	^{228}Ra	^{226}Ra	^{228}Ra/^{226}Ra
			(dpm m^{-3})		
W1	3 June 03	$<$3	220$\pm$20	150$\pm$10	1.47$\pm$0.17
W2	3 June 03	$<$3	143$\pm$10	96$\pm$10	1.50$\pm$0.19
W3	3 Jun 03	$<$3	576$\pm$40	446$\pm$30	1.29$\pm$0.14
W4	9 Oct 02	$<$3	518$\pm$41	139$\pm$11	3.72$\pm$0.41
W5	9 Oct 02	$<$3	389$\pm$30	290$\pm$20	1.34$\pm$0.15
W6	9 Oct 02	$<$3	335$\pm$30	290$\pm$22	1.16$\pm$0.12
W7	9 Oct 02	$<$3	135$\pm$10	288$\pm$20	0.47$\pm$0.06
W8	15 May 03	$<$3	172$\pm$10	182$\pm$10	0.95$\pm$0.10
W9	15 May 03	$<$3	74$\pm$10	85$\pm$10	0.87$\pm$0.11
W10	16 May 03	$<$3	135$\pm$10	185$\pm$10	0.73$\pm$0.08
W11	28 April 05	3.7	1070$\pm$81	311$\pm$23	3.45$\pm$0.37
W12	28 April 05	3.2	2920$\pm$213	703$\pm$51	4.16$\pm$0.43
W13	28 April 05	8.0	1690$\pm$124	334$\pm$25	5.06$\pm$0.53
W14	28 April 05	8.9	2190$\pm$168	515$\pm$40	4.25$\pm$0.46

* Samples 1-10 were from wells used for irrigation or livestock and salinities are assumed to be $<$3. Samples 11-14 were from monitoring wells and salinity was determined using a YSI Model 30 Sonde.

Table 2.4: September 2002 Gulf of Mexico transect of surface water dissolved radium activity.

	Latitude	Longitude	Distance Offshore (km)	$^{228}\mathrm{Ra}$ (dpm m^{-3})	$^{226}\mathrm{Ra}$ (dpm m^{-3})	$^{228}\mathrm{Ra}/^{226}\mathrm{Ra}$
1	27° 43N	97° 5W	6	491±41	166±13	2.95±0.33
2	27° 39N	96° 60W	17	438±36	152±12	2.87±0.32
3	27° 36N	96° 54W	28	475±39	169±13	2.81±0.31
4	27° 29N	96° 43W	49	286±22	118±9	2.42±0.26
5	27° 18N	96° 35W	160	71±7	59±5	1.19±0.16

Table 2.5: Uncertainty estimates for parameters used in water, salt, and Ra balances.

Variable	Uncertainty	Basis for Uncertainty Estimate
A	5%	Bay Area: We estimate that 5% of the total 75 km^2 open bay area is intertidal based on the mean tidal range of 15 cm and the extent of bay shallows.
D	10%	Bay Depth: Based on our judgment of the accuracy of bay bathymetry and mean bay depth. In comparison, the uncertainty of the waterlevel guage heights is considered negligible.
V, FT, ET	11%	Bay and Tidal Volumes: The result of the bay area and depth uncertainties.
R	5%	River Discharge: Based on the estimated accuracy of stream guaging (*Sauer and Meyer*, 1992).
$\bar{s}_{ET}$	17 to 95%*	Ebb Tide Salt Concentration: Based on 1 standard deviation of the salinity measurements taken during each Nueces Bay sampling period. Natural variability changed with salinity level; high variability (67%) at low salinities and lower variability (12%) at higher salinities. This variability trend was used to estimate the uncertainties in the time series salinity observations from the TCOON SALT05 salinity recorder which were used to estimate Nueces Bay mean salinity.
$\bar{s}_{FT}$	28%*	Flood Tide Salt Concentration: We estimate a 20% uncertainty associated with representing Nueces Bay flood tide salinities using only the UTMSI salinity recorder in Aransas Pass.
$\bar{s}_{R}$	28%*	River Salt Concentration: We estimate a 20% uncertainty associated with representing Nueces River salinities with the one salinity recorder at TCOON station SALT 05.
Ra_R	^{228}Ra: 15% ^{226}Ra: 13%	River Ra Activity: The combination of one standard deviation of the dissolved July 2002 flood water samples and an uncertainty estimate of 50% for the desorbable Ra associated with riverine particulate material.
Ra_{FT}	^{228}Ra: 3% ^{226}Ra: 8%	Flood Tide Ra Activity: Half the range between the two 19 and 27 May 2003 station 1 samples.
Ra_{ET}	^{228}Ra: 24% ^{226}Ra: 32%	Ebb Tide Ra Activity: One standard deviation of the combined 19 and 27 May 2003 samples.

* The uncertainties in all salt concentrations are the result of carrying the uncertainties in salinity through the equation for the density of seawater (*Millero and Poisson*, 1981). Neglecting higher order terms and the effects of temperature, the relative uncertainty in density is the same as that of salinity and from Equation 2.4 the relative uncertainty in salt concentration is the relative uncertainty in salinity times $\sqrt{2}$.

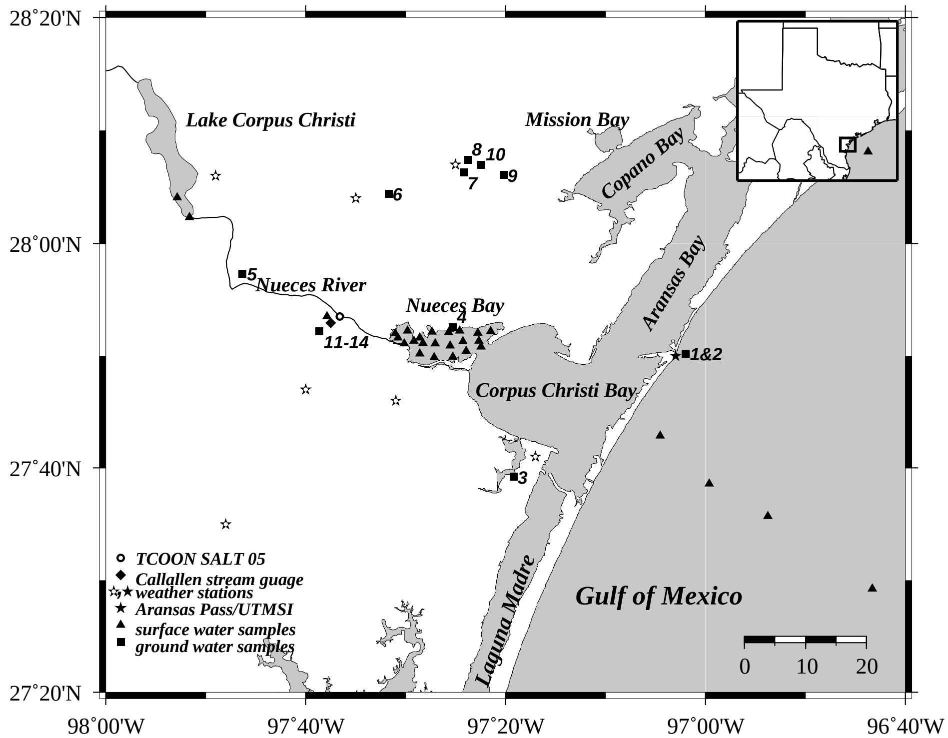

Figure 2.1: The Coastal Bend region of Texas indicating the locations of Nueces Bay, the Aransas Pass connection to the Gulf of Mexico labeled (solid star), and the final Nueces River impoundment at Lake Corpus Christi. Samples collected for this study are indicated by solid squares for well samples and solid triangles for surface water samples; the farthest offshore surface water sample (27° 18’ 11.5” N, 95° 34’ 44.4” W) is shown on the inset map. Well samples are numbered as in Table 2.3. National Weather Service affiliated stations used to determine net precipitation are indicated by hollow stars. The Nueces River stream gauge at Callallen is indicated by a solid diamond.

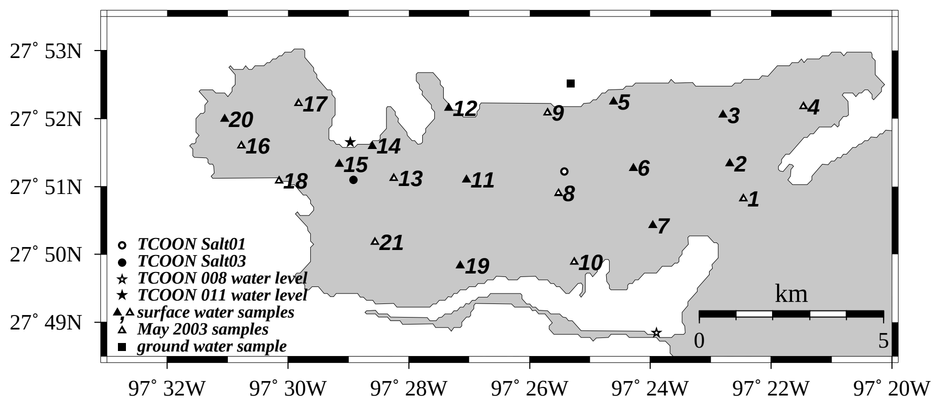

Figure 2.2: Details of station locations in Nueces Bay. Triangles indicate surface water samples. Only 10 of the April and July 2002 stations were reoccupied during the two May 2003 surveys; these 10 stations are indicated by hollow triangles. The one well sample in this immediate area (Table 2.3)) is indicated by a solid square. TCOON salinity recorders are indicated by circles. TCOON water level recorders are stars.

Figure 2.3: The author sampling from a well used for cattle watering.

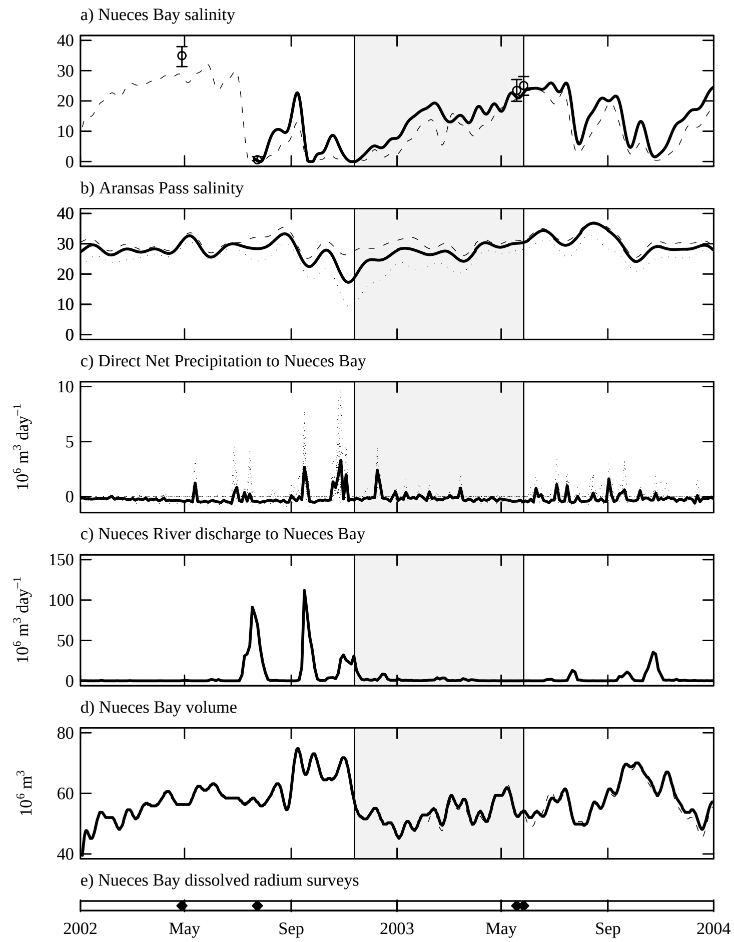

Figure 2.4: Time series data for Nueces Bay covering the sampling periods. Data shown as solid lines are used to determine fluxes for the recovery period from November 2002 flooding (period indicated with gray shading). Supporting data are shown as dotted or dashed lines. For a) Nueces Bay salinity the solid line is TCOON station Salt01, the dashed line is TCOON Salt03, and the circles with whiskers represent the mean and range of the salinities measured during the Ra surveys; for b) Aransas Pass salinity the dashed line is daily maximum, the dotted line is daily minimum, and the solid line is daily mean; for c) direct net precipitation, the dotted lines are precipitation and evaporation from area weather stations and the solid line is the spatial mean; for d) Nueces River discharge the solid line is daily volumetric discharge; for e) Nueces Bay volume the solid line is bay volume based on water height at TCOON station 008 and the dashed line from TCOON station 011; and for f) Nueces Bay Ra survey dates are diamonds.

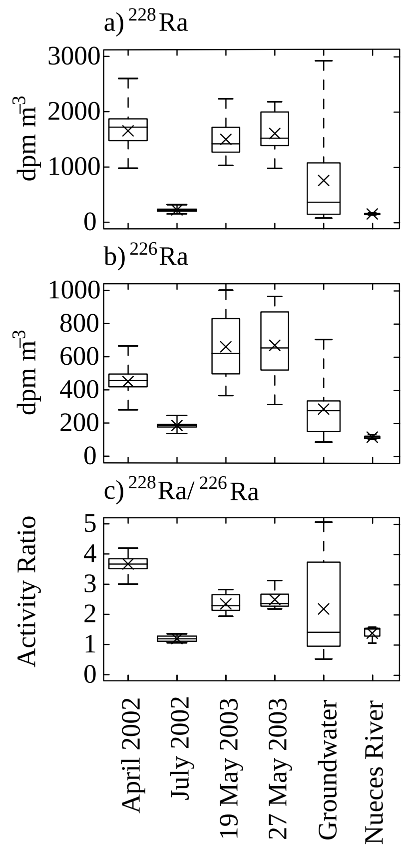

Figure 2.5: Dissolved activity of a) $^{228}\mathrm{Ra}$, b) $^{226}\mathrm{Ra}$, and c) the activity ratio of $^{228}\mathrm{Ra}/^{226}\mathrm{Ra}$ of Nueces Bay and associated waters summarized in box plots where box width is proportional to the square root of sample size, box height encompasses the 25th and 75th quantiles, the horizontal line is the median, the x symbol is the mean, and the whiskers extend to the extreme values. Nueces Bay Ra activities are generally quite high with the exception of the July 2002 period when the bay was completely flushed and mean salinity was 0.3. Nueces Bay Ra activities during April 2002 and both May 2003 periods were greater than the activities in all other waters sampled within the region, including groundwater.

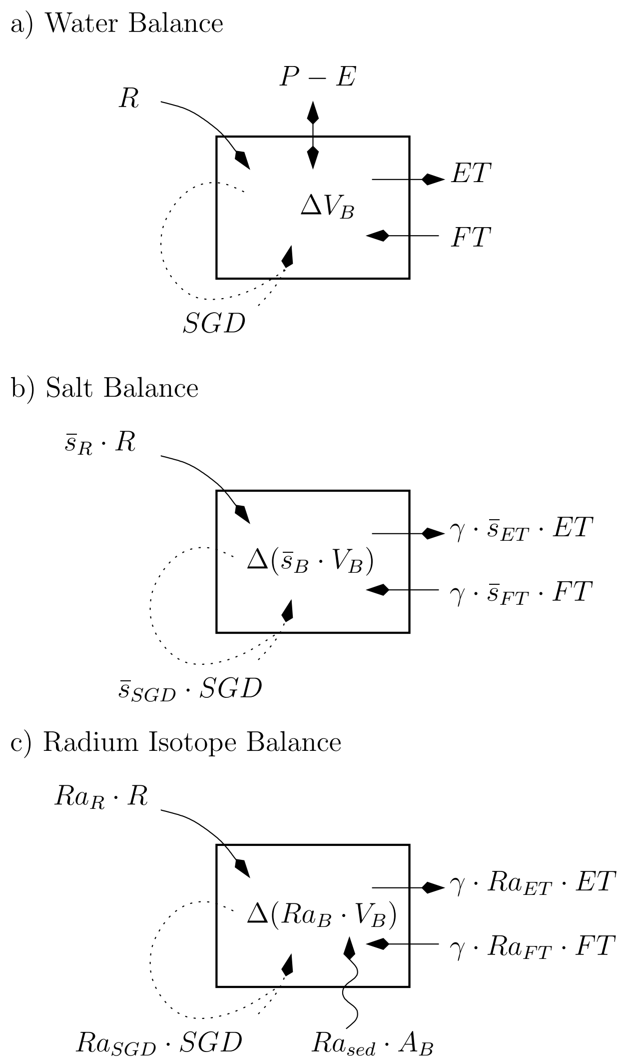

Figure 2.6: Schematic of mass balance model used in analysis (Equations 2.2, 2.3, and 2.5). Bay volume a) is a function of river discharge (R), net precipitation ($P - E$), ebb tide (ET), flood tide (FT), and potentially submarine fluid discharges (SGD) such as SGD and oil-field brine leakage. For b) the bay dissolved salt concentration, net precipitation is assumed to be a negligible direct flux of salt to the bay though it does affect the salt concentration indirectly by influencing the bay water balance. For c) the bay dissolved Ra activity, net precipitation is similarly assumed to be a negligible direct flux of Ra while diffusion of Ra from sediment porewater (Ra_{sed}) is an additional input. SGD represents the unknown but suspected fluxes of salt and Ra from submarine fluid discharges.

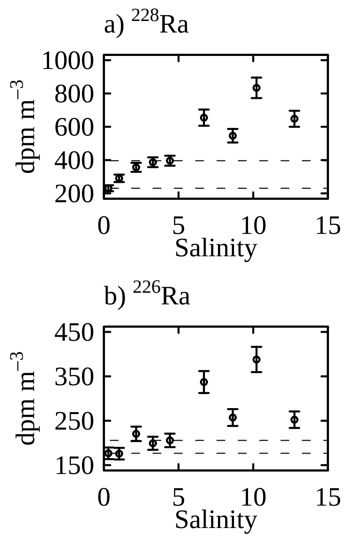

Figure 2.7: Dissolved a) $^{228}\mathrm{Ra}$ and b) $^{226}\mathrm{Ra}$ activity of the Nueces River plume as it entered Nueces Bay in May 2004. The nonlinear increase in $^{228}\mathrm{Ra}$ activity below a salinity of 5 suggests particle desorption as described by *Krest et al.* (1999). If entirely attributable to particle desorption the contribution would be 170 dpm m^{-3}, the increase in activity between the dashed horizontal lines. The increase in $^{226}\mathrm{Ra}$ does not indicate such a well defined contribution from particle desorption but if desorption is similar to that of $^{228}\mathrm{Ra}$ then the contribution would be 30 dpm m^{-3}.

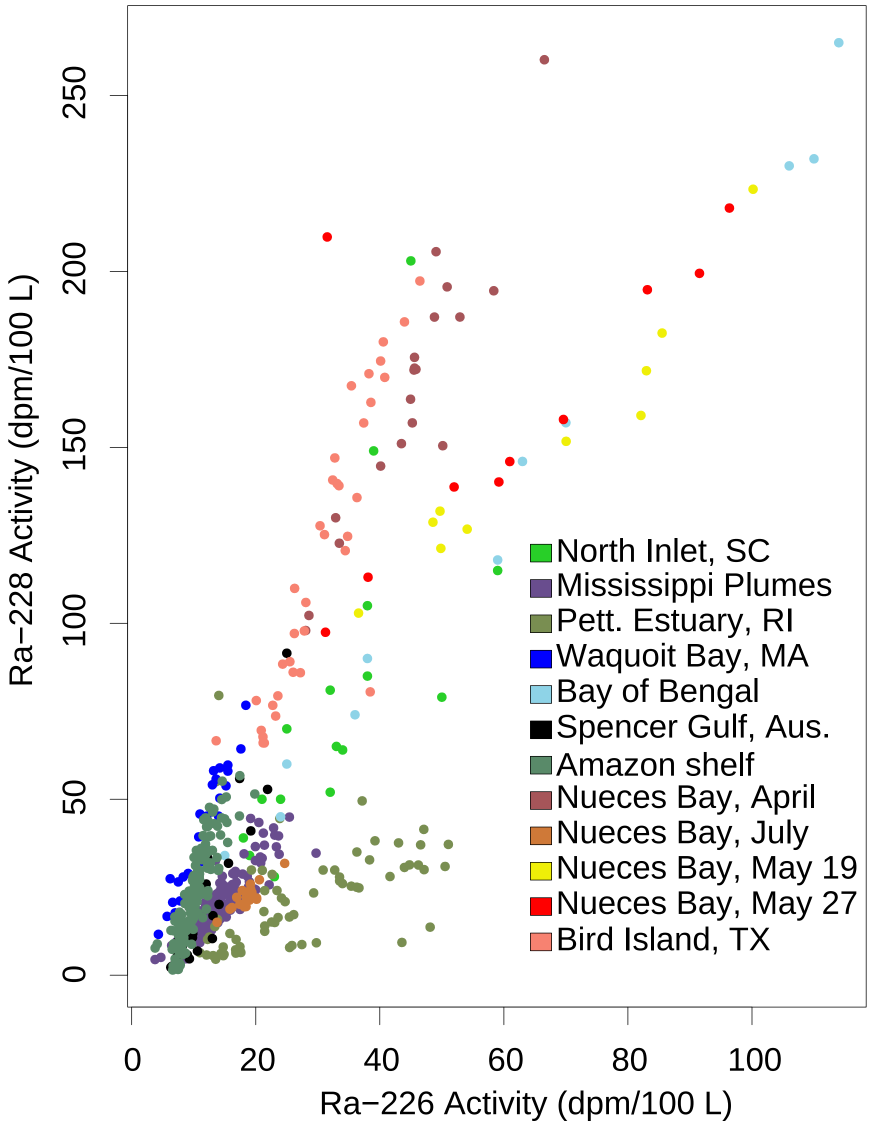

Figure 2.8: Measured ^{226}Ra and ^{228}Ra activities compared to literature values. The maximum observed ^{226}Ra activity in Nueces Bay was 1000±78 dpm m^{-3}, similar to the Bay of Bengal maximum ^{226}Ra activity of 1140 dpm m^{-3} (*Moore*, 1997). In other coastal waters observed ^{226}Ra activities have been <600 dpm m^{-3} (e.g., Spencer Gulf Australia; the waters of Amazon shelf; North Inlet, South Carolina; Waquoit Bay, Massachusetts; and Pettaquamscutt River estuary, Rhode Island) (*Charette et al.*, 2001; *Kelly and Moran*, 2002; *Moore et al.*, 1995; *Rama and Moore*, 1996; *Veeh et al.*, 1995).

Chapter 3

Detecting submarine groundwater discharge using radium isotopes and continuous electrical resistivity profiling

3.1 Abstract

A synoptic geophysical and geochemical survey was used to investigate the occurrence and spatial distribution of submarine water discharges to upper Nueces Bay, Texas. [1] The survey was conducted in the 9.2 km^2 head of Nueces Bay where a previous Ra mass balance suggested a significant submarine groundwater discharge. The 17 kilometer survey incorporated continuous resistivity profiling; measurements of surface water salinity,

[1] This chapter was published in a slightly modified version as *Breier et al.* (2005) and is reproduced by permission of the American Geophysical Union. 0094-8276/05/2005GL024639$05.00

temperature, and dissolved oxygen; and point measurements of dissolved $^{226}\mathrm{Ra}$, $^{228}\mathrm{Ra}$, $^{224}\mathrm{Ra}$, and $^{223}\mathrm{Ra}$. The survey revealed areas of interleaving, vertical fingers of high and low conductivity extending up through 7 meters of bay bottom sediments into the surface water, located within 100 m of surface salinity and dissolved Ra maxima ($^{226}\mathrm{Ra} > 600$ dpm m^{-3}). At these locations there were also peaks in water temperature and lows in dissolved oxygen. These results indicate either brackish submarine groundwater discharge or the leakage of oil-field brine from submerged petroleum pipelines; the latter is supported by the proximity of the water chemistry perturbations to known hydrocarbon pipelines. The presence of localized high Ra submarine inputs in this area of Nueces Bay is consistent with previous dissolved Ra surveys which indicated that this area has consistently higher dissolved Ra activities. This study demonstrates the utility of sediment resistivity profiling as part of a comprehensive characterization of submarine discharge using a sequence of 1) large scale chemical tracer assessments, 2) detailed synoptic surveys including resistivity profiling, and ultimately 3) targeted water chemistry samples and direct physical measurements.

3.2 Introduction

Submarine discharges have been detected directly and indirectly in numerous areas using seepage meters and surface water enrichments in tracers such as dissolved Ra, Rn, and $\mathrm{CH_4}$ (e.g., *Burnett et al.*, 2001; *Charette et al.*, 2003). In some cases these submarine discharges clearly consist of advected groundwater (e.g., *Swarzenski et al.*, 2001); however, in many cases the nature of the discharge is difficult to determine and may be the result of several different processes such as: groundwater advection, seawater recirculation, density driven convection of hypersaline salt marsh water, the release of sediment porewater due to sediment compaction or resuspension, or leakage of oil-field brines from submerged petroleum pipelines (*Krest et al.*, 1999; *Rama and Moore*, 1996; *Simmons et al.*, 1991). These sources differ in their chemical composition and resulting impact on coastal systems. Therefore a complete understanding of the implication of submarine water discharge requires that we treat these sources separately and identify and quantify their individual contributions.

Locating and determining the source of a suspected submarine discharge is difficult because there is significant spatial and temporal variability in the flux (*Burnett et al.*, 2003). No single method currently used to measure submarine discharge sufficiently describes any particular system because they do not relate estimates at large and small scales (i.e., total discharge to an area vs. discharge at a point location). While natural chemical tracers (e.g., Ra, Rn, and CH_4) are useful at estimating total discharge to a large area (i.e., a bay), they cannot be used to pinpoint the source of discharge because water column mixing weakens and spatially integrates the signal. Conversely, while direct spot measurement with seepage meters can be used to measure discharge at any single point, and characterize that discharge chemically, they are poor at characterizing large areas because they do not accurately reflect spatial variation in the system and can miss significant localized discharges altogether. Additional techniques that can provide more detailed spatial and temporal data are needed to complement tracer and seepage meter measurements.

Sediment resistivity profiling is a technique commonly used by geologists and can be used to obtain information on the vertical distribution of bay bottom sediment that porewater conductivity (*Jones*, 1991; *Sharma*, 1976). Sediment resistivity profiling can delineate transitions between sediment facies as well as salinity gradients within bay bottom sediments. This type of spatially detailed information can contribute significantly to the comprehensive characterization of submarine discharges. The application of sediment resistivity measurements to investigating submarine groundwater discharge is relatively new.

Stieglitz (2005) used a push-point electrode to delineate changes in surface sediment conductivity through areas of suspected groundwater discharge. *Bratton et al.* (2004) used continuous resistivity profiling and dissolved Rn measurements to locate areas of apparent groundwater discharge within the Upper Neuse River Estuary, North Carolina. In August 2004, this study of Nueces Bay was conducted using continuous resistivity profiling and synoptic sampling of dissolved Ra isotopes, salinity, water temperature, and dissolved O_2.

The goals of this study were to 1) further develop the application of continuous resistivity profiling and synoptic geochemical measurements for submarine discharge studies and 2) apply it to this continuing investigation of submarine discharge to Nueces Bay, Texas. The previous surveys of dissolved Ra in Nueces Bay revealed generally high dissolved Ra activities particularly at the head of the bay (Chapter 2). A Ra mixing model for Nueces Bay indicated a submarine water discharge similar in magnitude to the Nueces River discharge (Chapter 2); this discharge is larger than expected given the arid conditions, low hydraulic gradient, and small tidal range. Therefore, I hypothesized that density driven convection (*Simmons et al.*, 1991) of hypersaline water in the salt marsh might also contribute to the submarine discharge. The leakage of oil-field brine (formation water) coproduced from submerged petroleum wells and pipelines is also a distinct possibility (Chapter 2). Convection or upwelling of hypersaline water in sediments along the marsh or leakage of oil-field brine would be seen as vertical fingers of higher conductivity on a conductivity profile (an inverted resistivity profile) and should be coincident with high salinity and dissolved Ra in the overlying surface waters.

3.3 Methods

3.3.1 Study Area

Nueces Bay is a secondary bay of the Corpus Christi Bay system of Texas, with an area of 75 km^2, a mean depth of 0.7 meters, and a mean tidal range of 15 cm. At its western end, the Nueces River delta comprises a low, 60 km^2 area of salt marshes, mudflats, and shallow water (Figure 3.1).

A bluff along the bay's north shore, including the White's Point peninsula, rises 10 m above the salt marsh and river valley. Except for several man-made diversions into the marsh, much of the Nueces River currently bypasses the Nueces delta and discharges directly into Nueces Bay. The Nueces River outlet on the south shore and White's Point peninsula on the north shore define a sheltered portion of the bay adjacent to the delta that will be referred to as the head of Nueces Bay. This portion of the bay was selected for resistivity profiling because of the high dissolved Ra activities found during four previous Ra surveys of Nueces Bay (Chapter 2, *Breier and Edmonds*, submitted). Nueces Bay experiences dramatic annual swings in salinity driven by high annual evaporation rates and periods of intense precipitation during the late summer and fall. Hypersaline conditions in the summer are common, particularly in the salt marsh at the head of Nueces Bay where sediment porewater salinities are typically between 35 and 80 and can reach as high as 320 (*Dunton et al.*, 2004). Nueces Bay salinity typically ranges between 15 and 30 however this survey followed recent rain storms and the salinity at the head of the bay was 2 to 7.

3.3.2 Continuous Resistivity Profiling

Continuous resistivity profiling is a controlled source electromagnetic technique for measuring the vertical and horizontal distribution of electrical resistivity in submarine sediments (*Jones*, 1991). Sediment resistivity is a function of sediment type, porosity, porewater salinity, and temperature. Using a dipole-dipole electrical array, the bulk resistivity of sediments can be measured by creating an electric current with one dipole electrode pair and measuring the potential field at another dipole electrode pair. Since the induced current creates a curved potential field a surface electrode array can measure the bulk resistivity of subsurface formations to a depth proportional to the spacing between the dipoles. Progressively increasing the dipole spacing increases the measurement depth. Additional measurements that include new and previously surveyed material are made by moving the electrode array laterally along the survey line. In practice, dipole spacing is varied by alternating between different electrode pairs and in the case of marine studies surveying can be done continuously by towing the electrode array behind a boat. The actual resistivity at a specific depth and location is estimated from the collection of bulk resistivity estimates using an inverse modelling algorithm similar to that used in seismic profiling.

The study area was surveyed on 14 August 2004 using an AGI Marine Supersting R8-IP resistivity meter with a towed array of 8 electrodes. The survey (Figure 3.1) focused on the shoreline looking for evidence of density driven circulation. The river mouth and channel were also carefully surveyed looking for changes in sediment structure associated with the river. Two east-west transects were made for contrast and completeness but proved interesting in their own right. During the survey boat speed was kept below 4 km hr^{-1} to maintain electrode contact with the water.

A Lowrance GPS and sonar were connected to the resistivity controller so that position and water depth could be recorded along with the apparent resistivity measured at the electrodes. Data were postprocessed with an inverse modelling algorithm developed by AGI to estimate the resistivity. Resistivity results are reported as their inverse, conductivity (mS cm^{-1}), to facilitate comparison with surface water salinity.

3.3.3 Dissolved $^{226}\mathrm{Ra}$, $^{228}\mathrm{Ra}$, $^{224}\mathrm{Ra}$, and $^{223}\mathrm{Ra}$

$^{226}\mathrm{Ra}$, $^{228}\mathrm{Ra}$, $^{224}\mathrm{Ra}$, and $^{223}\mathrm{Ra}$ are members of the three naturally occurring radioactive decay series and are each the product of Th decay. Ra is more soluble than Th particularly as salinity increases. Therefore in saturated, brackish sediments such as coastal aquifers and bay bottom deposits the Ra produced from sediment-bound Th partitions into the porewater. This makes Ra a natural tracer of groundwater discharge to the coastal ocean (*Rama and Moore*, 1996). In addition, Ra isotopes range in half-life from 3.8 days to 1600 years and are thus responsive to processes occurring at a variety of rates and time scales (*Moore*, 2000; *Moore and Arnold*, 1996).

In this study surface water samples (25 L) for dissolved Ra analysis (n=28) were collected from approximately 30 cm below the surface while the boat was moving using a sampling loop continuously pumped at 2 L min^{-1}. Samples were filtered in the laboratory through a 1 $\mu\mathrm{m}$ polypropylene cartridge filter and the Ra extracted onto a subsequent column of MnO_2-impregnated acrylic fiber at a flow rate of less than 1 L min^{-1}. Short lived $^{224}\mathrm{Ra}$ and $^{223}\mathrm{Ra}$ were measured using the delayed coincidence counting method developed by *Moore and Arnold* (1996). Long lived $^{226}\mathrm{Ra}$ and $^{228}\mathrm{Ra}$ were then measured on a high purity germanium well gamma detector following the procedure outlined by *Rutgers van der Loeff and Moore* (1999).

3.3.4 Surface Water Parameters and Survey Groundtruthing

Surface water salinity, temperature, and dissolved O_2 were recorded with a YSI Model 6000 sonde. The sonde was set in a flow cell in the surface water sampling loop. Measurements were logged at 2 second intervals and synchronized with resistivity logging.

In April 2005 after the initial survey results were complete, a groundtruthing survey was conducted to qualitatively classify the surficial bay bottom sediments along the original survey line. At each Ra sample location a 60 cm long, 7 cm diameter sediment core was collected and used to visually classify bottom sediments by silt, clay, and sand fraction. Sediments were visually classified based on the presence and distribution of sand and shell and the extent that the extruded cores held their shape. The location of submerged oyster reefs, pipeline markers, and emergent petroleum well heads near the survey path were also noted.

3.4 Results and Discussion

The survey covered 17 km within the 9.2 km^2 head of Nueces Bay. The entire sediment conductivity profile, with details of notable sections, is shown in Figure 3.3. Care must be taken not to overinterpret features in the profile because conductivity varies in response to several factors (temperature, sediment type, porewater salinity, and porosity) and because the inversion algorithm can produce false conductivity features from incorrect depth soundings. Instead I have focused on the overall conductivity structure and on features that correlate with surface water data. Most of the survey profile consists of evenly stratified layers of lower conductivity surface waters and higher conductivity sediments (Figure 3.3a, b). This is consistent with low salinity surface waters overlying mud and clay sediments containing higher salinity porewater. In addition there is an area of low sediment conductivity (Figure 3.3c) in the center of the bay between km 8.5 and 11 (Figure 3.1 Area I). There is also an area of high sediment conductivity (Figure 3.3d) between km 13.5 and 14.7 that contains features that are probably buried petroleum pipeline cross-sections (Figure 3.1 Area II). The Nueces River channel cross section is also clearly visible near km 14.9 (Figure 3.3d). The interleaving low and high conductivity fingers in Area I at km 8.4, 8.8, 9.4, and 9.6 (Figure 3.3c) are suggestive of brackish water plumes discharging to the bay and appear to correspond with features in the surface water data. Similar features elsewhere in the conductivity profile (Figure 3.3b) do not correlate with the surface water data and therefore are not discussed further as explained above.

These higher conductivity fingers are the most interesting features of the survey and appear to correspond with features in the surface water data. The conductivity fingers in Area I at km 8.4 and 8.8 extend from the bottom of the profile (7.5 m total depth) to the surface water and are within 100 m of the two surface salinity maxima (S$>$7) at km 8.5 and 8.9 (Figures 3.1, 3.3c, and 3.4b). At these locations there are also peaks in surface water temperature and drops in dissolved O_2 (Figure 3.4). In addition, of the 28 Ra samples collected, sample 12 taken between these conductivity fingers had the highest dissolved Ra activity (e.g., $^{226}Ra > 600$ dpm m^{-3}) for all four isotopes (Figure 2.5 and Table 3.1). Such high spatial correlation between sediment conductivity and surface water chemistry suggests a submarine discharge in this area. Increased dissolved Ra and salinity (S$>$5) along with decreased dissolved O_2 also occur from km 13.5 to 14.7 in Area II which contains the petroleum pipelines (Figure 3.3d, 3.4, and 2.5).

It initially seems surprising that the strongest submarine discharge indications occurred in Area I as opposed to closer to the shoreline. Simple models based on the Ghyben-Herzberg relation predict that submarine groundwater discharge should be greatest at the shoreline where the hydraulic gradient is highest (*Schwartz and Zhang*, 2003). However, simple models and generalizations neglect the actual complexity of coastal sediments (*Moore*, 1999). In this case, sediment groundtruthing revealed an area in the center of the bay where surficial bay bottom sediments had a much higher sand fraction than the bay margins (Table 3.2 and Figure 3.1). This area corresponds with the area of low sediment conductivity between km 8.5 and 11, suggesting that the sandy sediments in this part of the bay are at least several meters deep. The sediments around the Nueces River mouth are also very sandy as are sediments along a portion of the shoreline north of White's Point.

In contrast, the bay bottom sediments in the rest of the study area consist of silt, mud, and clay with presumably low permeability. Therefore preferential groundwater discharge to the center of the bay vice the margins may be consistent with the actual distribution of bay bottom sediments. However limited and unsuccessful attempts to use seepage meters and porewater samplers in the center of the bay showed that some of these visually sandier sediments were also very low in permeability.

The strong spatial correlation between sediment conductivity features and trends in surface water chemistry in Areas I and II are potentially due to one or a combination of the following: 1) tidal mixing of fresh and saline surface water, 2) brackish groundwater discharge, or 3) leakage of produced water from buried petroleum pipelines and wells. The known presence of pipelines in Area II is suggestive of this as the source of the features observed in this area. While the data in Area I are suggestive of brackish groundwater discharge it is not conclusive. Additional data such as seepage meter measurements or a time series of sediment resistivity and surface water chemistry measurements are necessary to determine whether the surface water features and conductivity fingers are directly related. Leakage of produced water from petroleum pipelines and wells in Area I is also possible. Pipeline or well leakage could release high salinity brine as well as petroleum into the sediments or directly into the bay. Such a brine would likely have all the characteristics seen in the surface water between km 8.4 and 8.9: high salinity, high dissolved Ra, elevated temperature, and low dissolved O_2. Additional data such as the presence of hydrocarbons or low Br/Cl ratios (*Davis et al.*, 1998) are needed to conclude that pipeline or well leakage is occurring. Finally although little evidence of density driven convection was found at the shoreline of the salt marsh, the channels and bayous of the marsh were not surveyed, thus convection from the marsh cannot be eliminated as a discharge source.

3.5 Conclusions

Synoptic surveying of sediment conductivity and surface water chemistry have provided a more complete understanding of submarine discharges to Nueces Bay and identified specific locations for further research. The results suggest that within the head of Nueces Bay groundwater discharge and/or produced water leakage occurs largely in one, possibly two, relatively localized areas. Future studies of Nueces Bay should focus on these areas looking for chemical evidence of produced water leakage from petroleum pipelines and direct physical measurements of seepage.

Sediment resistivity profiling is a powerful technique that can provide valuable data to more comprehensively characterize submarine discharges. Sediment resistivity measurements can link large and small scale studies when used in a sequence of 1) large scale tracer assessments, 2) detailed synoptic surveys including resistivity profiling, and 3) targeted water chemistry samples and direct physical measurements. In this study resistivity provided unique data that complemented dissolved Ra and surface water measurements. Further improvements in resistivity data can be achieved in the future by employing more accurate methods for measuring bathymetry.

Table 3.1: Upper Nueces Bay synoptic survey Ra activities.

Sample	^{226}Ra	^{228}Ra	^{224}Ra	^{223}Ra
		(dpm m^{-3})		
1	424±33	642±53	455±50	36.1±5.1
2	420±33	570±54	185±27	6.5±1.1
3	443±34	734±61	512±92	41.2±6.4
4	477±38	707±64	832±140	44.9±5.6
5	475±39	713±55	1147±380	16.2±2.5
6	466±35	732±59	501±73	23.1±3.3
7	543±41	882±69	915±192	39.5±5.7
8	470±37	774±68	122±27	4.3±0.9
9	462±36	718±60	1058±265	36.3±5.0
10	626±49	901±79	220±40	6.2±1.0
11	530±42	863±75	93±18	6.8±1.2
12	633±49	1054±90	1302±372	51.3±7.4
13	537±42	757±66	500±82	43.4±6.7
14	545±42	696±59	584±120	40.7±6.9
15	481±38	599±57	472±137	34.5±5.8
16	461±37	710±65	174±66	7.4±1.3
17	405±33	618±57	782±206	37.4±6.4
18	476±38	682±61	493±113	35.4±6.3
19	492±38	726±60	537±93	38.5±6.6
20	567±45	948±83	470±97	28.2±4.6
21	580±44	1020±81	679±179	40.6±7.4
22	631±49	918±79	616±258	30.8±4.8
23	538±41	817±66	371±88	27.4±3.5
24	447±36	673±60	63±21	2.4±0.6
25	448±34	764±62	611±264	30.5±5.4
26	532±41	801±66	122±28	5.7±1.2
27	454±36	754±67	91±22	5.2±1.1
28	431±34	896±72	384±108	16.2±3.0

Table 3.2: Upper Nueces Bay Sediment Survey.

Station	Sediment Type[†]	Comments
1	mud	Buried pipeline sign.
2	mud	Contained some shells.
3	mud	
4	clay/mud	Mostly clay.
5	clay/mud	Contained some shells.
6	mud	
7	mud	
8	clay/mud	
9	mud	
10	clay/mud/sand	
11	mud	
12	sand/mud/shells	
13	sand/mud/shells	
14	sand/mud/shells	
15	sand/mud/shells	Progressively more mud below 5 cm.
16	mud/sand	
17	mud	
18	mud/shells	Shells on surface.
19	oyster reef	
20	mud	
21	clay/mud	Some sand and shell at surface.
22	mud	Buried pipeline sign.
23	sand/mud	Layered surface of sand/mud, 20 cm down is sand, 40 cm down is mud.
24	sand/mud	Progressively more mud below 5 cm.
25	sand/mud	Approximately 80% sand.
26	sand/mud	Progressively more mud below 5 cm.
27	mud/shells	
28	mud/shells	

[†] Sediments were visually classified based on the presence and distribution of sand and shell and the extent that the extruded cores held their shape.

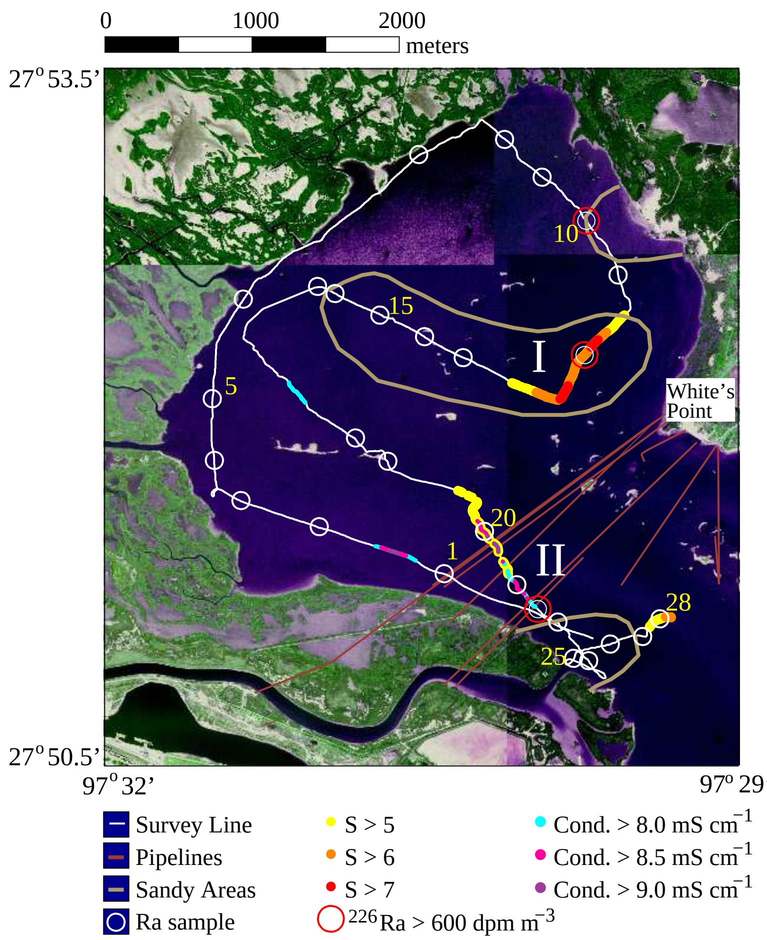

Figure 3.1: Upper Nueces Bay showing the salt marsh to the west and the Nueces River channel to the south. The survey proceeded west from the river mouth, clockwise along the shoreline, making two transects through the bay, and finished with transects across and along the outlet of the Nueces River channel. Ra sample locations are marked as white circles with every fifth sample and the last sample labeled. The highest activity dissolved Ra samples are marked by red circles. Areas of elevated surface salinity are colored yellow to red and areas of high mean subsurface conductivity are colored yellow to purple. Area I had subsurface conductivity features that were within 100 m of surface salinity and water temperature highs and dissolved O_2 lows. Area II, containing several petroleum pipelines, also had subsurface conductivity features, elevated surface Ra activity and salinity, and low surface dissolved O_2.

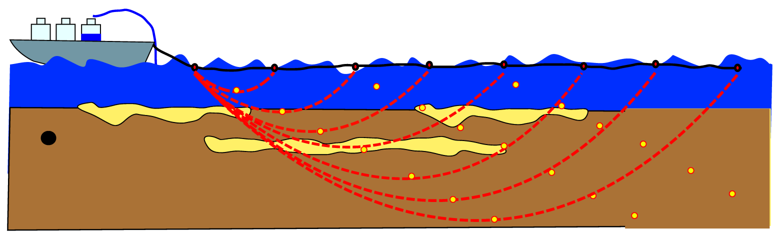

Figure 3.2: Schematic diagram of marine resistivity profiling. In marine applications of continuous resistivity profiling, an electrode array is towed at low speed by a boat. Resistance data is collected by applying an electric potential to the different electrode combinations and measuring the induced electric currents (*Jones*, 1991). Since the electric fields are curved the horizontal spacing of the electrodes determines the depth of the measurement. The raw resistance data simply indicates the combined resistance of all the material along the electric field line for a particular electrode pair at a specific point along the survey. After all the raw data is collected it is post processed using an inversion algorithm that fits a 2D conductivity field to the raw resistance data.

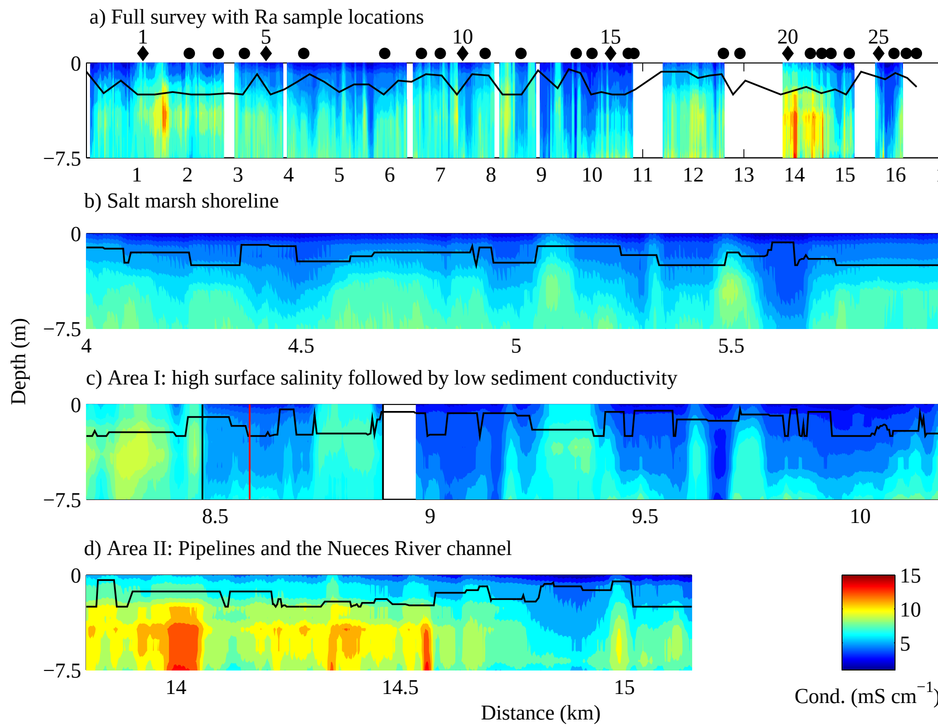

Figure 3.3: Results of the conductivity survey including a) the full survey path; b) a segment along the salt marsh shoreline; c) Area I , west of White's Point, with elevated surface salinity; and d) Area II containing pipeline indications and the Nueces River channel. In c), the location of the surface salinity maxima (S>7) are indicated by vertical black lines and the survey maximum Ra activity (sample 12) by a vertical red line. Water depth is indicated by a black line in all panels. The blank areas in the survey starting at km 10.9, 12.8, 15.3, and 16.2 are where raw data was too sparse to permit an inverted conductivity solution. Raw data can not be collected when an electrode breaches the water surface. In this survey wind speed increased in the afternoon to the point that in some parts of the bay the waves were large enough to regularly expose the electrodes to the air in the wave troughs.

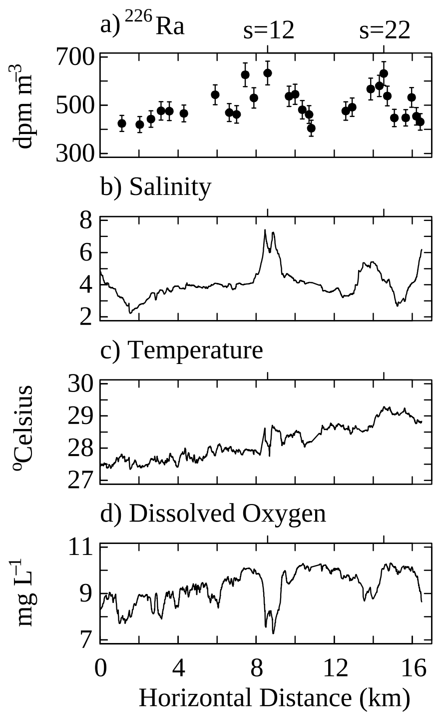

Figure 3.4: Results of the survey for a) dissolved $^{226}\mathrm{Ra}$, samples 12 and 22 are marked with ticks on all frames; b) surface salinity, c) water temperature; and d) dissolved $\mathrm{O_2}$. Water temperature and dissolved $\mathrm{O_2}$ generally increased during the course of the day. The influence of the Nueces River is apparent in the low surface salinity and dissolved $^{226}\mathrm{Ra}$ activity near survey km 15.5; another surface salinity low near km 1.5 may be a plume or eddy of Nueces River water.

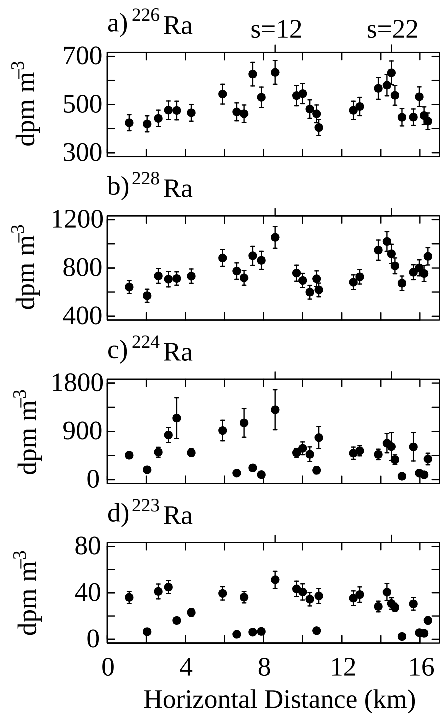

Figure 3.5: Results for dissolved a) $^{226}\mathrm{Ra}$, b) $^{228}\mathrm{Ra}$, c) $^{224}\mathrm{Ra}$, and d) $^{223}\mathrm{Ra}$. Long lived $^{226}\mathrm{Ra}$ and $^{228}\mathrm{Ra}$ activities exhibit very similar trends, peaking in two locations. Short lived $^{223}\mathrm{Ra}$ is nearly bimodal either high or low while $^{224}\mathrm{Ra}$ shares both the trends of $^{223}\mathrm{Ra}$ and those of $^{226}\mathrm{Ra}$ and $^{228}\mathrm{Ra}$.

Chapter 4

Ra isotopes and methane reveal pattern in submarine discharges to three Texas Coastal Bend Bays

4.1 Abstract

Previous studies of Nueces Bay, Texas have indicated a large submarine Ra source at the head of the bay (Chapters 2 and 3). In this study, Nueces Bay dissolved Ra activities and CH_4 concentrations are compared with those of two adjacent bays. The bays differ in 1) the relative importance of river discharge and net evaporation, 2) terrestrial aquifer level, and 3) the scale and density of their submerged petroleum infrastructures. Dissolved ^{226}Ra,^{228}Ra,^{223}Ra, and ^{224}Ra activities were measured in the three bays at three separate periods during the course of their seasonal flushing cycles. In addition during the final set of surveys, dissolved CH_4 was measured to obtain an independent indication of submarine fluid discharge. These results show that the seasonal increase in dissolved ^{226}Ra activity for

Nueces Bay is substantially larger than for either Copano Bay or Baffin Bay. The Nueces Bay station with the maximum ^{226}Ra exhibited a 4.7 dpm day^{-1} increase between the last two survey periods. In comparison, the Baffin Bay station with the maximum ^{226}Ra activity exhibited only a 2.7 dpm day^{-1} increase during a similar period and Copano Bay ^{226}Ra activities held steady between the last two surveys. For Nueces Bay, this increase cannot be readily explained by either evaporative concentration or riverine supply. Nueces Bay also has significantly higher CH_4 concentrations than either Copano or Baffin Bay. The CH_4 concentrations are highest at the head of Nueces Bay in the same area where dissolved ^{226}Ra activities were highest. These results indicate that the Ra supply to Nueces Bay is unusually large even regionally. The most relevant differences between the three bays that might account for this are 1) the proportionally larger salt marsh at the head of Nueces Bay and 2) the higher density of petroleum wells and pipelines. Though submarine groundwater discharge cannot be ruled out it cannot completely account for the observations. Leakage of oil-field brine can be inferred when these results are considered along with the the size of the Ra imbalance indicated in Chapter 2.

4.2 Introduction

Previous studies of Nueces Bay, Texas, found exceptionally high dissolved ^{226}Ra and ^{228}Ra activities particularly at the head of the bay (Chapters 2 and 3). In the initial surveys of Nueces Bay (Chapter 2), the maximum observed ^{226}Ra activity was 1000$\pm$78 dpm m^{-3}. For comparison the ^{226}Ra measured in other coastal waters has typically been $<$600 dpm m^{-3} (e.g., Spencer Gulf Australia; the waters of the Amazon shelf; North Inlet, South Carolina; Waquoit Bay, Massachusetts; and Pettaquamscutt River estuary, Rhode Island) (*Charette et al.*, 2001; *Kelly and Moran*, 2002; *Moore et al.*, 1995; *Rama and Moore*, 1996; *Veeh et al.*, 1995) (Figure 2.8). Only in the Bay of Bengal have comparable dissolved

^{226}Ra activities been observed (maximum of 1140 dpm m^{-3}) and the high values were attributed to submarine groundwater discharge (*Moore*, 1997). Similarly, a mixing model for Nueces Bay suggested that a submarine Ra supply on the order of 390×10^6 dpm day^{-1} was necessary to account for the high bay ^{226}Ra activities (Chapter 2). This submarine Ra input is large; it represents 100 times the Ra supplied by the Nueces River. Initial surveys also showed that dissolved Ra activities were highest at the head of Nueces Bay; subsequent geochemical and geophysical surveys in this area indicated that there were one or perhaps two relatively localized submarine Ra sources (Chapter 3). The geochemical and geophysical surveys showed dissolved Ra maxima coincident with 1) interleaving, vertical conductivity fingers in bay bottom sediments and 2) maxima in surface salinity and water temperature and minima in dissolved O_2. Together these results suggested two possible submarine Ra sources: 1) brackish submarine groundwater discharge (SGD) (*Burnett et al.*, 2003) and 2) the leakage of oil-field brine from the numerous submerged petroleum wells and pipelines (*Hudak and Wachal*, 2001).

The goal of this study was to evaluate these two potential sources of Ra by comparing the dissolved Ra activities of Nueces Bay to those of adjacent bays (Copano and Baffin) that differ in 1) the relative importance of river discharge and net evaporation, 2) terrestrial aquifer level, and 3) the scale and density of their submerged petroleum infrastructure (Figure 4.1 and Table 4.1). Dissolved ^{226}Ra, ^{228}Ra, ^{223}Ra, and ^{224}Ra activities were measured in each bay at three separate periods during the course of their seasonal flushing cycle to enable comparisons by absolute Ra activities, activity ratios, and seasonal changes in Ra activity. In addition to measuring dissolved Ra activities, dissolved CH_4 was also measured in the final set of surveys to obtain an independent indication of submarine fluid discharge.

Long lived ^{226}Ra and ^{228}Ra and short lived ^{224}Ra and ^{223}Ra are enriched to differing degrees in brackish groundwater and sediment porewaters; in particular long lived ^{226}Ra

(1600 year half-life) is greatly enriched in groundwater relative to river water, seawater, and sediment porewater making it a good general tracer of SGD (*Charette et al.*, 2001). However oil-field brines are also enriched in Ra (*Kraemer and Reid*, 1984); therefore, in this study high dissolved ^{226}Ra activities are considered an indication of either oil-field brine leakage or SGD. Similar to Ra, CH_4 is enriched in groundwater and porewaters of anoxic sediments due to methanogenesis and has also been used as a tracer of SGD (e.g., *Bugna et al.*, 1996; *Swarzenski et al.*, 2001). The dissolved CH_4 concentration of water in equilibrium with the atmosphere is approximately 2 nM while concentrations in groundwater can be several orders of magnitude greater.

The previous studies of Nueces Bay made use of 1) bay scale Ra surveys and mixing models and 2) detailed geochemical and geophysical measurements in a portion of Nueces Bay where Ra activities were highest (Chapter 2, Chapter 3). This study takes a third approach of comparing bay Ra activities on a regional scale and by doing so addresses the basic question, "Are the absolute and seasonal changes in Nueces Bay Ra activities representative of other bays in the region?" It is demonstrated below that the seasonal increase in dissolved ^{226}Ra for Nueces Bay is larger and more rapid than for either Copano Bay or Baffin Bay. This suggests that the Ra supply to Nueces Bay is substantially larger than for the other two bays and of the differences between the bays it is the petroleum infrastructure density that most readily correlates with a large submarine Ra input to Nueces Bay.

4.3 Methods

4.3.1 Study Area

Among the bays and estuaries of the Texas Coastal Bend are Copano Bay, Nueces Bay, and Baffin Bay. These three bays have adjacent watersheds and share a common primary connection with the Gulf of Mexico through Aransas Pass (Figure 4.2). These three bays differ in salinity, river inflow, bay water residence time, net precipitation, the relative size of the wetlands to the bay area, and terrestrial aquifer level (Table 4.1). Regionally, precipitation decreases from east to west such that Copano Bay typically receives the most rainfall and Baffin Bay the least (Table 4.1). The Nueces River is the largest of the three watersheds. However, most of the drainage is impounded in reservoirs; the unimpounded (free) watershed is actually smaller than either the Baffin or Copano watersheds. While river inflow from these watersheds generally follows the regional precipitation trend, Nueces River discharge is augmented by discharge from its impounded watershed. Nueces Bay also has a larger wetland system relative to bay size than the other two bays (Table 4.1). The regional aquifer system is a network of confined and unconfined layers of silt, clay, sand, and gravel. Groundwater level generally follows the coastal topography except around Baffin Bay where municipal use and low recharge has caused water levels to drop below sealevel (Figure 4.1).

Oil and gas production in the region is long-established and pervasive both on land and in the bays. There are a total of 624 wells in the three bays combined; Copano Bay has the most wells, Baffin Bay has the fewest wells, and Nueces Bay has the densest concentration of wells (Figure 4.3, Table 4.1) (*Texas Railroad Commission*, 2005). A quarter of these wells actively produce oil, gas, and or a mixture of both (active wells). Half of all the wells were actively producing oil or gas at one time but production has now ceased or diminished to the point where they have been shut down (inactive wells). Of these inactive wells a few are shut off but maintained to potentially be restarted in the future; the rest have been permanently plugged by filling in the bottom of the well with cement. A quarter of the wells never produced oil or gas (dry wells). In addition to the wells themselves there are numerous submerged and buried pipelines that transfer petroleum and gas from the wells to shore facilities as well as refined petroleum products between facilities across the bays.

Along with oil and gas, active wells also produce saline water (referred to here as oil-field brine). The relative amount of water varies from well to well. Oil field brine chemistry also varies from well to well but typical brines are very saline and have high dissolved Ra activities (*Hudak and Wachal*, 2001; *Kraemer and Reid*, 1984). Oil field brine is separated from the petroleum product and disposed of by injection into deep disposal wells (typically into oil formations that are no longer productive). Wells may leak through compromised well casings and plugs or at surface valves and flanges. The potential exists for any of these wells (and pipelines) to leak though there is insufficient data to evaluate which type of well might be more likely to leak. In this study the total number of wells within a bay is used as a qualitative indication of leakage probability and bays are compared based on the number of wells divided by the bay volume.

4.3.2 Sample Collection

Surface water samples (50 L) for dissolved Ra analysis were collected from Copano Bay, Nueces Bay, and Baffin Bay at three periods during their seasonal flushing cycles (Table 4.2, 4.3, 4.4, Figure 4.3, and Figure 4.4). The first set of samples (July 2004) followed a period of heavy rain, when river discharges were high and bay salinities were reduced to seasonal lows. During this initial period, Nueces Bay samples (n=12) were collected on 10 and 12 July 2004, Copano Bay samples (n=12) on 13 July 2004, and Baffin Bay samples (n=12) on 15 July 2004. The goal of the second set of samples was to observe each bay at a period when salinities were midway to their final seasonal maxima. This goal was met for the samples collected from Baffin Bay (n=8) and Nueces Bay (n=8) on 8 December 2004 and 26 January 2005, respectively. The samples collected from Copano Bay (n=8) on 1 December 2005 ultimately proved closer to the seasonal salinity maximum than did the final samples. The final set of samples was timed to observe each of the three bays near the end of their seasonal flushing cycles when they approached their highest salinities. During this final period, Copano Bay samples (n=12) were collected on 18 May 2005, Nueces Bay samples (n=12) on 25 and 27 May 2005, and Baffin Bay samples (n=8) on 8 June 2005. Samples were collected by submersible pump and stored in 25 L polyethylene bottles. Water temperature and salinity were determined using a YSI Model 30 Sonde.

Samples were also collected from the tidal inlet at Aransas Pass, the primary rivers feeding the three bays, and regional water wells, lakes, ponds, marshes (Figure 4.2). Aransas Pass samples (50 L, n=32) were collected biweekly from The University of Texas at Austin Marine Science Institute (UTMSI) pier lab from 16 July 2004 to 29 July 2005 either by submersible pump or as grab samples (Table 4.5). River samples (75 L, n=4) were collected from the Mission and Aransas Rivers in the Copano Bay watershed and Los Olmos Creek in the Baffin Bay watershed. The other large drainage in the Baffin watershed (San Fernando Creek) was dry when sampling was attempted (11 May 2005). Nueces River sampling was included in the bay surveys. Groundwater samples (25-75 L, n=20) were collected from wells equipped with downhole pumps, flowing under artesian pressure, or using a portable pump (Table 4.6). Surface samples (n=5) were also collected from brackish ponds, salt marshes, and intertidal areas. Porewaters were sampled using a 1.8 m MHE Products stainless steel minipiezometer; in only two cases were sediments permeable enough to collect sufficient water for Ra analysis.

4.3.3 Ra Activity Measurements

Samples for Ra analysis were filtered in the laboratory through a 1 $\mu\mathrm{m}$ polypropylene cartridge filter and the Ra extracted onto a subsequent column of MnO_2-impregnated acrylic fiber at a flow rate of less than 1 L min^{-1}. Short lived ^{224}Ra and ^{223}Ra were measured using the delayed coincidence counting method of *Moore and Arnold* (1996). ^{226}Ra and ^{228}Ra were then measured on a high purity Ge well gamma detector following the procedure outlined by *Rutgers van der Loeff and Moore* (1999) and described in Chapter 2. The ^{228}Ra and ^{226}Ra activities of the precipitates were determined by gamma counting the daughter nuclides ^{228}Ac and ^{214}Pb by their 911 and 351 keV gamma emissions respectively. The 1σ counting error is reported for all measurements and was typically 5-10%. Reported activities are decay-corrected to time of sample collection.

In most studies, MnO_2 fibers prepared in this way are assumed to quantitatively extract Ra from water samples at flow rates of $<$1-2 L min^{-1}. Extraction efficiency in this study was verified to be $>$95% by using two MnO_2 columns in series for several samples and determining the relative amounts adsorbed to the primary and secondary columns. A combined collection and counting efficiency for the gamma detector was determined by preparing two solutions of known ^{228}Ra and ^{226}Ra activity from standards and precipitating, collecting, and counting these standards in the same way as the samples. Counting efficiencies for the delayed coincidence detectors were determined by counting a MnO_2 fiber column of known ^{224}Ra and ^{223}Ra activity prepared by Matt Charette at the Woods Hole Oceanographic Institution.

4.3.4 CH_4 Measurements

Air free water samples (120 mL) for CH_4 analysis were collected in 150 ml polyethylene gas tight syringes and stored submerged with ice in the field. Samples were analyzed the same day, typically within 8 hours of collection on an SRI 8610C gas chromatograph (GC). Prior to analysis samples were allowed to equilibrate to room temperature in a water bath. To extract the dissolved CH_4, 20 ml of He was added to each syringe, the He/sample mixture was shaken vigorously for 3 minutes and allowed to equilibrate for 15 minutes prior to injecting the head space gas into the GC. Extraction efficiency for these sample and headspace volumes was determined to be 70% by stripping and analyzing several samples twice and comparing the CH_4 concentrations. For gas separation two capillary columns, a 2 m molecular sieve 5A and a 15 m Porapak Q, were used in series. The GC was equipped with a pulse discharge detector and flame ionization dectector both capable of detecting CH_4. While results for both detectors are similar the flame ionization dectector data are reported because this detector is more selective for CH_4 and peaks are more readily quantifiable and less subject to noise. The GC was calibrated using mixtures of ultra high purity He and a 100 ppm CH_4 in He standard gas mixture. The CH_4 partial pressures measured with the GC were corrected for extraction efficiency and converted to dissolved CH_4 concentrations using an expression of the Ideal Gas Law and Dalton's Law of Partial Pressures:

$$\mathrm{C}_{\mathrm{CH}_4} = \mathrm{P}_{\mathrm{CH}_4} \frac{P}{(273.15\,\mathrm{K} + T)} \left(\frac{1.00\,\mathrm{mol}\ 273.15\,\mathrm{K}}{1.00\,\mathrm{atm}\ 22.4\,\mathrm{L}} \right) \frac{V_{hs}}{V_w} \frac{1}{E_{eff}} \tag{4.1}$$

where C_{CH_4} is the dissolved molar concentration, P_{CH_4} is the mole fraction measured with the GC, P is air pressure (atm), T is air temperature (Celsius), V_{hs} is the volume of the headspace gas, V_{hs} is the water sample volume, and E_{eff} is gas extraction efficiency.

4.4 Results and Discussion

As observed previously for Nueces Bay (Chapter 2), the dissolved Ra activities of all three bays are high relative to other coastal waters; over the entire study period the mean ^{226}Ra activities for Copano Bay, Nueces Bay, and Baffin Bay were 393$\pm$122 dpm m^{-3}, 431$\pm$247 dpm m^{-3}, and 615$\pm$171 dpm m^{-3}, respectively (Figure 4.5 and Table 4.3). Bay water Ra activities are also high relative to many but not all groundwater samples; 7 of the groundwater samples had dissolved ^{226}Ra activities $>$ 680 dpm m^{-3} and three were higher than 1150 dpm m^{-3} (Figure 4.6 and Table 4.6). To move beyond these points, the analysis will now consider the differences in the temporal trends in Ra activity between the bays and the spatial relationships between Ra activities, CH_4 concentrations, and petroleum well distribution.

4.4.1 Seasonal Trends

The primary differences between Copano Bay, Nueces Bay, and Baffin Bay salinities and Ra activities (Tables 4.2-4.4, Figure 4.7) are clearly due to differences in the volume and timing of river discharge relative to net evaporation. For all three bays, precipitation and river discharge were unusually high during the two months prior to the study period such that by the first set of surveys all three bays had been flushed to seasonal low salinities and Ra activities (Figure 4.7). During the study period, Nueces Bay received the greatest river inflow followed by Copano Bay then Baffin Bay (U.S. Geological Survey, 2005). Residence time with respect to gauged river inflow was 30 days for Nueces Bay, 391 days for Copano Bay, and over 35 years for Baffin Bay (Table 4.1). In comparison, residence time with respect to direct net evaporation (or in this case evaporation) is typically 262 days for Nueces Bay, 428 days for Copano Bay, and 524 days for Baffin Bay. Considered together it is clear that Nueces Bay is a net exporter of water to the regional bay system and Baffin Bay a net importer (inverse estuary). Compared to Nueces Bay, Copano Bay is only a marginal exporter of water. The consistently lower salinities and Ra activities of Copano Bay can largely be attributed to the importing of substantially more river water from the northern watersheds than either Nueces Bay or Baffin Bay.

Though unremarkable in terms of total river discharge, Copano Bay is notable for both peak and greatest sustained discharge (Table 4.1). During the study period Copano Bay experienced two river inflow events (one minor and one major). During the remainder of the study period river discharge was consistently at least 63,600 m^3 day^{-1} (Figure 4.4a).

Nueces Bay experienced four major inflow events between which river discharge dropped to as low as 300 m^3 day^{-1}. No major river inflow events were recorded by the river gauges in the Baffin Bay watershed and gauged river discharge was sustained at 600 m^3 day^{-1} though it is likely that much of this discharge evaporated, infiltrated the ground or was otherwise diverted prior to reaching Baffin Bay. However the Baffin river gauges do not include a large part of the watershed so the guaged discharge may underestimate actual river inflow (Figure 4.2). This suggests that with respect to river inflow Copano Bay was functioning near steady state. This appears to be reflected in the Copano Bay salinities, ^{226}Ra, and ^{228}Ra activities which peaked during or prior to the second survey (Figure 4.7a, b, and c). Baffin Bay on the other hand did not reach steady state with respect to salinity, ^{226}Ra, or ^{228}Ra activities all of which increased steadily during the study period as water was imported from the regional bay system and concentrated by evaporation.

In the case of Nueces Bay, the river discharge and bay salinity records (Figure 4.4a and b) show that bay hydrology and general chemistry are episodic and Nueces Bay ^{226}Ra and ^{228}Ra activities (Figure 4.7b and c) show large seasonal increases. The episodic nature of Nueces river discharge may explain the variability in the short lived ^{223}Ra and ^{224}Ra results (Figure 4.7d and e). For Nueces Bay ^{223}Ra and ^{224}Ra, the initial elevated activities and the very high final activities are probably due to input of bay bottom porewater by sediment resuspension during episodic river discharge. The increased activity from such episodic inputs of short lived isotopes would decrease rapidly due to dilution and radioactive decay. For Copano Bay and Baffin Bay similar initial inputs are also suggested by the seasonal decrease in the ^{224}Ra to ^{228}Ra ratio (Figure 4.7f). Both Copano Bay and Baffin Bay probably received their largest inputs of ^{223}Ra and ^{224}Ra during the period of high river discharge prior to the study period.

Taken together the trends in river discharge, salinity, and Ra activity discussed above show that the three bays function differently during their seasonal flushing cycles. Copano Bay quickly reaches steady state at salinities between 7 and 10 and relatively low Ra activities. Baffin Bay operates as an inverse estuary ultimately reaching the highest salinities (up to 37.5) and the highest ^{228}Ra activities (up to 3232 dpm m^{-3}) measured in the three bays during the study. Nueces Bay salinity and Ra activity increase unsteadily throughout the study ultimately achieving ^{226}Ra activities as high as those of Baffin Bay but at significantly lower salinities.

Nueces Bay salinity, ^{226}Ra, and ^{228}Ra activity (Figure 4.7a, b, and c) increased by as much or more than for Baffin Bay and in less time. This is in apparent contradiction with the fact that Nueces Bay received substantially greater river discharge both in absolute terms and proportional to bay volume. The next step is to consider whether either riverine input or evaporation can explain such a large seasonal increase.

4.4.2 River Input and Evaporation Effects

The dissolved ^{226}Ra activity of Nueces River water is $<$ 200 dpm m^{-3} (Chapter 2) and can only dilute the high ^{226}Ra activities of Nueces Bay. However Ra also desorbs from riverine particulate material as salinity increases; desorption is nearly complete when the mixture reaches a salinity of 5 (*Krest et al.*, 1999). Could the Ra desorption from riverine particulate supply the needed ^{226}Ra in Nueces Bay? In chapter 2 it was concluded from dissolved Ra measurements across the 0-12 salinity gradient that the desorbable ^{226}Ra contribution from the Nueces River near mean river discharge was 30 dpm m^{-3}. It is possible that the desorbable contribution might increase during or just after large episodic discharge events but the largest such event during this study did not result in substantially higher bay ^{226}Ra activities; the highest ^{226}Ra activity during the initial survey was 305 dpm m^{-3} (Table 4.3 station N5) at a salinity of 5.7. Therefore I conclude that riverine Ra supply cannot lead to the high ^{226}Ra activities of Nueces Bay. This is supported by the fact that in Copano Bay, ^{226}Ra activities decreased after a large river discharge event between the second and third surveys (Table 4.5).

To evaluate the effects of evaporation, Nueces Bay will now be compared with Baffin Bay where evaporation is the largest net flux of water. Nueces Bay salinity and ^{226}Ra and ^{228}Ra activities increased as much or more than Baffin Bay and did so in a shorter time span. Stations B9 in Baffin Bay and N16 in Nueces Bay illustrate how large the increase in ^{226}Ra was for Nueces Bay (Figure 4.8). During the 182 days between the second and third surveys the ^{226}Ra activity at B9 increased from 676$\pm$49 to 1164$\pm$100 dpm m^{-3} and the salinity increased from 27.4 to 37.5. In comparison it took only 120 days for the ^{226}Ra activity in the area of N16 to increase from 560$\pm$42 (N1) to 1122$\pm$87 (N16) dpm m^{-3} while the salinity increased from 13.20 to 19.3. The direct net evaporation in these areas can be estimated by assuming the system is closed to Ra exchange. The progressive increase in activity would then be:

$$A_f = \frac{A_i}{\left(1 - \frac{E}{D}\right)^n} \tag{4.2}$$

where A_f is the final activity, A_i is the initial activity, E is the daily direct net evaporation rate, D is the water depth, and n is the number of days between final and initial activities.

In fact neither Baffin Bay nor Nueces Bay is closed to the addition of Ra regenerated in bay bottom sediments, though for long lived ^{226}Ra this contribution is small (*Charette et al.*, 2001; *Krest et al.*, 1999). In Chapter 2 an upper limit of 0.6 dpm m^{-2} day^{-1} was estimated for the regenerated ^{226}Ra contribution based on previous Nueces Bay surveys and Ra mixing models. By using Equation 4.2 to create a daily sequence with regenerated ^{226}Ra added daily, the evaporation rate can be found iteratively. The net evaporation rate for Baffin Bay at B9 is 77 cm yr^{-1} based on the 182 day change in ^{226}Ra activity and a depth of 0.93 m (for this portion of Baffin Bay) (*Diener*, 1975). This calculation exactly matches the mean of 77 cm yr^{-1} from precipitation and pan evaporation measurements for the period of record (Table 4.1). In the case of Nueces Bay, even if the N16 area were closed to lateral Ra exchange it would still require a net evaporation rate of 120 cm yr^{-1} to cause the observed increase in ^{226} Ra activity. This is much greater than the Baffin Bay rate and more than double the 54 cm yr^{-1} mean based on precipitation and pan evaporation measurements in the Nueces area (Table 4.1). In addition this part of Nueces Bay mixes with lower Ra activity waters both from the river (hence the lower salinities) and from the regional bay system. Therefore an even higher net evaporation rate would be necessary than the one calculated. Consequently, I conclude that while evaporation is sufficient to explain the behavior of Ra in Baffin Bay, it is insufficient to explain the large increase and high absolute values of dissolved ^{226}Ra activity in Nueces Bay.

This large increase in ^{226}Ra activities in Nueces Bay suggests that the Ra supply to Nueces Bay is enhanced relative to Baffin Bay and Copano Bay. In particular the area at the head of Nueces Bay stands out as an area of high Ra activity. This area has had the highest ^{226}Ra activities in four out of the six Nueces Bay sampling periods conducted during this and the previous study (Chapter 2); the two times when this was not the case were during the lowest salinity surveys immediately after the bay had been flushed by river discharge (Figure 4.9). Besides river discharge, three things make Nueces Bay stand out from Copano Bay and Baffin Bay: 1) its extensive salt marsh system, 2) positive hydraulic gradient of the watertable towards the bay (Figure 4.1), and 3) the density of its submerged petroleum infrastructure. The potential influence of these factors will be evaluated by comparing dissolved ^{226}Ra activities with CH_4 concentrations and petroleum well distributions.

4.4.3 CH_4 Concentrations

Results from the May-June 2005 surveys show that Nueces Bay CH_4 concentrations are significantly greater than either of the two other bays (Table 4.7) approaching the concentrations of the well samples (Table 4.8). Bay CH_4 concentrations were compared using unpaired, two-sided t-tests for samples with unequal variances, non-detects were removed, and, in the case of Nueces Bay, salt marsh samples were not included. The mean CH_4 concentration in the open water of Nueces Bay was 22.6 nM with a high at station N16 of 67.7 nM. CH_4 concentrations in the Nueces salt marsh were as high as 114 nM. Copano Bay and Baffin Bay mean CH_4 concentrations were 6.41 and 3.96 nM respectively. For comparison, the mean CH_4 concentration in the ten groundwater samples for which CH_4 were measured was 159 nM with a maximum of 302 nM.

The highest CH_4 concentrations (67.7, 73.9, and 114 nM) were found in and near the salt marsh at the head of Nueces Bay at the same stations with the highest ^{226}Ra and ^{228}Ra activities (Figure 4.10). Beyond this association there was no other discernible relationship between CH_4 concentrations and Ra activities in Nueces Bay. In Copano Bay, CH_4 concentrations and ^{226}Ra and ^{228}Ra activities showed some correlation with higher levels in the southern part of the bay and near the bay outlet (Figure 4.10). In Baffin Bay there was no discernible relationship between CH_4 concentrations and Ra activities (Figure 4.10).

The most compelling observation relative to the petroleum infrastructure is that CH_4 concentrations, seasonal increases in Ra activity, and petroleum well density are all highest in Nueces Bay. Comparing CH_4 concentrations and Ra activities against the petroleum well spatial distribution provides little additional information because there are so many petroleum wells and most of them probably do not leak (Figure 4.3). Nueces Bay has wells and pipelines throughout the bay such that nearly every sample station has a potential oil-field brine source in the near vicinity. For instance, the head of Nueces Bay, with the highest CH_4 concentrations and ^{226}Ra and ^{228}Ra activities, contains 48 wells including 13 outside of the high density area shown on Figure 4.3. For Copano Bay, the well and pipeline distribution is patchier with large groups of wells in the south bay and near the bay mouth; areas that generally have higher CH_4 concentrations and Ra activies. For Baffin Bay, there are very few wells outside of the areas indicated on Figure 4.3 and the only discernable connection is that station B9, which of all bay samples had the greatest ^{226}Ra activity, is in an area with numerous petroleum wells.

4.4.4 Evidence of High Dissolved ^{226}Ra Activity Submarine Discharges

The results indicate some important differences between Nueces Bay and the other two bays. First, the seasonal increases in salinity and dissolved ^{226}Ra and ^{228}Ra activities were substantially larger for Nueces Bay than for the other bays despite proportionally greater river discharge. Second, Nueces Bay CH_4 concentrations were significantly higher than those of the other two bays and there was a clear association between high CH_4 concentrations and high Ra activities in the head of Nueces Bay. Of the physical, hydrologic, and anthropogenic differences between the three bays two stand out as pertinent to the differences in the Nueces Bay results 1) the proportionally larger salt marsh at the head of Nueces Bay and 2) the high density of the petroleum infrastructure (Table 4.1). The proportionally larger amount of cropland in the free Nueces watershed is also notable but when cropland is compared in either absolute terms or relative to bay size the correlation with high Nueces Bay Ra activity breaks down.

For CH_4 the high concentrations in the Nueces salt marsh suggest this may be a strong input to the bay. The salt marsh may also be an important source of Ra to Nueces Bay. The highest dissolved ^{226}Ra activity measured in Nueces Bay was 1122$\pm$87 dpm

m^{-3} at station N16 in the head of the bay. Besides station B9 in Baffin Bay, only four other samples in the study had higher ^{226}Ra than station N16. Three were well samples (Table 4.6 samples W16, W19, and W34) and one was a porewater sample from an intertidal inlet on the barrier island (Table 4.9 station S8); none were in the Nueces watershed. Four surface water samples were nearly this high with ^{226}Ra activities $>$ 1000 dpm m^{-3} (Table 4.9 S2, S5,S6, and S7); two were in the Nueces salt marsh. Thus, high Ra activity water is present in the salt marsh, but the activities are too low to account for the high open water activities at station N16 when dilution is considered. It seems likely that the salt marsh porewaters would have sufficiently high ^{226}Ra activities, similar to the porewater at station S8 on the barrier island (1654 dpm m^{-3}). *Rama and Moore* (1996) made extensive measurements of Ra production in the salt marsh sediments of North Inlet, South Carolina, and determined that ^{226}Ra production in the first 15 cm of the marsh sediments was 1.2 x 10^{-5} dpm cm^{-2} day^{-1}. If we assume that ^{226}Ra production rates are similar in the Nueces wetland system (75 km^2: Table 4.1) then the ^{226}Ra production would be 9 x 10^6 dpm day^{-1}. This is small in comparison to the 218 x 10^6 dpm day^{-1} input necessary to balance the Nueces Bay ^{226}Ra budget (Chapter 2). In addition the salt marsh sediments are mainly mud and clay with low permeabilities so it is not clear how large amounts of Ra produced in the salt marsh sediments would be delivered to the bay on a regular basis. Finally, synoptic geophysical and geochemical surveys conducted along the edge of the salt marsh indicate no sign of submarine fluid discharge (Chapter 3).

These same surveys did find evidence of high dissolved Ra submarine discharges near petroleum wells and pipelines in the head of Nueces Bay. Samples of local oil-field brine have dissolved ^{226}Ra activities that range between 100 and 34,700 dpm m^{-3} with a mean of 10,000 dpm m^{-3}; their salinities range between 7.5 and 36.3 with a mean of 25.5 (*Kraemer and Reid*, 1984). A previous Ra mixing model of Nueces Bay indicated the size of the submarine ^{226}Ra input was $218 \times 10^6 \pm 105\%$ dpm day^{-1} (Chapter 2). Based on the mean measured local oil-field brine ^{226}Ra activity of 12,000 dpm m^{-3} it would take an oil-field brine leakage rate of 18,200 m^3 day^{-1} to supply the needed ^{226}Ra. The only data available with which to compare this estimate with are previous permitted brine discharges. Oil field brine discharge to coastal waters is no longer permitted but in the early 1990s the active discharge to Nueces Bay was 2,478 m^3 day^{-1} (*Caudle*, 1993). This was in fact only a fraction of the historic permitted discharge, which had been as high as 10,438 m^3 day^{-1} (*Armstrong and Ward*, 1998). In comparison a present-day leakage rate of 18,200 m^3 day^{-1} is unrealistic. Obviously if higher activity brine is leaking this would reduce the rate; using the highest measured ^{226}Ra activity of local brine samples of 34,700 dpm m^{-3} (*Kraemer and Reid*, 1984) reduces the leakage estimate to 6,290 m^3 day^{-1}. In fact actual local brine samples may be significantly higher than the measured values. *Kraemer and Reid* (1984) note that because brine samples were often collected from holding tanks a significant amount of the dissolved Ra probably precipitated with barite that often forms as the warm brine cools. An oil-field brine sample from Galveston, Texas had a ^{226}Ra activity of 695,000 dpm m^{-3} and nine samples from the Louisiana coast had activities $>$1x10^6 dpm m^{-3} (*Kraemer and Reid*, 1984). A leakage rate of 200 to 300 m^3 day^{-1} of such fluids could easily account for the ^{226}Ra activities seen at N16 and the submarine Ra supply estimated from previous mixing models.

The results of this study indicate a large submarine input of Ra at the head of Nueces Bay. Considered together with previous results the evidence suggests that the dissolved ^{226}Ra activity of the input is very high. SGD cannot be ruled out and may play an important role in the high Ra activities observed in Nueces Bay. However I conclude that it is unlikely that SGD alone could explain the seasonal trends and absolute activities observed in the open waters of Nueces Bay while oil-field brine potentially could.

4.5 Conclusions

These results show that the seasonal increase in dissolved ^{226}Ra activity for Nueces Bay is substantially larger than for either Copano Bay or Baffin Bay. This increase cannot be explained readily by either evaporation or riverine supply. In addition Nueces Bay has significantly higher CH_4 concentrations than either Copano or Baffin Bay. The CH_4 concentrations are highest at the head of Nueces Bay in the same area where dissolved ^{226}Ra activities were highest in every non-flood stage Nueces Bay survey (i.e., 4 out of 6 periods). These results suggest that the Ra supply to Nueces Bay is unusually large in a regional context. The most relevant differences between the three bays that might account for this are 1) the proportionally larger salt marsh at the head of Nueces Bay, 2) the higher hydraulic gradient towards Nueces Bay, and 3) the higher density of petroleum wells and pipelines. Though SGD cannot be ruled out, leakage of oil-field brine is strongly suggested when these results are considered along with those from previous studies (Chapters 2 and 3).

The actual leakage rate depends on the radium activity of the leaking brine which is highly variable and not well characterized. Based on available data, the leakage rate is potentially from 200 to 6,290 m^3 day^{-1}. The results of synoptic geochemical and geophysical surveys suggest the leakage may be greatest at two areas in the head of Nueces Bay. The wells and pipelines in these areas should be inspected and if they are in fact leaking brine samples should be collected to determine their dissolved ^{226}Ra activity. From the activity of the leakage it would be possible to determine whether or not other wells might also be leaking.

The leakage of oil-field brine needs to be understood because it has potentially important ecological consequences especially in the shallow and restricted waters of the Texas Coastal Bend. Oilfield brine is very saline, up to S=37 (*Kraemer and Reid*, 1984), and therefore denser than the water in most of the regional bays. Oilfield brine is also anoxic and can have high concentrations of total organic carbon (*Veil et al.*, 2005). Significant leakage of such water in restricted areas could accumulate during dry periods promoting stratification and anoxia in bottom waters; which does in fact occur in some areas of the Texas Coastal Bend. Oilfield brine can also be high in nitrogen particularly dissolved inorganic N. A recent survey of permitted oil-field brine discharges from 50 oil rigs in the Gulf of Mexico by *Veil et al.* (2005) showed that mean brine dissolved inorganic N was 76±52 mg/l while total N (total Kjeldahl N + NO_3^- +NO_2^-) total N was 85±52 mg/l. Again in restricted areas during dry periods, a persistent leakage of the kind suggested by the results could modify the bay inorganic/organic N ratio and potentially change the competitiveness of some algal species as suggested by *Laroche et al.* (1997).

Table 4.1: Physiography and other characteristics of Baffin, Nueces, and Copano Bays and their watersheds.

	Baffin	Nueces	Copano
Bay Area (km^2)*	228	75	171
Mean Bay Depth (m)*	1.8	0.7	1.1
Bay Volume (10^6 m^3)*	410	55	188
Mean Precipitation (cm yr^{-1})**	77	95	102
Mean Direct Evaporation (cm yr^{-1})**	154	148	135
River Inflow: 9 July 2004 to 8 June 2005***			
Minimum (m^3)	600	300	63600
Maximum (10^6 m^3)	1.56	17.6	26.0
Mean (10^6 m^3)	0.03	1.81	0.48
Bay Volume/Maximum River Inflow (days)	262	3	7
Bay Volume/Mean River Inflow (days)	13400	30	391
Bay Volume/Net Evaporation (days)	524	262	428
Watershed Area (km^2)†	8599	947‡	5869
rangeland	63.9%	11.9%	27.2%
cropland	31.8%	67.2%	34.8%
forest	1.2%	7.5%	31.1%
urban	1.2%	4.6%	3.8%
wetland	1.3%	7.9%	1.9%
wetland area/bay area	49%	100%	65%
Total oil and gas wells††	59	184	381
well density (wells/bay volume)	0.14	3.36	2.03
Active Wells			
Oil	2%	15%	3%
Gas	31%	9%	6%
Mixed	3%	9%	9%
Inactive Wells			
Oil	12%	24%	31%
Gas	14%	18%	8%
Mixed	2%	8%	15%
Dry Wells	37%	17%	27%

* (*Diener*, 1975)
** For 1961 to 2002 (*Texas Water Development Board*, 2005b).
*** (U.S. Geological Survey, 2005)
† (*U.S. Geological Survey*, 2005a)
‡ This is the free Nueces watershed; the total Nueces watershed is 44,000 km^2.
†† (*Texas Railroad Commission*, 2005)

Table 4.2: Salinity and dissolved Ra activity for Copano Bay.

Station	Collected	Salinity	^{226}Ra (dpm m^{-3})	^{228}Ra (dpm m^{-3})	^{224}Ra (dpm m^{-3})	^{223}Ra (dpm m^{-3})	^{228}Th (dpm m^{-3})
C1*	13 Jul 04	1.25	303±22	367±30	384±167	12.3±2.6	64.8±21
C2	13 Jul 04	1.83	255±20	364±32	197±66	9.45±1.9	46.6±7.5
C3	13 Jul 04	1.75	259±20	349±31	377±168	10.8±2.3	55.2±18
C4	13 Jul 04	4.38	269±21	633±52	364±127	16.3±3.4	27.4±4.5
C5	13 Jul 04	4.30	243±19	642±52	456±166	14.3±3	7.44±1.3
C6	13 Jul 04	1.75	253±19	408±32	496±198	6.79±1.7	3.33±0.6
C7	13 Jul 04	1.65	267±21	387±35	1332±684	-	4.7±1.6
C8	13 Jul 04	1.95	263±20	412±36	664±277	12.3±2.7	4.02±0.68
C9	13 Jul 04	3.06	249±19	446±38	627±295	15.3±3.3	6.87±2.2
C10	13 Jul 04	2.10	299±23	468±41	-	18.9±4.5	5.24±0.89
C11	13 Jul 04	2.31	256±19	431±33	-	9.72±2.4	7.16±2.3
C12	13 Jul 04	3.99	259±20	535±46	-	18±4.1	88.9±14
C2	01 Dec 04	8.80	548±40	1205±89	48.5±17	2.2±0.41	5.57±1.8
C3	01 Dec 04	8.60	639±47	1335±101	41.3±7	3.3±0.58	5.36±0.9
C5	01 Dec 04	9.60	514±38	1156±89	41.2±13	3.3±0.59	3.74±1.2
C8	01 Dec 04	8.70	595±47	1265±111	61±10	6.85±1.2	15.6±2.9
C9	01 Dec 04	10.50	475±35	1307±97	587±192	38.9±6.3	4.8±1.6
C10	01 Dec 04	9.60	532±40	1201±94	66.7±12	6.81±1.1	7.13±1.2
C11	01 Dec 04	11.10	423±31	1141±87	510±104	34.4±5.5	5.92±1
C12	01 Dec 04	10.10	386±28	1028±76	141±47	9.26±1.6	13.1±4.2
C1	18 May 05	6.20	536±42	940±83	64.9±22	3.95±0.75	8.44±2.7
C2	18 May 05	6.60	507±40	1010±88	-	3.53±0.66	-
C3	18 May 05	7.60	361±28	836±68	48.7±8.2	6.75±1.2	11±1.9
C4	18 May 05	8.20	370±30	970±85	52.5±9	6.61±1.1	11.3±1.9
C5	18 May 05	8.80	337±26	1006±80	45.6±8.9	4.75±0.86	4.68±0.84
C6	18 May 05	6.30	493±39	1051±90	29.8±5.4	3.2±0.59	8.69±1.5
C7	18 May 05	7.60	460±37	922±86	62.2±21	3.66±0.67	8.52±2.8
C8	18 May 05	7.60	334±26	789±63	70.5±23	4.59±0.79	6.91±2.2
C9	18 May 05	7.70	395±32	935±83	33.2±6.3	3.59±0.65	9.41±1.5
C10	18 May 05	6.80	534±40	1008±80	104±36	4.88±0.85	9.45±3
C11	18 May 05	7.50	466±34	1023±77	40.2±8.6	4.34±0.74	15.2±2.5
C12	18 May 05	8.20	504±40	1051±92	74.3±27	3.61±0.69	6.04±2

* First letter of sample name indicates the bay the sample is from: Copano Bay (C), Nueces Bay (N), or Baffin Bay (B), e.g. C1 is Copano Bay station 1.

Table 4.3: Salinity and dissolved Ra activity for Nueces Bay.

Station	Collected	Salinity	^{226}Ra (dpm m^{-3})	^{228}Ra (dpm m^{-3})	^{224}Ra (dpm m^{-3})	^{223}Ra (dpm m^{-3})	^{228}Th (dpm m^{-3})
NR*	12 Jul 04	0.00	183±14	206±17	312±117	13±2.6	17.2±5.6
N0†	10 Jul 04	3.27	251±22	461±48	438±152	24.1±5	26.3±4.2
N1	12 Jul 04	0.00	170±13	271±25	307±109	13.6±2.6	15.9±5.1
N2	10 Jul 04	1.08	236±18	316±29	491±178	12.4±2.6	25.9±4.2
N3	10 Jul 04	0.40	186±15	242±25	369±169	9.5±2.1	9.43±3
N4	10 Jul 04	2.00	230±17	344±27	386±149	16.1±3.2	22.5±7.2
N5	10 Jul 04	5.72	305±23	653±52	673±258	29±5.7	39.2±13
N8	10 Jul 04	1.40	248±19	367±31	543±241	11.2±2.4	22.2±7.1
N9	10 Jul 04	3.46	276±22	486±43	485±191	22.1±4.4	27±8.7
N10	10 Jul 04	0.45	135±10	144±13	163±46	10.4±2	9.55±1.6
N16	12 Jul 04	0.00	188±14	289±24	333±128	13.3±2.7	20±6.4
N17	12 Jul 04	0.00	213±17	355±31	251±67	16.1±3.1	20.8±3.4
NR	26 Jan 05	8.90	364±27	701±52	37.1±12	3.97±0.73	1.93±0.63
N0	26 Jan 05	24.80	276±21	921±71	27±4.5	3.37±0.62	4.1±0.72
N1	26 Jan 05	13.20	560±42	1269±99	66.7±13	4.22±0.75	1.67±0.31
N2	26 Jan 05	14.80	389±29	914±69	51.3±8.9	5.94±0.96	3.04±0.55
N4	26 Jan 05	23.50	304±23	847±66	37.7±12	2.8±0.48	2.16±0.71
N8	26 Jan 05	19.10	384±29	930±72	24.1±5	2.5±0.45	1.88±0.35
N16	26 Jan 05	13.30	483±35	1072±80	59.7±21	4.2±0.79	3.14±1
N17	26 Jan 05	13.40	525±38	1158±86	82.5±28	5.98±1.1	2.6±0.85
NR	27 May 05	18.20	719±61	1604±155	76.1±15	5.55±0.98	6.75±1.1
N0	25 May 05	27.20	337±26	1137±88	76.9±19	7.06±1.3	3.69±0.6
N1	27 May 05	20.20	891±66	2053±155	2521±873	105±18	21.5±7
N2	25 May 05	22.10	654±49	1671±127	1208±231	111±18	57.4±9.8
N3	27 May 05	21.40	802±64	1799±155	200±70	10.3±1.9	12.5±4
N4	25 May 05	26.80	395±30	1318±103	121±21	11±1.8	3.44±0.61
N5	25 May 05	26.70	380±32	1325±111	2315±779	158±26	58.2±19
N8	25 May 05	24.40	545±40	1567±115	651±119	47±7.5	7.67±1.3
N9	25 May 05	26.50	482±38	1628±130	201±70	9.01±1.6	3.93±1.3
N10	25 May 05	21.50	702±52	1718±131	109±41	4.71±0.87	3.44±1.1
N16	27 May 05	19.30	1122±87	2612±215	351±90	14.3±2.5	10.6±1.8
N17	27 May 05	20.60	864±67	2014±166	2359±539	125±21	7.28±1.4

† First letter of sample name indicates the bay the sample is from: Copano Bay (C), Nueces Bay (N), or Baffin Bay (B), e.g. N1 is Nueces Bay station 1.

* Station NR is the station nearest the Nueces River discharge to Nueces Bay.

Table 4.4: Salinity and dissolved Ra activity for Baffin Bay.

Station	Collected	Salinity	^{226}Ra (dpm m^{-3})	^{228}Ra (dpm m^{-3})	^{224}Ra (dpm m^{-3})	^{223}Ra (dpm m^{-3})	^{228}Th (dpm m^{-3})
B3*	15 Jul 04	30.80	450±36	1746±141	2223±1144	46.3±10	226±72
B4	15 Jul 04	22.70	473±35	1572±116	-	30.9±7.4	164±52
B5	15 Jul 04	19.40	515±38	1491±110	-	39.8±9.3	13.2±4.2
B6	15 Jul 04	15.50	587±43	1450±110	-	37.6±8.7	88.6±14
B7	15 Jul 04	16.80	549±41	1586±120	-	45.3±11	244±78
B8	15 Jul 04	16.40	530±39	1414±107	-	42±9.8	286±92
B9	15 Jul 04	14.20	467±35	1307±100	-	43.6±10	11.1±1.8
B10	15 Jul 04	14.80	484±39	1400±117	-	49.1±12	148±47
B11	15 Jul 04	13.50	499±37	1283±98	-	45.9±11	41.3±6.7
B12	15 Jul 04	12.40	469±34	1243±92	-	9.06±2.6	15.2±2.5
B3	08 Dec 04	34.90	316±25	1341±106	46.9±18	1.93±0.39	4.5±1.5
B4	08 Dec 04	33.90	481±36	1924±144	17±4.2	1.27±0.24	3.17±0.62
B7	08 Dec 04	30.10	591±44	1918±142	59.7±20	6.17±1.1	4.82±1.6
B8	08 Dec 04	30.10	619±45	2048±149	688±123	55.9±8.9	31.6±5.5
B9	08 Dec 04	27.40	676±49	2151±157	930±185	72.6±13	52.1±8.5
B10	08 Dec 04	28.50	669±50	2144±163	46.6±9.8	2.76±0.5	4.66±0.86
B11	08 Dec 04	27.70	687±51	2165±162	953±182	74.2±12	14.9±2.5
B4	08 Jun 05	37.60	588±46	2336±182	597±110	40.4±6.5	16.1±2.6
B5	08 Jun 05	36.60	658±49	2471±184	134±47	7.01±1.3	16.9±5.5
B6	08 Jun 05	37.40	828±60	2867±209	146±30	10.9±1.8	13.1±2.2
B7	08 Jun 05	36.70	753±55	2823±205	1059±207	62.9±11	12.8±2.1
B8	08 Jun 05	36.60	762±61	3099±247	188±36	12.7±2.2	15.6±2.6
B9	08 Jun 05	37.50	1164±100	3232±297	103±23	6.31±1.1	15.5±2.7
B10	08 Jun 05	37.00	785±57	2880±210	128±46	7.57±1.4	16.8±5.4
B11	08 Jun 05	36.80	773±57	2850±211	87.2±19	5.87±1	8.58±1.4

* First letter of sample name indicates the bay the sample is from: Copano Bay (C), Nueces Bay (N), or Baffin Bay (B), e.g. B1 is Baffin Bay station 1.

Table 4.5: Salinity and dissolved Ra activity for Aransas Pass.

Sample	Collected	Salinity	^{226}Ra (dpm m^{-3})	^{228}Ra (dpm m^{-3})	^{224}Ra (dpm m^{-3})	^{223}Ra (dpm m^{-3})	^{228}Th (dpm m^{-3})
1	16 Jul 04	-	138±10	252±21	-	15.6±4.4	33.9±11
2	29 Jul 04	34.60	144±11	339±30	1133±576	25.9±5.4	4.64±1.5
3	13 Aug 04	-	124±9.4	258±21	106±22	8.86±1.7	5.34±0.93
4	26 Sep 04	27.00	203±16	452±39	290±96	21.7±3.6	4.82±1.6
5	28 Sep 04	-	293±22	960±71	303±51	37.8±6	5.81±0.98
6	08 Oct 04	27.30	164±13	438±35	248±85	18.1±3.1	3.76±1.2
7	08 Oct 04	25.30	208±16	606±49	17.6±4.2	3.51±0.65	13.1±2.2
8	22 Oct 04	35.70	111±8.6	195±17	230±59	14.3±2.5	3.58±0.65
9	22 Oct 04	34.70	-	-	69.1±26	4.25±0.83	2.23±0.74
10	05 Nov 04	32.60	181±13	488±37	-	-	16.7±3
11	07 Nov 04	27.50	256±20	862±68	-	62±9.8	-
12	19 Nov 04	19.70	274±21	953±75	-	3.8±0.69	-
13	21 Nov 04	23.70	279±21	926±71	-	11.8±1.9	-
14	07 Dec 04	13.10	230±18	685±55	-	17.9±3.1	-
15	09 Dec 04	12.40	241±19	675±54	19.6±7.9	0.799±0.19	3.14±1
16	16 Dec 04	26.20	171±13	429±33	119±22	8.09±1.3	3.53±0.61
17	19 Dec 04	15.00	198±16	522±45	227±75	20.4±3.4	5.88±1.9
18	07 Jan 05	27.30	189±15	456±39	115±38	5.76±1	1.38±0.47
19	11 Jan 05	24.10	176±13	454±35	29.6±9.6	2.2±0.39	1.27±0.42
20	03 Feb 05	28.90	201±16	595±48	13.3±4.8	0.59±0.11	1.99±0.67
21	04 Feb 05	14.40	149±11	256±21	17.6±3.9	1.05±0.19	2.66±0.46
22	23 Feb 05	23.50	151±11	327±26	8.99±1.6	1.13±0.2	1.82±0.34
23	23 Feb 05	22.20	201±16	480±42	31.4±10	2.64±0.45	2.07±0.68
24	09 Mar 05	12.00	245±19	635±51	20.3±4	2.42±0.45	3.71±0.68
25	10 Mar 05	12.50	257±20	653±52	23.7±8.1	2.43±0.46	5.22±1.7
26	25 Mar 05	21.70	210±16	511±42	-	2.89±0.54	-
27	12 Apr 05	-	127±11	176±20	34.4±13	1.48±0.27	2.73±0.89
28	04 May 05	31.40	161±14	320±31	95.7±40	3.4±0.68	9.39±3
29	24 May 05	33.20	199±15	207±19	18.6±6.2	1.43±0.27	2.64±0.86
30	06 Jul 05	-	131±11	238±24	33.1±11	2.94±0.57	2.03±0.65
31	15 Jul 05	34.30	154±13	302±32	28.9±9.6	3.32±0.62	3.78±1.3
32	29 Jul 05	33.00	205±16	584±46	47.5±8.6	7.31±1.2	3.94±0.67

Table 4.6: Salinity and dissolved Ra activity for regional wells.

	Watershed	Collected	Salinity	^{226}Ra (dpm m^{-3})	^{228}Ra (dpm m^{-3})	^{224}Ra (dpm m^{-3})	^{223}Ra (dpm m^{-3})
W11	Nueces	28 Mar 05	3.70	311±23	1073±81	405±132	21.6±3.6
W12	Nueces	28 Mar 05	3.20	703±51	2924±213	592±103	52.6±8.3
W13	Nueces	28 Mar 05	8.00	334±25	1713±126	1281±425	51.9±8.4
W14	Nueces	28 Mar 05	8.90	515±40	2188±168	308±57	24.7±4
W15	Copano	28 Apr 05	3.90	680±49	1124±84	36.2±12	3.16±0.58
W16	Copano	28 Apr 05	3.60	1157±83	1293±94	175±42	5.91±1
W17	Copano	28 Apr 05	1.20	423±31	173±17	6.25±1.3	1.04±0.19
W18	Copano	28 Apr 05	2.20	805±59	587±47	52.6±19	5.38±0.93
W19	Copano	28 Apr 05	0.80	1505±108	73.1±10	3.15±4.2	4.52±0.78
W20	Copano	26 Jul 05	2.70	530±39	988±74	45±15	1.67±0.29
W21	Baffin	13 Jun 05	1.20	181±15	254±27	11.9±2.8	0.559±0.11
W22	Baffin	13 Jun 05	1.30	132±10	208±19	14.2±2.7	1.05±0.21
W23	Baffin	13 Jun 05	1.30	153±12	233±23	18.3±6.1	0.785±0.17
W24	Baffin	13 Jun 05	1.60	168±13	282±22	22±7.8	0.398±0.11
W25	Baffin	13 Jun 05	4.20	875±64	904±68	124±55	4.49±0.94
W26	Baffin	13 Jun 05	1.60	188±14	152±14	6.66±2.4	0.208±0.052
W27	Baffin	13 Jun 05	1.80	384±29	223±23	180±72	8.16±1.5
W28	Baffin	13 Jun 05	1.50	343±26	206±22	67.3±33	0.721±0.19
W29	Baffin	13 Jun 05	1.50	229±17	230±20	45.7±21	0.452±0.15
W30	Baffin	13 Jun 05	1.60	133±11	164±17	13.3±4	0.33±0.084
W31	Baffin	20 May 05	0.90	164±14	310±32	160±35	7.44±1.3
W32	Baffin	20 May 05	1.00	168±13	292±23	32.7±6.7	2.07±0.38
W33	Baffin	11 May 05	0.80	231±17	225±21	27.1±5.6	0.937±0.18
W34	Baffin	20 May 05	0.80	4542±326	291±26	4022±1483	193±33
W35	Other*	12 Apr 05	0.30	91±6.9	119±10	14.3±3.9	0.319±0.063

* On the north shore of Corpus Christi Bay and south of the Copano bay watershed.

Table 4.7: Methane concentrations in bay samples.

Sample	Station	Type	Collected	CH_4 (nM)
1	C1	bay	18 May 2005	8.21
2	C2	bay	18 May 2005	5.97
3	C3	bay	18 May 2005	4.34
4	C4	bay	18 May 2005	5.40
5	C5	bay	18 May 2005	7.91
6	C6	bay	18 May 2005	8.46
7	C7	bay	18 May 2005	8.51
8	C8	bay	18 May 2005	5.83
9	C9	bay	18 May 2005	6.36
10	C10	bay	18 May 2005	3.66
11	C11	bay	18 May 2005	4.80
12	C12	bay	18 May 2005	7.48
13	B4	bay	8 June 2005	5.91
14	B5	bay	8 June 2005	3.72
15	B6	bay	8 June 2005	3.51
16	B7	bay	8 June 2005	nd*
17	B8	bay	8 June 2005	3.22
18	B9	bay	8 June 2005	nd*
19	B10	bay	8 June 2005	3.45
20	B11	bay	8 June 2005	nd*
21	NR	bay	27 May 2005	33.12
22	NCH	salt marsh	27 May 2005	113.96
23	NSM	salt marsh	27 May 2005	73.91
24	N0	bay	25 May 2005	nd*
25	N1	bay	27 May 2005	17.70
26	N2	bay	25 May 2005	nd*
27	N3	bay	27 May 2005	11.61
28	N4	bay	25 May 2005	32.54
29	N5	bay	25 May 2005	5.30
30	N8	bay	25 May 2005	1.01
31	N9	bay	25 May 2005	17.55
32	N10	bay	25 May 2005	nd*
33	N16	bay	27 May 2005	67.69
34	N17	bay	27 May 2005	16.86

* nondetectable

Table 4.8: Methane concentrations in well samples.

Sample	Station	Type	Collected	CH_4 (nM)
35	W21	well	13 June 2005	175.38
36	W22	well	13 June 2005	103.44
37	W23	well	13 June 2005	85.54
38	W24	well	13 June 2005	86.27
39	W25	well	13 June 2005	121.40
40	W26	well	13 June 2005	302.39
41	W27	well	13 June 2005	242.28
42	W28	well	13 June 2005	105.53
43	W29	well	13 June 2005	232.33
44	W30	well	13 June 2005	137.35

* nondetectable

Table 4.9: Salinity and dissolved Ra activity of regional surface waters and surficial porewaters.

	Sample	Collected	Salinity	^{226}Ra (dpm m^{-3})	^{228}Ra (dpm m^{-3})	^{224}Ra (dpm m^{-3})	^{223}Ra (dpm m^{-3})
S1	Mission River	30 Nov 04	0.20	279±21	246±22	170±55	9.28±1.5
S2	Mission River	25 Jul 05	4.40	1040±79	1174±104	23.1±4.4	2.15±0.36
S3	Aransas River	07 Dec 04	0.90	266±19	483±36	74.2±26	1.59±0.3
S4	Hazel Bazemore pond	28 Mar 05	6.00	454±34	839±66	70.7±17	3.84±0.67
S5	Nueces marsh bayou	27 May 05	19.20	1079±79	2373±177	124±43	7±1.2
S6	Nueces marsh channel	27 May 05	25.90	1013±83	2240±203	132±25	10.3±1.8
S7	Los Olmos Creek	11 May 05	69.00	1034±75	3383±246	209±75	12.3±2.2
S8	Fish Pass*	28 Feb 05	43.90	1654±144	8507±729	-	73.4±12
S9	Nueces Bay*	18 Mar 05	1.80	678±99	292±88	279±100	12.4±2.8
S10	Bird Island	15 Jul 04	29.10	433±33	1877±142	3151±1657	82.4±18
S11	Laguna Madre	15 Jul 04	29.50	426±32	1904±144	-	7.34±2.3
S12	Bird Island	08 Dec 04	32.00	356±27	1452±109	1235±441	42.3±7.2
S13	Laguna Madre	08 Dec 04	33.70	391±30	1704±129	1337±449	70.7±12

* Sediment porewater samples.

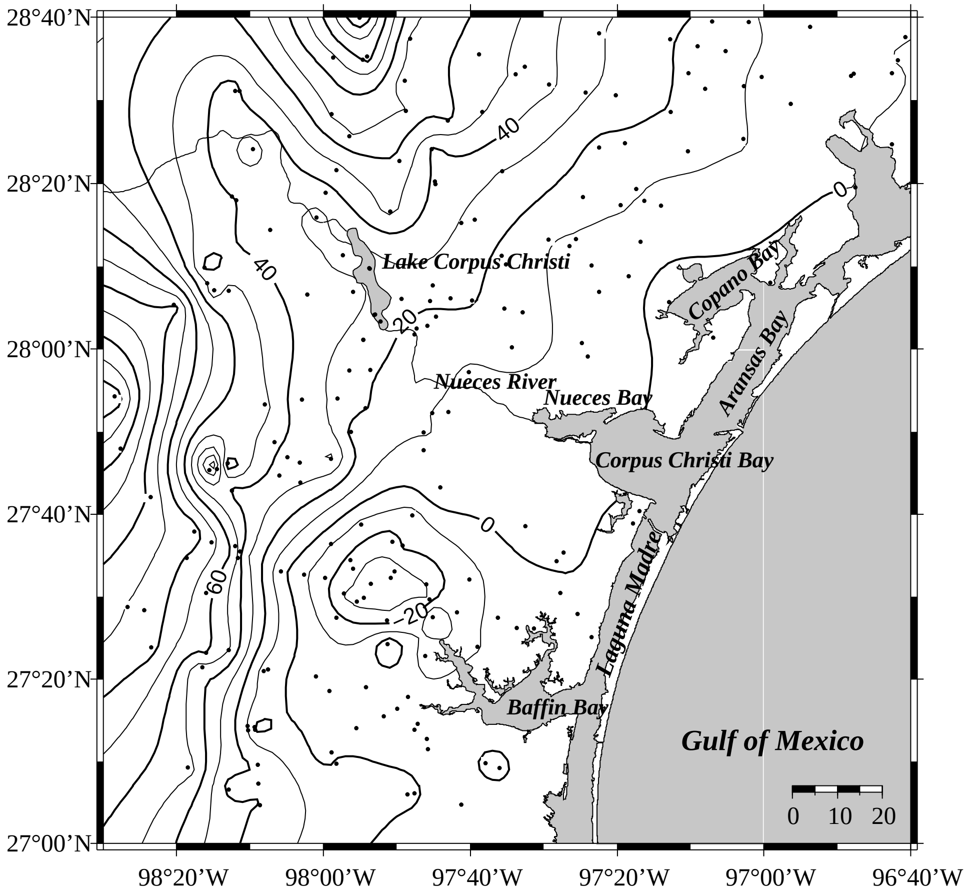

Figure 4.1: The regional groundwater equipotential surface relative to mean sea level contoured every 10 m. This shows the dramatic decrease in watertable elevation around Baffin Bay relative to Nueces Bay and Copano Bay. Water level measurements from 330 wells measured between 1995-2005 were used to create this map; the dots are the well locations. Where multiple observations of the same well were available the mean waterlevel was used. The data for this map was collected by the Texas Water Development Board (*Texas Water Development Board*, 2005a).

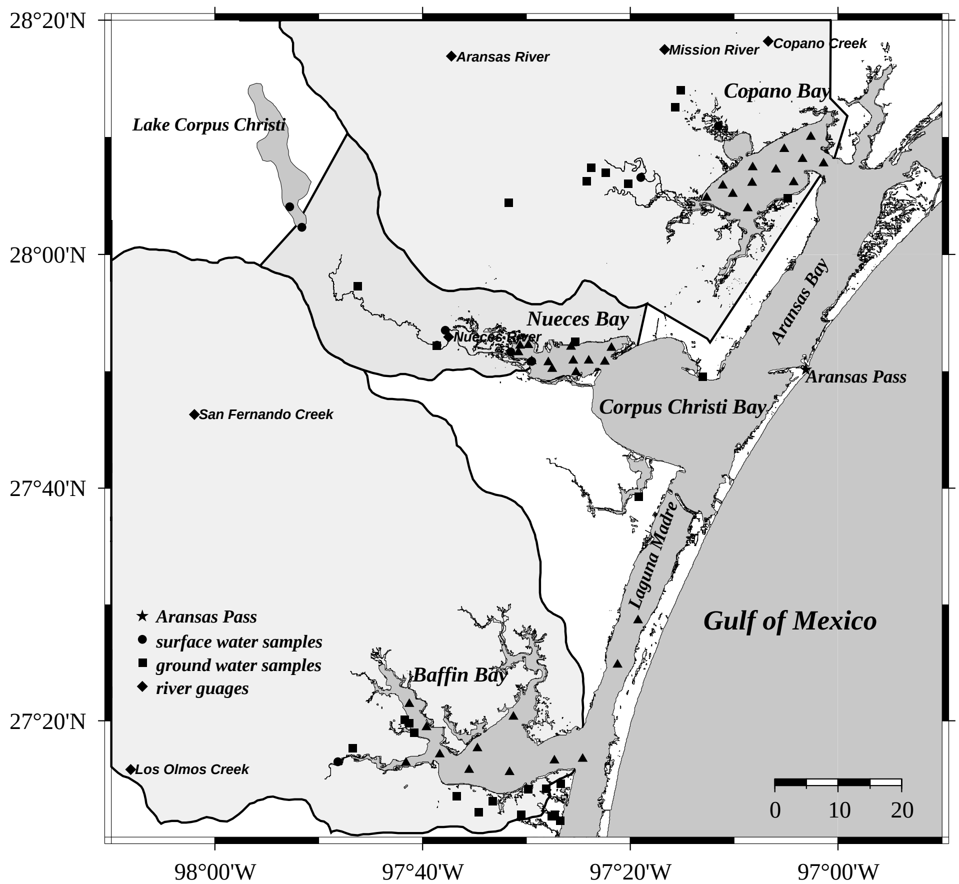

Figure 4.2: The Coastal Bend region of Texas showing the locations of Copano Bay, Nueces Bay, Baffin Bay, their watersheds, and the Aransas Pass connection to the Gulf of Mexico labeled with a solid star. Samples collected for this study are indicated by solid squares for well samples and solid triangles for surface water samples. The six stream gauges are indicated by solid diamonds.

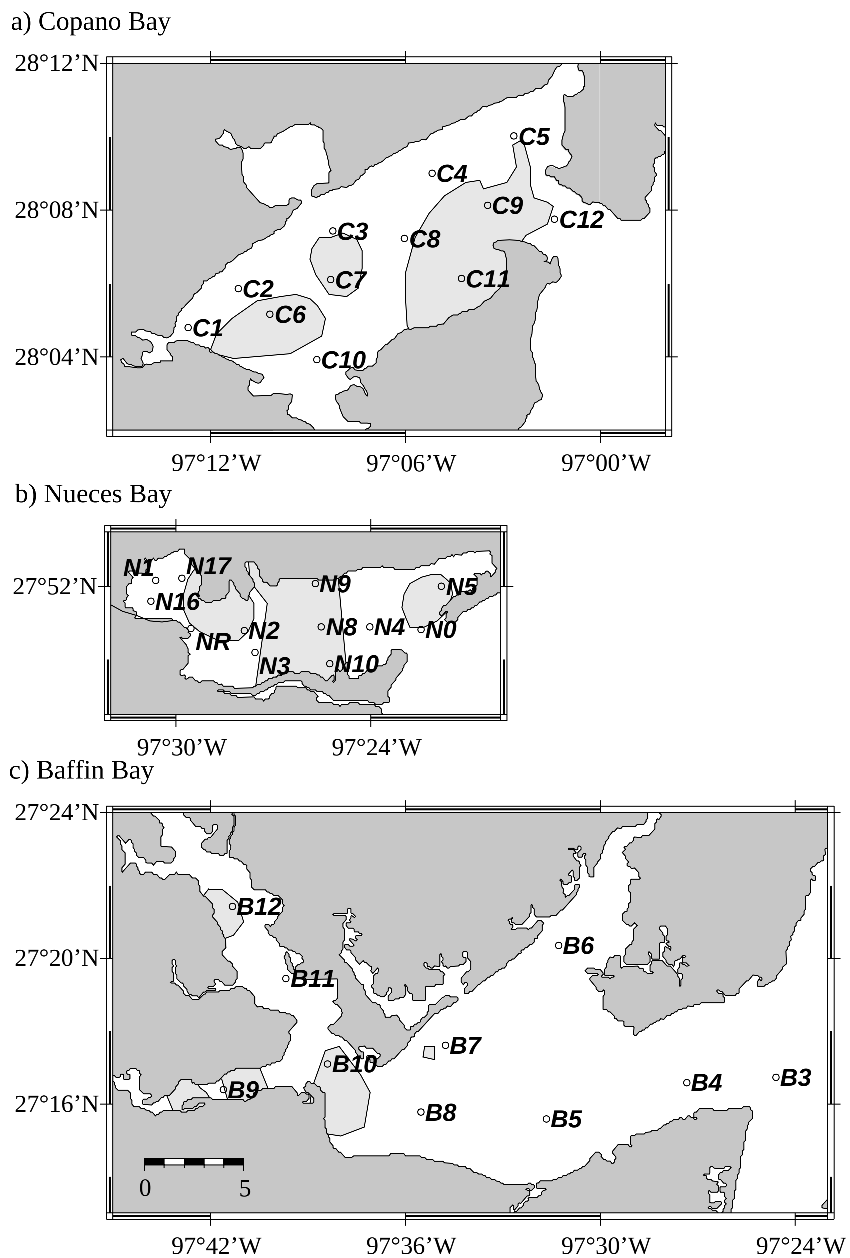

Figure 4.3: Sample station locations and areas with the highest number of petroleum wells and pipelines for a) Copano Bay, b) Nueces Bay and c) Baffin Bay. The gray shaded areas contain the majority of wells (>75%) in each bay though there are petroleum wells and pipelines outside these areas.

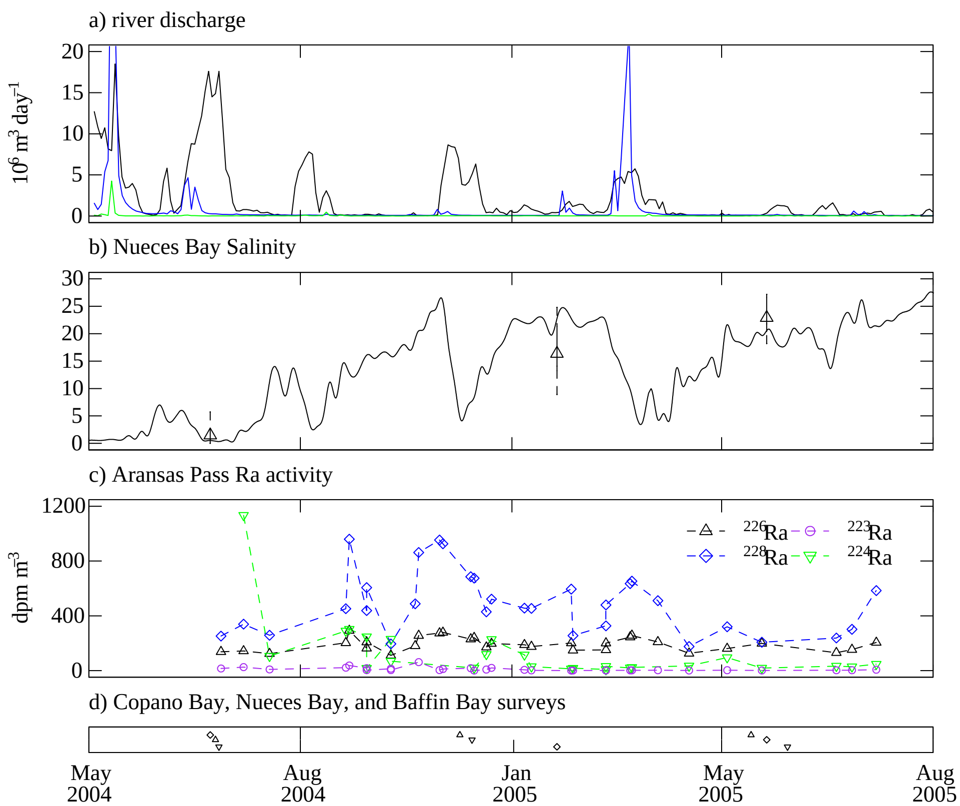

Figure 4.4: Time series data for a) gauged daily river discharge to Copano Bay (blue), Nueces Bay (black), and Baffin Bay (green); b) Nueces Bay salinity from the continuous salinity recorder at TCOON Salt03 near the center of Nueces Bay, the triangles with whiskers represent the mean and range of the salinities measured during the Nueces Bay Ra surveys; and c) the dissolved Ra activity at the tidal inlet at Aransas Pass; and d) the timing of the bay Ra surveys for Copano Bay (upward triangle), Nueces Bay (diamonds), and Baffin Bay (downward triangle).

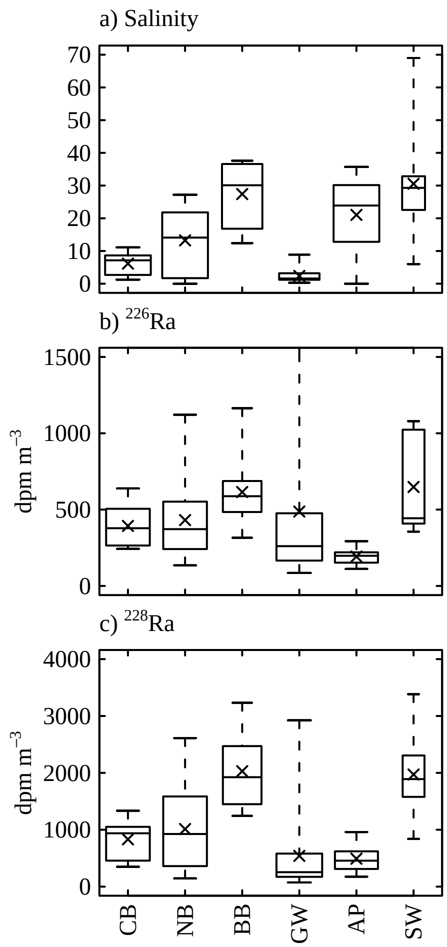

Figure 4.5: Combined results for the 2004-2005 samples: a) salinity, b) dissolved ^{226}Ra activity, and c) dissolved ^{228}Ra activity of Copano Bay (CB), Nueces Bay (NB), Baffin Bay (BB), the Aransas Pass (AP) tidal inlet, regional groundwater (GW), and associated rivers and surface waters (SW) summarized in box plots where box width is proportional to the square root of sample size, box height encompasses the 25th and 75th quantiles, the horizontal line is the median, the x symbol is the mean, and the whiskers extend to the extreme values.

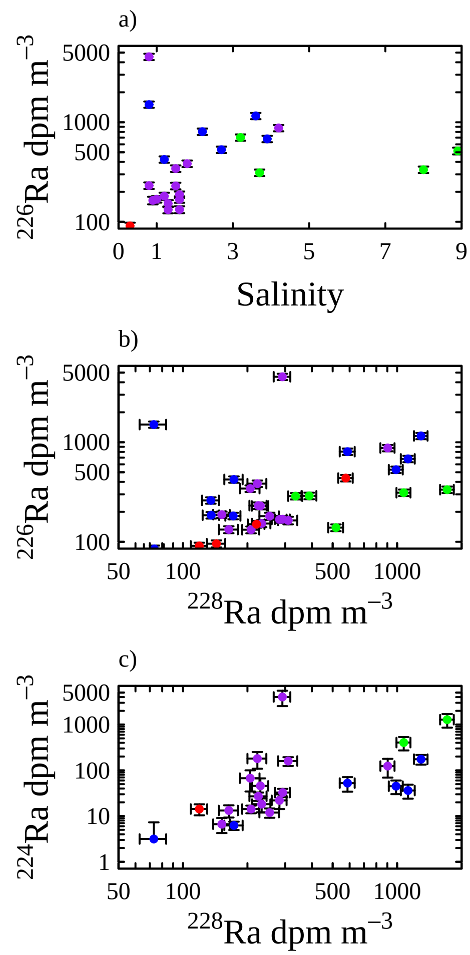

Figure 4.6: Regional groundwater a) ^{226}Ra activity versus salinity, b) ^{226}Ra activity versus ^{228}Ra activity, and c) ^{224}Ra activity versus ^{228}Ra activity. Samples are color coded by the watershed they are in: Copano wells are blue, Nueces wells are green, Baffin wells are purple, the red samples are wells located around Corpus Christi Bay or on the barrier islands. The observations can be grouped into several groundwater types: a low salinity high Ra activity groundwater, a high salinity moderate activity groundwater, and a low salinity low Ra activity groundwater. Surprisingly the two highest ^{226}Ra activities were from low salinity samples (the highest near Baffin Bay and the other in the Copano watershed near Refugio, Texas). The data includes 25 groundwater samples collected during this study and 10 groundwater samples collected previously (Chapter 2).

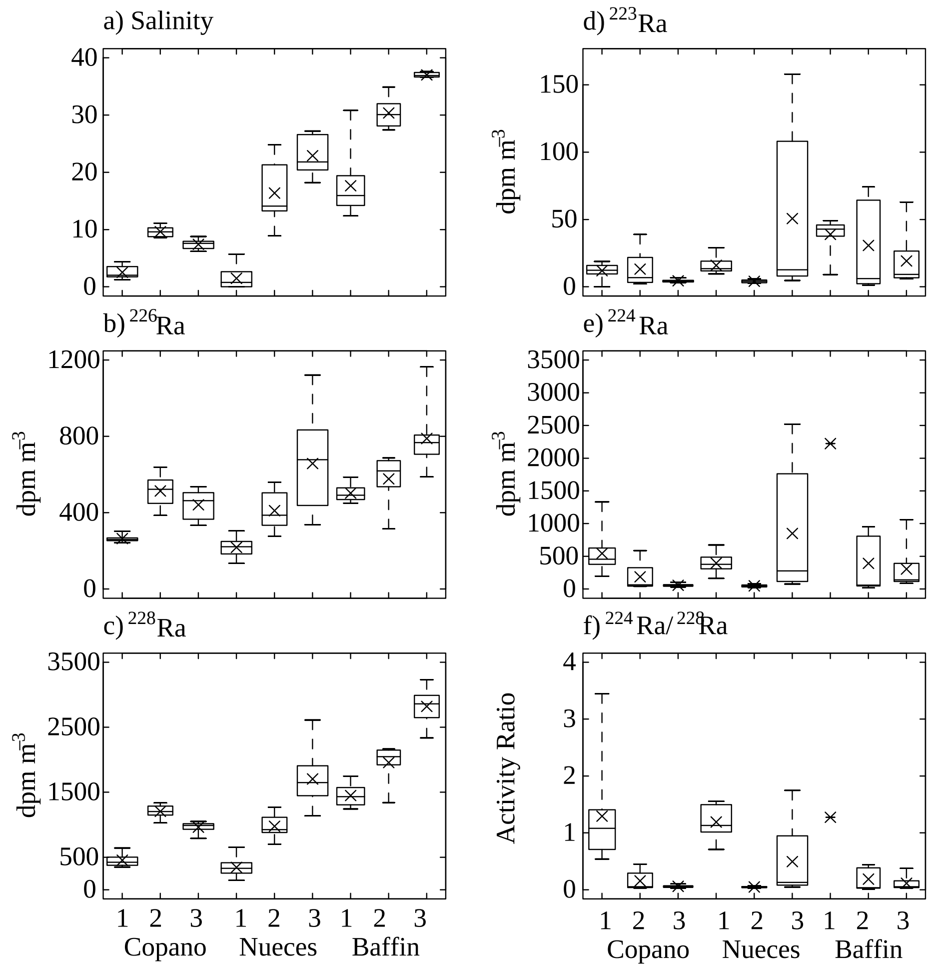

Figure 4.7: Seasonal comparisons between Copano Bay, Nueces Bay, and Baffin Bay a) salinity, b) dissolved ^{226}Ra activity, c) dissolved ^{228}Ra, d) ^{223}Ra activity, e) ^{224}Ra activity, and f) ^{224}Ra/^{228}Ra activity ratio summarized in box plots. Survey periods are labeled 1, 2, and 3 for their seasonal order.

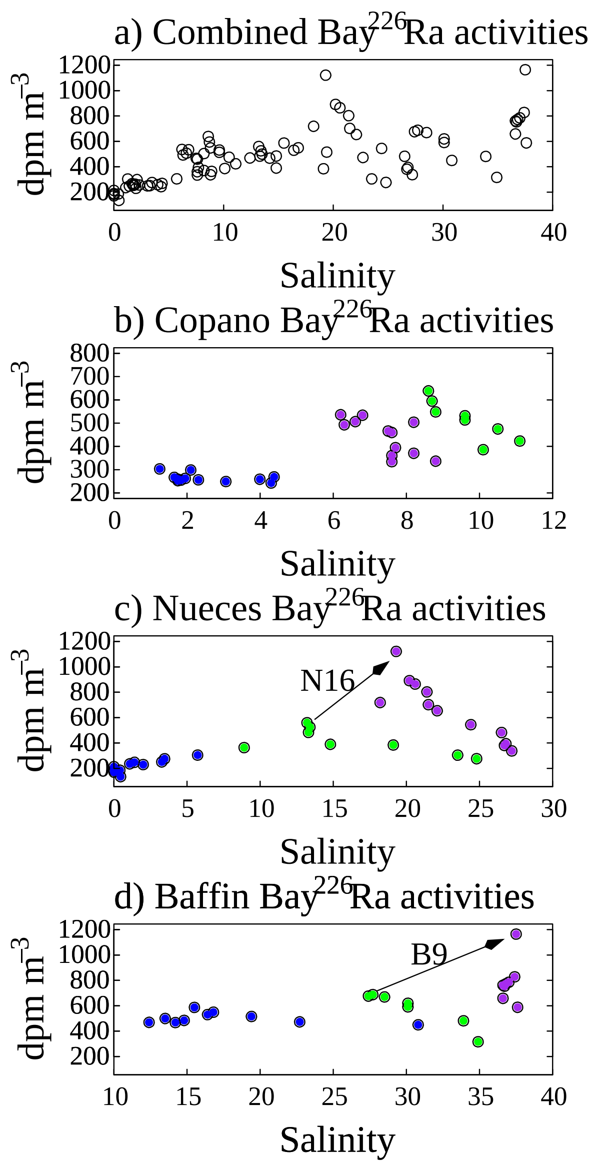

Figure 4.8: Dissolved ^{226}Ra activity versus salinity for all three survey periods for a) all three bays, b) Copano Bay, c) Nueces Bay, and d) Baffin Bay. For b), c), and d) the first survey samples are blue, second survey samples are green, and third survey samples are purple. Station B9 in Baffin Bay and N16 in Nueces Bay undergo the largest increases in dissolved ^{226}Ra activity and salinity.

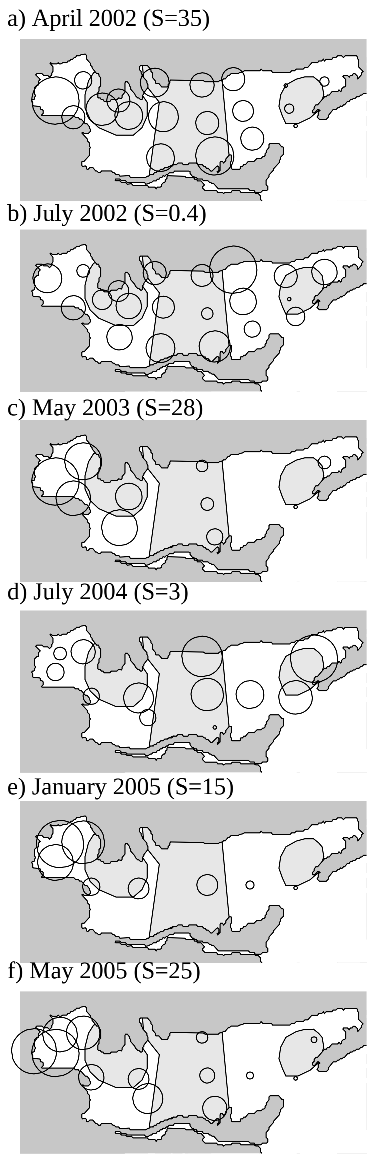

Figure 4.9: The spatial distribution of dissolved ^{226}Ra activity for all seven Nueces Bay surveys in this and the previous study (Chapter 2): a) April 2002, b) July 2002, c) May 2003, d) July 2004, e) January 2005, and f) May 2005. The mean salinity during the surveys are shown in the subtitles. Dissolved ^{226}Ra activities were highest at the head of Nueces Bay in all but two of the six surveys and those two surveys were immediately after Nueces Bay was flushed by high river discharge. Results are normalized for each period by subtracting the mean from each sample result and dividing by the standard deviation; circle sizes are not comparable between periods.

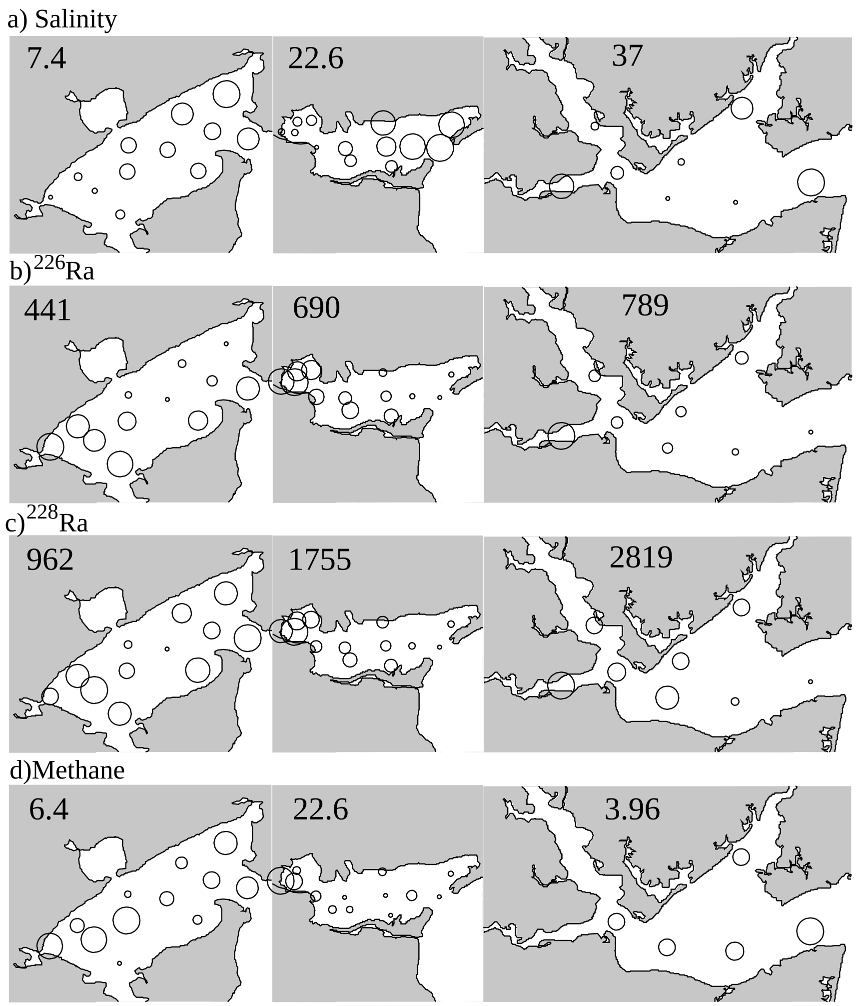

Figure 4.10: The spatial distribution of a) salinity, b)dissolved ^{226}Ra activity, c) dissolved ^{228}Ra activity, and d) CH_4 concentration for Copano Bay, Nueces Bay, and Baffin Bay during the final set of surveys (May-June 2005). Results are normalized for each bay by subtracting the mean from each sample result and dividing by the standard deviation. Circle sizes are not comparable between bays but the quantity means are shown for each bay.

Chapter 5

Conclusions: Identifying Submarine Fluid Discharges and their Impacts on Estuaries

The focus of this dissertation has been on developing methods and techniques for answering the question, "What is the submarine groundwater discharge (SGD) to Texas Coastal Bend Estuaries?" One of the things that made this particularly difficult to answer was the tide. This is initially surprising because the tide is so small along the Texas coast (15 cm range). The problem is the bays are shallow. Nueces Bay mean depth is <1 m so the tidal prism is actually 15% of the bay volume making the tides the biggest water fluxes in the bay. Although the relative tidal volume uncertainties are reasonable the absolute uncertainties are large, making mixing models (the main approach of Chapter 2) particularly uncertain. The other thing that made quantifying submarine groundwater discharge difficult was the potential confounding influence of oil-field brine leakage discovered during the course of this study. Oil field brine shares some of the same chemical traits as many coastal groundwater types, including enrichments in Ra and CH_4, but to an even greater degree.

In the end this dissertation is more notable for the approach and techniques used to evaluate submarine discharges rather than for producing precise estimates of discharge. First, the progressive series of smaller scale surveys has been effective in identifying areas of regionally high dissolved Ra activity and potential submarine discharges. Second, the novel combination of synoptic geophysical and geochemical surveys provided the type of complimentary surface water and sediment data that is needed to identify areas of groundwater and surface water interaction. Last, the regional geochemical intercomparison of bays indicated differences in Ra cycling between the bays.

5.1 Research Summary

The research was conducted along two complimentary lines: 1) a detailed study of submarine fluid discharge to Nueces Bay and 2) a regional comparison of SGD to Copano, Nueces, and Baffin Bays. In the first case, areas of submarine discharge within Nueces Bay were identified using a series of progressively more refined studies; starting at the regional level, down to the bay scale, and finally to specific subregions of the bay where discharge indications were strongest. In the second case, Copano, Nueces, and Baffin Bays were compared with one another in terms of changes in dissolved Ra activity over an annual wet-dry cycle.

Chapter 2 concerns the initial 2002–2003 field season that focused on Nueces Bay. The results provided evidence of a substantial submarine input of dissolved $^{226}\mathrm{Ra}$ to Nueces Bay. The dissolved Ra activities of Nueces Bay are among the highest observed in coastal estuaries; as great as 2600 dpm/m^3 for $^{228}\mathrm{Ra}$ and 660 dpm/m^3 for $^{226}\mathrm{Ra}$. Using a combination of salt and Ra mass balances I demonstrated that river discharge and bay bottom sediments cannot supply the Ra needed to balance tidal export. In the case of $^{226}\mathrm{Ra}$

there is an additional source of 218±105% 10^6 dpm/day that is 9 times the maximum estimated supply from bay bottom sediments and 50 times the Ra supplied by the Nueces River. Only a portion of this large flux can be supplied by SGD, given the Ra activity of local groundwater.

Chapter 3 concerns a synoptic geophysical and geochemical survey conducted to further investigate the occurrence and spatial distribution of submarine discharges of water to the head of Nueces Bay. Previous dissolved Ra measurements in the 12 km^2 head of bay (Chapter 2) had suggested a significant submarine groundwater discharge. The 17 kilometer survey incorporated continuous resistivity profiling, measurements of surface water salinity, temperature, and dissolved oxygen, and point measurements of dissolved Ra isotopes. The resistivity survey indicated vertical fingers of high conductivity extending up through 7 meters of bay bottom sediments into the surface water within 100 m of surface salinity and dissolved Ra maxima ($^{226}\mathrm{Ra}$ >600 dpm/m^3). At these locations there were also peaks in water temperature and lows in dissolved oxygen. These results indicate either submarine brackish groundwater discharge or the leakage of oil-field brine from submerged petroleum pipelines.

Chapter 4 concerns the final 2004–2005 field season that compares the Ra activities of Copano, Nueces, and Baffin Bays at three periods during the seasonal transition from relatively fresh water to seawater. Measurements of dissolved CH_4 are also used as independent indicators of oil-field brine leakage and SGD. These results show that the seasonal increase in dissolved ^{226}Ra activity for Nueces Bay is substantially larger than for either Copano Bay or Baffin Bay. This increase cannot be readily explained by either evaporation or riverine supply. In addition, Nueces Bay has significantly higher CH_4 concentrations than either Copano or Baffin Bay. The CH_4 concentrations are highest at the head of Nueces Bay in the same area where dissolved ^{226}Ra activities were highest in every non-flood stage Nueces Bay survey (4 out of 6 periods). These results clearly suggest that the Ra supply to Nueces Bay is unusually large. The most relevant differences between the three bays that might account for this are 1) the proportionally larger salt marsh at the head of Nueces Bay and 2) the higher density of petroleum wells and pipelines.

5.2 Conclusions

Considered together the results indicate a large submarine Ra flux at the head of Nueces Bay. The Ra activity of the flux is probably very high. While SGD cannot be ruled out and may play an important role in the high Ra activities observed in Nueces Bay it is unlikely that SGD alone could explain the seasonal trends and absolute activities observed in the open waters of Nueces Bay. The leakage of oil-field brine potentially could explain those activities.

The actual leakage rate (volume per unit time) depends on the radium activity of the leaking brine which is highly variable and not well characterized. Based on available data, the leakage rate is potentially from 200 to 6,290 m^3 day^{-1}. Because the results of Chapter 3 suggest the greatest leakage is in the head of Nueces Bay, the wells and pipelines in this area should be inspected and if they are in fact leaking brine samples should be collected to determine their dissolved ^{226}Ra activity. From the activity of the leakage it would be possible to determine whether or not other wells might also be leaking.

The leakage of oil-field brine needs to be understood because it has potentially important ecological consequences especially in the shallow and restricted waters of the Texas Coastal Bend. Oilfield brine is very saline, up to S=37 (*Kraemer and Reid*, 1984), and therefore denser than the water in most of the regional bays. Oilfield brine is also anoxic and can have high concentrations of total organic carbon which can deplete dissolved oxygen concentrations when mixed with surface waters. A recent survey of permitted oil-field brine discharges from 50 oil rigs in the Gulf of Mexico by *Veil et al.* (2005) showed that mean brine total organic carbon was 564 mg/l and mean biological oxygen demand was 957 mg/l. Significant leakage of such water in restricted areas could accumulate during dry periods promoting stratification and anoxia in bottom waters, a recurring problem in some areas of the Texas Coastal Bend.

Finally, turning to the question, "What is the nitrogen contribution of submarine groundwater discharge to Texas Coastal Bend estuaries?" This question cannot be directly answered at this time for two principal reasons: 1) the uncertainties on the water flux estimates are large and 2) it is unknown how much of the flux is oil-field brine and how much is groundwater. However either of these inputs would represent significant nutrient loadings to the bay. This would be especially true during dry periods when river inputs are low, particularly in the case of oil-field brine leakage which would not change seasonally. For groundwater the regional mean nitrate concentration is 1.7 mg L^{-1} N as NO_3^- (*Texas Water Development Board*, 2005a).[1] Assuming that 1) this is representative of brackish groundwater discharge, 2) nitrate is the dominate dissolved inorganic nitrogen species in brackish groundwater discharge, and 3) the submarine Ra input is entirely due to an advecting groundwater discharge of 31,100 m^3 day^{-1}, and 3) then the associated nitrogen input would be 19 million g N yr^{-1}. For Gulf of Mexico oil-field brines measured by *Veil et al.* (2005), ammonium is the dominate form of dissolved inorganic nitrogen and the mean concentration is 57.5 mg L^{-1} N as NH_4^+. Assuming this is 1) representative of oil-field brine leakage to Nueces Bay and 2) the submarine Ra input is entirely due to an oil-field brine input of 6,290 m^3 day^{-1} then the associated nitrogen input would be 132 million g N yr^{-1}. These inputs are less than estimates of nitrogen loading to Nueces Bay from wastewater

[1]Based on 778 NO_3^- measurements made during the period of record from 1931 to 2005 (*Texas Water Development Board*, 2005a). The samples were collected from 308 wells in the following counties: Aransas, Atascosa, Bee, Brooks, Calhoun, De Witt, Duval, Goliad, Jim Wells, Kennedy, Kleberg, Live Oak, McMullen, Nueces, Refugio, San Patricio, and Victoria.

(400-1500 million g N yr^{-1})(*Brock*, 2001) but they are not trivial.

Additional work is necessary to fully understand the chemical implications of these potential submarine water fluxes. Persistent leakage of the sizes suggested by the results has the potential for altering the DIN/DON ratio of bay water particularly in restricted areas during periods of low river discharge. Influencing DIN/DON ratios is same type of forcing mechanism that *Laroche et al.* (1997) concluded was the causal link between groundwater discharge and the initiation of harmful algal blooms in Peconic Bay, Long Island.

5.3 Future Studies

The results of this dissertation raise several questions that would be interesting to address in future studies. One line of investigation should address whether there is significant leakage from the oil-field network in Nueces Bay both in terms of dissolved Ra supply and in terms of ecologically relevant fluxes such as nitrogen and total organic carbon. This question could not be directly addressed in this dissertation because access to the location of the oil wells was not available until after all the data was collected. Now that the well and pipeline locations are readily available (*Texas Railroad Commission*, 2005), and with the results from this dissertation, it would be straightforward to develop a targeted and representative sampling plan to directly assess oil-field leakage in Nueces Bay. I believe a combination of targeted geochemical sampling and aerial thermal IR photography is the most efficient approach to such a study.

Dissolved Ra has the potential to be an excellent tracer of oil-field brine leakage because of the large dynamic range between oil-field brine Ra activities and those of bay water; however, a more thorough sampling of local endmember brines needs to carried out to make full use of Ra as a tracer of brine leakage. Particularly valuable would be samples of brine collected before separation tanks, i.e., before $BaSO_4$ has a chance to precipitate and remove a portion of the dissolved Ra. Additional oil-field brine indicators such as Br/Cl ratio, the presence of hydrocarbons, methane, and carbon isotopes of methane may also be useful in confirming whether leakage is occurring. However, the potential smaller dynamic range (relative to dissolved Ra) of these indicators may require that samples be collected close to a leak. Since oil-field brine is geothermally heated perhaps the easiest way to locate oil-field brine leakage in a shallow estuary such as Nueces Bay would be with thermal infrared photography. The potential submarine discharge features identified in the synoptic geochemical and geophysical survey results (Figure 3.4) appear to be over 0.5° Celsius above background bay temperatures. Such a temperature difference is detectable by thermal IR cameras such as the FLIR Thermovision A40M which can measure temperature differences less than 0.1° Celsius.

Another line of investigation could explore salt marsh hydrology and Ra cycling. The results of this dissertation indicate that the Nueces salt marsh may be a significant source of Ra to Nueces Bay. This would be consistent with conclusions from studies of other salt marshes such as North Inlet, South Carolina (*Rama and Moore*, 1996), and Great Sippewissett Marsh, Massachusetts (*Charette et al.*, 2003). However more work is required to determine what processes are actually contributing the dissolved Ra. Specifically work needs to be done to determine whether significant groundwater advection occurs within the marsh and its bayous. This could be done with surveys similar to those conducted in Chapter 2 of this dissertation. In addition, installation of shallow wells in the marsh to obtain groundwater samples would also be worthwhile. The flux of Ra from the marsh sediments should also be examined in detail including 1) measurements of sediment Th concentrations, 2) experiments to determine the desorbable sediment bound Ra fraction, and 3) flux chamber experiments to evaluate the total Ra supply from diffusion, sediment compaction, and bioirrigation.

Finally, there is reason to believe that Texas Coastal Bend bay dissolved nitrogen speciation may be driven in part by the submarine discharges suggested by this dissertation. Such a relationship would be modulated by the strong seasonal and interannual fluctuations in the regional precipitation cycle. Therefore, evaluating the ecological effects of such submarine discharges would greatly benefit from long term time series such as the 11 year record of algal cell counts, bay nitrogen concentrations, and terrestrial watertable levels which *Laroche et al.* (1997) used to evaluate brown tide bloom initiation in Peconic Bay, Long Island, New York.

Appendix A

Well Sampling and Locations

Table A.1: Well locations and data.

ID	Latitude	Longitude	Well Owner	Well Power
W1	27.836000	-97.033333	Jake and Helen Garret	Downhole Pump
W2	27.836000	-97.033333	UTMSI	Downhole Pump
W3	27.653970	-97.319950	Moorehead	Downhole Pump
W4	27.875270	-97.422000	Koonce	Windmill
W5	27.954730	-97.771720	San Patricio Catholic Church	Downhole Pump
W6	28.073420	-97.528940	Sinton Municipal Golf Course	Downhole Pump
W7	28.104630	-97.403500	Welder Wildlife Refuge	Windmill
W8	28.123230	-97.396510	Welder Wildlife Refuge	Windmill
W9	28.100660	-97.336750	Welder Wildlife Refuge	Windmill
W10	28.115830	-97.373890	Welder Wildlife Refuge	Downhole Pump
W11	27.870090	-97.644150	Nueces River Authority	none
W12	27.870090	-97.644150	Nueces River Authority	none
W13	27.870090	-97.644150	Nueces River Authority	none
W14	27.870090	-97.644150	Nueces River Authority	none
W15	28.233800	-97.252830	Fennessey Ranch	Downhole Pump
W16	28.233800	-97.252830	Fennessey Ranch	Artesian Flowing
W17	28.208970	-97.261760	Fennessey Ranch	Artesian Flowing
W18	28.233800	-97.252830	Fennessey Ranch	Artesian Flowing
W19	28.208970	-97.261760	Fennessey Ranch	Artesian Flowing
W20	28.079660	-97.080790	Ploch	Downhole Pump

Table A.1: Continued.

ID	Latitude	Longitude	Well Owner	Well Power
W21	27.225340	-97.612350	Kenedy Ranch	Downhole Pump
W22	27.201910	-97.577030	Kenedy Ranch	Downhole Pump
W23	27.217670	-97.555210	Kenedy Ranch	Downhole Pump
W24	27.198650	-97.508940	Kenedy Ranch	Downhole Pump
W25	27.196080	-97.459820	Kenedy Ranch	Downhole Pump
W26	27.189720	-97.446430	Kenedy Ranch	Artesian Flowing
W27	27.198400	-97.454817	Kenedy Ranch	Artesian Flowing
W28	27.235183	-97.497883	Kenedy Ranch	Windmill
W29	27.236000	-97.468867	Kenedy Ranch	Artesian Flowing
W30	27.243367	-97.445700	Kenedy Ranch	Artesian Flowing
W31	27.330040	-97.689080	Hill	Downhole Pump
W32	27.334400	-97.695760	A. R. Brown	Downhole Pump
W33	27.316640	-97.680600	Riveria City Park	Downhole Pump
W34	27.293900	-97.779520	Rudealot	Windmill
W35	27.825965	-97.217681	Thauburn	Downhole Pump
W36†	28.22059	-97.27502	Fennessey Ranch	Windmill
W37†	28.22613	-97.2616	Fennessey Ranch	Artesian Flowing
W38†	28.24212	-97.26394	Fennessey Ranch	Artesian Flowing
W39†	28.2331	-97.28163	Fennessey Ranch	Windmill
W40†	28.24327	-97.25245	Fennessey Ranch	Windmill

† Well was not sampled for Ra isotopes.

The University of Texas at Austin
Marine Science Institute
750 Channel View Drive
Port Aransas, TX 78373

EMAIL: jbreier@utmsi.utexas.edu *PHONE: (361) 749-6823*

Limited - Free Nitrate and Radium Well Sampling

November 30, 2004

To All Texas Coastal Bend Well Owners,

We are conducting a study of groundwater discharge to Texas Coastal Bend Bays including Nueces, Baffin, and Copano. As part of this study we need to sample regional well water for nitrate and radium concentrations. Low levels of nitrate are normal while high levels can be an indication of human impacted water generally from fertilizers and human and animal waste. Radium is a naturally occurring element which occurs in very low concentrations and can only be measured with very sensitive lab equipment.

Well sampling is simple and usually takes less than a half hour. Samples can be collected from pump and windmill discharges. Wells not continuously flowing must be pumped for several minutes prior to sampling. If a holding tank is connected to the well, samples must be collected between the pump and holding tank which typically means the holding tank must be temporarily disconnected.

Well owners will receive the results of the nitrate and radium measurements. Sampling in this phase of the study will be limited to less than thirty wells and wells will not be accepted if nearby wells of similar depth have already been sampled - so apply soon! To apply call (361) 749-6773 and leave your name, number, and the general location of your well (such as 5 miles southeast of Sinton).

Sincerely,

John (Chip) Breier

Figure A.1: This letter was posted and handed out throughout the study area in order to identify well owners willing to have their wells sampled.

Appendix B

Bay and Surface Water Station Locations

Table B.1: Station locations for 2002-2003 Nueces Bay Ra study.

Station	Latitude	Longitude
1	27.846950	-97.374333
2	27.855617	-97.378067
3	27.867550	-97.379950
4	27.869583	-97.357783
5	27.870717	-97.410183
6	27.854500	-97.404683
7	27.840433	-97.399400
8	27.848350	-97.425350
9	27.868017	-97.428433
10	27.831483	-97.421033
11	27.851600	-97.450833
12	27.869200	-97.455667
13	27.852050	-97.470783
14	27.859900	-97.476767
15	27.855433	-97.485850
16	27.859967	-97.512933
17	27.870400	-97.497117
18	27.851417	-97.502533
19	27.830517	-97.452433
20	27.866483	-97.517517
21	27.836317	-97.476000

Table B.2: Surface water sample station locations.

Sample	Water	Latitude	Longitude
S1[†]	Mission River	28.183006	-97.192170
S2[†]	Mission River	28.183006	-97.192170
S3[†]	Aransas River	28.109871	-97.316770
S4[†]	Hazel Bazemore pond	27.870090	-97.644150
S5[†]	Nueces marsh bayou	27.860810	-97.525460
S6[†]	Nueces marsh pond	27.860600	-97.525490
S7[†]	Los Olmos Creek	27.274620	-97.802960
S8[†]	Fish Pass Porewater	27.680030	-97.172330
S9[†]	Nueces Bay Porewater	27.847433	-97.492183
S10[†]	Bird Island (B1)	27.476967	-97.321450
S11[†]	Laguna Madre (B2)	27.414133	-97.353983
S12[†]	Bird Island (B1)	27.476967	-97.321450
S13[†]	Laguna Madre (B2)	27.414133	-97.353983
NR1[‡]	Nueces River	27.847440	-97.492180
NR2[‡]	Nueces River	28.038570	-97.860730
NR3[‡]	Nueces River	27.891910	-97.630810
NR4[‡]	Nueces Bay	27.847440	-97.492180
NR5[‡]	Nueces Bay	27.853660	-97.490970
NR6[‡]	Nueces Bay	27.850970	-97.492500
NR7[‡]	Nueces Bay	27.839200	-97.436110
NR8[‡]	Nueces Bay	27.839120	-97.435430
NR9[‡]	Nueces Bay	27.851960	-97.489100
NR10[‡]	Nueces Bay	27.838280	-97.418530
NR11[‡]	Nueces Bay	27.850130	-97.485340
NR12[‡]	Nueces Bay	27.842390	-97.388350

[†] The surface water samples reported in Table 4.8.
[‡] The Nueces River and Nueces Bay samples reported in Table 2.2.

Table B.3: Sample station locations for upper Nueces Bay synoptic geophysical and geochemical study.

Station	Latitude	Longitude
1	27.852500	-97.500556
2	27.855556	-97.508889
3	27.857222	-97.514444
4	27.859722	-97.516111
5	27.863611	-97.516389
6	27.869444	-97.514167
7	27.878333	-97.501944
8	27.879167	-97.495833
9	27.876944	-97.493333
10	27.874167	-97.490278
11	27.870833	-97.488056
12	27.865833	-97.490556
13	27.865833	-97.498889
14	27.867222	-97.501667
15	27.868611	-97.504722
16	27.869722	-97.507778
17	27.870278	-97.508889
18	27.861111	-97.506389
19	27.859444	-97.504167
20	27.855278	-97.497500
21	27.851944	-97.495278
22	27.850278	-97.493889
23	27.849444	-97.492500
24	27.847222	-97.490556
25	27.847222	-97.491667
26	27.848056	-97.488889
27	27.848611	-97.486667
28	27.849722	-97.485556

Table B.4: Station locations for 2004-2005 regional Ra study.

Station	Bay	Latitude	Longitude
B3	Baffin	27.278717	-97.410050
B4	Baffin	27.276450	-97.455767
B5	Baffin	27.259667	-97.527800
B6	Baffin	27.339317	-97.521467
B7	Baffin	27.293617	-97.579500
B8	Baffin	27.262883	-97.592000
B9	Baffin	27.273083	-97.693333
B10	Baffin	27.284917	-97.639883
B11	Baffin	27.324100	-97.661183
B12	Baffin	27.357133	-97.688800
C1	Copano	28.080083	-97.211467
C2	Copano	28.097633	-97.185750
C3	Copano	28.123917	-97.137250
C4	Copano	28.150217	-97.086383
C5	Copano	28.167200	-97.044300
C6	Copano	28.085950	-97.169383
C7	Copano	28.101717	-97.138417
C8	Copano	28.120417	-97.100417
C9	Copano	28.135617	-97.057750
C10	Copano	28.065467	-97.145417
C11	Copano	28.102300	-97.071200
C12	Copano	28.129300	-97.023450
NR	Nueces	27.847433	-97.492183
N0	Nueces	27.846950	-97.374333
N1	Nueces	27.869500	-97.510233
N2	Nueces	27.846433	-97.464883
N3	Nueces	27.836450	-97.459517
N4	Nueces	27.848300	-97.400517
N5	Nueces	27.866783	-97.363733
N8	Nueces	27.848350	-97.425350
N9	Nueces	27.868017	-97.428433
N10	Nueces	27.831483	-97.421033
N16	Nueces	27.859967	-97.512933
N17	Nueces	27.870400	-97.497000

Appendix C

Nutrient Concentrations

Measurements of dissolved nutrients were made on the majority of groundwater and bay water samples (Table C.6). Nutrient samples were collected in 25 mL polyethylene bottles, filtered to 0.45 μm using silica-free filters, and frozen until analysis. Dissolved nutrient concentrations (nitrate+nitrite ($NO_3^- + NO_2^-$), ammonium (NH_4^+), orthophosphate (PO_4^{3-}), and amorphous silica (SiO_2)) were measured following traditional methods using a Lachat Quikchem 8000 autoanalyzer. Samples were run in duplicate against standards prepared in low-nutrient Gulf of Mexico seawater (*Yamane and Asito*, 1992).

Table C.1: Nutrient Concentrations for Nueces Bay, April 2002

Station	PO_4^{3-} (μM)	$\mathrm{SiO_2}$ (μM)	$\mathrm{NO_3^-} + \mathrm{NO_2^-}$ † (μM)
1	0.59	76.91	0.54
2	0.26	185.58	0.90
3	0.12	104.01	0.68
4	0.52	129.95	1.48
5	0.23	177.39	0.59
6	0.12	167.16	0.84
7	0.01	221.56	0.64
8	0.42	280.80	1.17
9	0.18	190.91	0.43
10	0.29	300.70	0.68
11	1.29	301.79	6.56
12	0.07	275.39	0.70
13	1.18	272.52	5.06
14	1.22	326.05	7.00
15	1.30	268.56	5.78
16	0.95	280.03	0.26
17	1.46	297.84	6.19
18	1.24	260.60	0.23
19	0.51	280.25	0.25

† Nutrient analysis for ammnonium not reported due to measurement difficulties.

Table C.2: Nutrient Concentrations for Nueces Bay, July 2002

Station	PO_4^{3-} (μM)	$\mathrm{SiO_2}$ (μM)	$\mathrm{NO_3^-} + \mathrm{NO_2^-}$ † (μM)
1	3.70	313.02	3.88
2	2.92	377.95	2.54
3	3.49	363.14	0.73
4	2.31	678.12	1.03
5	2.71	457.77	0.48
6	2.28	395.68	1.14
7	3.33	418.33	0.75
8	2.49	324.10	1.53
9	2.40	394.59	1.13
10	2.57	289.56	1.82
11	2.72	377.21	4.74
12	2.65	510.67	0.49
13	2.11	639.65	6.64
14	1.79	344.94	16.30
15	2.22	474.59	6.57
17	2.26	638.72	4.63
18	2.57	338.71	6.37
19	2.64	536.99	5.28
20	3.50	445.99	7.26
21	3.24	253.66	2.23

† Nutrient analysis for ammonium not reported due to measurement difficulties.

Table C.3: Nutrient Concentrations for Nueces Bay, 19 May 2003

Station	PO_4^{3-} (μM)	SiO_2 (μM)	NH_4^{+} † (μM)
1	0.15	56.16	3.37
4	0.37	169.46	0.27
8	0.41	75.85	0.38
9	0.74	181.43	0.08
10	0.49	102.52	0.12
13	0.62	131.39	0.84
16	0.53	70.94	1.77
17	0.44	78.37	0.15
18	0.46	70.25	0.06
21	0.24	58.41	0.13

† Nutrient analysis for $NO_3^- + NO_2^-$ not reported due to measurement difficulties.

Table C.4: Nutrient Concentrations for Nueces Bay, 27 May 2003

Station	PO_4^{3-} (μM)	$\mathrm{SiO_2}$ (μM)	$\mathrm{NH_4^+}$† (μM)
1	0.11	43.72	0.15
4	0.54	157.43	0.20
8	0.18	64.61	0.54
9	0.65	79.74	0.81
10	0.48	118.64	0.10
13	0.77	118.12	68.60
16	0.26	76.47	22.97
17	0.55	78.84	1.00
18	0.53	106.08	5.47
21	0.58	84.60	0.52

† Nutrient analysis for $\mathrm{NO_3^-} + \mathrm{NO_2^-}$ not reported due to measurement difficulties.

Table C.5: Bay nutrient concentrations for 2004-2005 regional Ra study.

ID	Collected	NH_4^+ (μM)	PO_4^{3-} (μM)	SiO_2 (μM)	$NO_3^- + NO_2^-$ (μM)
B1	8 Dec 04	0.16	0.08	180.85	0.00
B2	8 Dec 04	0.27	0.07	183.63	0.00
B3	8 Dec 04	0.09	0.26	181.51	0.00
B4	8 Dec 04	9.32	0.11	129.45	0.18
B7	8 Dec 04	0.21	0.17	212.29	0.23
B8	8 Dec 04	0.26	0.49	220.72	0.00
B9	8 Dec 04	0.44	0.13	229.27	0.00
B10	8 Dec 04	0.22	0.38	190.59	0.00
B11	8 Dec 04	0.23	0.10	207.70	0.06
C2	1 Dec 04	0.14	1.53	274.61	1.24
C3	1 Dec 04	0.20	1.85	259.81	0.50
C5	1 Dec 04	20.08	1.73	233.48	0.25
C8	1 Dec 04	10.25	0.57	246.87	0.10
C9	1 Dec 04	23.42	1.24	219.17	1.07
C10	1 Dec 04	6.00	1.99	246.89	0.97
C11	1 Dec 04	4.70	1.44	215.55	2.38
C12	1 Dec 04	0.33	0.74	232.14	0.54
NR	26 Jan 05	0.29	1.61	150.48	3.65
N0	26 Jan 05	0.01	0.31	75.88	0.06
N1	26 Jan 05	0.22	2.46	66.06	0.20
N2	26 Jan 05	0.06	1.70	119.27	0.26
N4	26 Jan 05	0.01	0.13	95.46	0.14
N8	26 Jan 05	0.12	1.04	76.86	0.22
N16	26 Jan 05	0.09	1.86	94.30	0.12
N17	26 Jan 05	0.56	2.22	108.50	0.13

Table C.5: Continued.

ID	Collected	NH_4^+ (μM)	PO_4^{3-} (μM)	SiO_2 (μM)	$NO_3^- + NO_2^-$ (μM)
B4	8 Jun 05	1.18	0.21	247.76	0.00
B5	8 Jun 05	43.45	1.85	226.20	2.97
B6	8 Jun 05	2.74	0.69	236.56	6.67
B7	8 Jun 05	8.12	0.83	245.76	5.73
B8	8 Jun 05	1.27	0.24	242.86	5.02
B9	8 Jun 05	0.02	0.11	213.66	0.06
B10	8 Jun 05	11.30	1.35	240.84	4.40
B11	8 Jun 05	7.66	1.22	242.95	8.46
C1	18 May 05	0.20	0.39	71.87	0.10
C2	18 May 05	0.26	1.29	90.29	0.28
C3	18 May 05	0.11	1.39	104.38	0.06
C4	18 May 05	0.11	1.01	50.95	0.12
C5	18 May 05	0.36	1.63	124.44	0.22
C6	18 May 05	0.12	2.14	117.32	0.11
C7	18 May 05	0.14	1.59	107.11	0.15
C8	18 May 05	0.11	1.87	127.25	0.07
C9	18 May 05	0.49	1.89	60.13	2.31
C10	18 May 05	0.23	0.20	89.67	0.11
C11	18 May 05	0.17	1.76	115.41	0.13
C12	18 May 05	0.11	0.90	91.96	0.13
NR	27 May 05	0.05	0.58	147.99	0.00
N0	25 May 05	0.00	0.57	70.78	0.02
N1	27 May 05	0.57	2.08	101.28	0.30
N2	25 May 05	0.00	0.32	85.27	0.17
N3	27 May 05	0.06	0.47	93.99	0.04
N4	25 May 05	0.00	0.66	77.75	0.08
N5	25 May 05	0.01	0.46	79.39	0.07
N8	25 May 05	0.00	0.91	87.28	0.09
N9	25 May 05	0.00	0.66	80.74	0.05
N10	25 May 05	0.04	0.38	72.51	0.45
N16	27 May 05	0.14	1.27	126.72	0.15
N17	27 May 05	1.30	0.37	107.17	0.69

Table C.6: Well sample nutrient concentrations.

ID	Collected	NH_4^+ (μM)	PO_4^{3-} (μM)	SiO_2 (μM)	$NO_3^- + NO_2^-$ (μM)
W1	3 Jun 03	11.6	2.5	275.4	6.9
W2	3 Jun 03	4.6	0.3	347.8	10.8
W3	3 Jun 03	4.1	0.6	355.4	4.4
W4	9 Oct 02	7.7	nd	196.9	177.5
W5	9 Oct 02	1.2	0.0	346.1	4.0
W6	9 Oct 02	1.2	0.1	173.3	0.9
W7	9 Oct 02	1.0	0.2	296.4	nd
W8	15 May 03	1.4	0.2	310.8	0.2
W9	15 May 03	0.3	0.2	309.5	0.9
W10	16 May 03	0.9	-	311.5	nd
W11	28 Mar 05	0.1	0.4	146.1	2.5
W12	28 Mar 05	0.2	0.7	102.4	0.3
W13	28 Mar 05	0.1	1.2	124.8	0.0
W14	28 Mar 05	0.0	0.2	57.1	0.1
W15	28 Apr 05	12.2	0.2	100.1	0.0
W16	28 Apr 05	6.9	0.2	101.2	0.0
W17	28 Apr 05	3.13	0.4	92.3	0.0
W18	28 Apr 05	6.8	0.3	106.2	0.4
W19	28 Apr 05	-	-	-	-
W20	26 Jul 05	14.3	2.1	117.5	0.1
W21	13 Jun 05	0.1	0.2	106.4	1.9
W22	13 Jun 05	0.1	0.2	105.3	0.5
W23	13 Jun 05	0.1	0.1	91.1	3.6
W24	13 Jun 05	0.1	0.1	97.6	1.2
W25	13 Jun 05	0.1	0.1	78.5	0.4
W26	13 Jun 05	0.0	0.2	99.7	0.0
W27	13 Jun 05	0.0	0.2	108.4	0.1
W28	13 Jun 05	0.1	0.2	114.0	1.4
W29	13 Jun 05	0.1	0.3	110.9	0.2
W30	13 Jun 05	0.1	0.3	114.1	2.2
W31	20 May 05	1.0	0.2	113.7	0.1
W32	20 May 05	0.7	0.2	105.8	0.2
W33	11 May 05	0.0	0.3	110.8	2.9
W34	20 May 05	nd	0.3	123.7	0.1
W35	12 Apr 05	33.1	8.6	91.3	33.9
W36	28 Apr 05	0.80	0.5	99.6	0.2
W37	28 Apr 05	6.46	0.3	109.7	0.1
W38	28 Apr 05	12.21	0.4	105.3	nd
W39	28 Apr 05	6.49	0.3	105.5	0.1
W40	28 Apr 05	3.01	0.5	111.7	0.0

† Well was not sampled for Ra isotopes.

Bibliography

Abdullah, K. C., The Holocene eustatic record as recorded in the offshore incised valley fill deposits of the Brazos River, Ph.D. thesis, Rice University, 1995.

Armstrong, N. E., and G. H. Ward, Analysis of point source discharges (including oil-field brine discharges) in the Corpus Christi Bay National Estuary Program study area, *CCBNEP-30*, Corpus Christi Bay National Estuary Program, 1998.

Basu, A. R., S. B. Jacobson, R. J. Poreda, C. B. Dowling, and P. K. Aggarwal, Large groundwater strontium flux to the oceans from the Bengal Basin and the marine strontium isotope record, *Science*, *293*, 1470–1473, 2001.

Bersezio, R., A. Bini, and M. Giudici, Effects of sedimentary heterogeneity on groundwater flow in a Quaternary pro-glacial delta environment: joining facies analysis and numerical modelling, *Sedimentary Geology*, *129*, 327–344, 1999.

Bokuniewicz, H. J., Analytical descriptions of subaqueous groundwater seepage, *Estuaries*, *15*, 458–464, 1992.

Brandenberger, J., P. Louchouarn, B. Herbert, P. Tissot, Geochemical and hydrodynamic controls on trace metal cycling in a seasonally stratified US sub-tropical reservoir, *Applied Geochemistry*, *19*, 1601–1623, 2004.

Bratton, J. F., J. F. Crusius, J. K. Meunier, T. B. Spruill, and B. M. Wrege, Use of continuous resistivity profiling to detect low-salinity ground water beneath the Upper Neuse River Estuary, North Carolina, *EOS Trans. AGU, 85*, Fall Meet. Suppl., Abstract H24A–04, 2004.

Breier, J. A., and H. N. Edmonds, High ^{226}Ra and ^{228}Ra activities in Nueces Bay, Texas indicate submarine saline discharges, *Marine Chemistry*, submitted.

Breier, J. A., C. F. Breier, and H. N. Edmonds, Detecting submarine groundwater discharge with synoptic surveys of sediment resistivity, radium, and salinity, *Geophysical Research Letters 32*, L23612, doi:10.1029/2005GL024639, 2005.

Breier, J. A., H. N. Edmonds, and T. A. Villareal, Submarine groundwater discharge and associated nutrient fluxes to the Corpus Christi Bay system, *Contract 2002483416*, Texas Water Development Board, 2004.

Brock, D. A., Nitrogen budget for low and high freshwater inflows, Nueces Estuary, Texas, *Estuaries*, *24*, 509–521, 2001.

Brune, G., *Springs of Texas*, vol. I, Branch-Smith, Fort Worth, TX, 1981.

Bugna, G. C., J. P. Chanton, J. E. Cable, W. C. Burnett, and P. H. Cable, The importance of groundwater discharge to the methane budgets of nearshore and continental shelf waters of the northeastern Gulf of Mexico, *Geochimica et Cosmochimica Acta, 60*, 4735–4746, 1996.

Burnett, W. C., M. Taniguchi, and J. Oberdorfer, Measurement and significance of the direct discharge of groundwater into the coastal zone, *Journal of Sea Research, 46*, 109–116, 2001.

Burnett, W. C., H. Bokuniewicz, M. Huettel, W. S. Moore, and M. Taniguchi, Groundwater and porewater inputs to the coastal zone, *Biogeochemistry*, *66*, 3–33, 2003.

Burnett, W. C., et al., Assessing methodologies for measuring groundwater discharge to the ocean, *Eos, Transactions AGU*, *83*, 177–123, 2002.

Buskey, E. J., B. Wysor, and C. Hyatt, The role of hypersalinity in the persistence of the Texas brown tide in the Laguna Madre, *Journal of Plankton Research*, *20*, 1553–1565, 1998.

Cable, J. E., G. C. Bugna, W. C. Burnett, and J. P. Chanton, Application of $^{222}\mathrm{Rn}$ and CH_4 for assessment of groundwater discharge to the coastal ocean, *Limnology and Oceanography*, *41*, 1347–1353, 1996.

Cable, J. E., W. C. Burnett, and J. P. Chanton, Magnitude and variation of groundwater seepage along a florida marine shoreline, *Limnology and Oceanography*, *38*, 189–205, 1997a.

Cable, J. E., W. C. Burnett, J. P. Chanton, D. R. Corbett, and P. H. Cable, Field evaluation of seepage meters in the coastal marine environment, *Estuarine, Coastal, and Shelf Science*, *45*, 367–375, 1997b.

Caudle, C. S., An impact assessment of produced water discharges to Nueces Bay, , Texas Water Commission, 1993.

Cech, I., M. Lemma, C. W. Kreitler, and H. M. Prichard, Radium and radon in water supplies from the Texas gulf coast aquifer, *Water Research*, *22*, 109–121, 1988.

Chapelle, F. H., *The Hidden Sea*, Geosciences Press, Tucson, Arizona, 1997.

Charette, M. A., and K. O. Buesseler, Submarine groundwater discharge of nutrients and copper to an urban subestuary of Chesapeake Bay (Elizabeth River), *Limnology and Oceanography*, *49*, 376–385, 2004.

Charette, M. A., K. O. Buesseler, and J. E. Andrews, Utility of radium isotopes for evaluating the input and transport of groundwater-derived nitrogen to a Cape Cod estuary, *Limnology and Oceanography*, *46*, 465–470, 2001.

Charette, M. A., R. Splivallo, C. Herbold, M. S. Bollinger, and W. S. Moore, Salt marsh submarine groundwater discharge as traced by radium isotopes, *Marine Chemistry*, *84*, 113–121, 2003.

Corbett, D. R., K. Dillon, W. Burnett, and J. Chanton, Estimating the groundwater contribution into Florida Bay via natural tracers, $^{222}\mathrm{Rn}$ and $\mathrm{CH_4}$, *Limnology and Oceanography*, *45*, 1546–1557, 2000.

Davis, S. N., D. O. Whittemore, and J. Fabryka-Martin, Uses of chloride/bromide ratios in studies of potable water, *Ground Water*, *36*, 338–350, 1998.

Diener, R. A., Cooperative Gulf of Mexico estuarine inventory and study - Texas: area description, *Technical Report NMFS CIRC-393*, National Oceanic and Atmospheric Administration, 1975.

Division of Nearshore Research, Texas Coastal Ocean Observation Network: Stations SALT01, SALT03, SALT05, 011, and 008, Texas A&M University at Corpus Christi, Corpus Christi, Texas, *http://dnr.cbi.tamucc.edu/TCOON*, 2003.

Dunton, K. H., H. Alexander, and K. Jackson, Emergent vegetation and soil characteristics, In *Rincon Bayou diversion project annual report 2002-2003*, pp. 31–39, The University of Texas at Austin Marine Science Institute, Port Aransas, Texas, 2004.

Fetter, C. W., *Applied Hydrogeology*, Prentice-Hall, Upper Saddle River, New Jersey, 1994.

Freeze, R. A., and J. A. Cherry, *Groundwater*, Prentice-Hall, Englewood Cliffs, New Jersey, 1979.

Gramling, C. M., D. McCorkle, A. E. Mulligan, and T. L. Woods, A carbon isotope method to quantify groundwater discharge at the land sea interface, *Limnology and Oceanography*, *48*, 957–970, 2003.

Hancock, G. L., I. T. Webster, P. W. Ford, and W. S. Moore, Using Ra isotopes to examine transport processes controlling benthic fluxes into a shallow estuarine lagoon, *Geochimica et Cosmochimica Acta*, *64*, 3685–3699, 2000.

Hudak, P. F., Regional trends in nitrate content of Texas groundwater, *Journal of Hydrology*, *228*, 37–47, 2000.

Hudak, P. F., and D. J. Wachal, Effects of brine injection wells, dry holes, and plugged oil/gas wells on chloride, bromide, and barium concentrations in the Gulf Coast Aquifer, southeast Texas, USA, *Environment International*, *26*, 497–503, 2001.

Hussain, N., T. M. Church, and G. Kim, Use of $^{222}\mathrm{Rn}$ and $^{226}\mathrm{Ra}$ to trace groundwater discharge into Chesapeake Bay, *Marine Chemistry*, *65*, 127–134, 1999.

Johannes, R. E., The ecological significance of the submarine discharge of groundwater, *Marine Ecology Progress Series*, *3*, 365–373, 1980.

Jones, E. J., Investigations of the seafloor using electrical methods, In *Marine Geophysics*, pp. 217–241, Wiley, Chichester, England, 1991.

Karpen, V., L. Thomsen, and E. Suess, A new ’schlieren’ technique application for fluid flow visualization at cold seep sites, *Marine Geology*, *204*, 145–159, 2004.

Kehew, A. E., *Applied Chemical Hydrogeology*, Prentice Hall, Upper Saddle River, New Jersey, 2000.

Kelly, R. P., and S. B. Moran, Seasonal changes in groundwater input to a well mixed estuary estimated using radium isotopes and implications for coastal nutrient budgets, *Limnology and Oceanography*, *47*, 1796–1807, 2002.

Kraemer, T. F., and D. F. Reid, The occurrence and behavior of radium in saline formation water of the U.S. gulf coast region, *46*, 153–174, 1984.

Kreitler, C. W., and D. C. Jones, Natural soil nitrate: the cause of the nitrate contamination of ground water in Runnels county, Texas, *Ground Water*, *13*, 53–61, 1975.

Krest, J. M., and J. W. Harvey, Using natural distributions of short lived radium isotopes to quantify groundwater discharge and recharge, *Limnology and Oceanography*, *48*, 290–298, 2003.

Krest, J. M., W. S. Moore, and Rama, $^{226}\mathrm{Ra}$ and $^{228}\mathrm{Ra}$ in the mixing zones of the Mississippi and Atchafalaya Rivers: indicators of groundwater input, *Marine Chemistry*, *64*, 129–152, 1999.

Langevin, C. D., Simulation of ground-water discharge to Biscayne Bay, southeastern florida, *WRIR 00-4251*, U.S. Geological Survey, 2001.

Laroche, J., R. Nuzzi, R. Waters, K. Wyman, P. G. Falkowski, and D. W. R. Wallace, Brown tide blooms in Long Island's coastal waters linked to interannual variability in groundwater flow, *Global Change Biology*, *3*, 397–410, 1997.

Michael, H. A., J. S. Lubetsky, and C. F. Harvey, Characterizing submarine groundwater discharge: a seepage meter study in Waquoit Bay, Massachusetts, *Geophysical Research Letters*, *30*, 1–4, 2003.

Millero, F. J., and A. Poisson, International one-atmosphere equation of state of seawater, *Deep-Sea Research*, *128*, 625–629, 1981.

Moore, W. S., Radium isotope measurements using germanium detectors, *Nuclear Instruments and Methods in Physics Research*, *223*, 407–411, 1984.

Moore, W. S., Large groundwater inputs to coastal waters revealed by $^{226}\mathrm{Ra}$ enrichments, *Nature*, *380*, 612–614, 1996.

Moore, W. S., High fluxes of radium and barium from the mouth of the Ganges-Brahmaputra River during low river discharge suggest a large groundwater source, *Earth and Planetary Science Letters*, *150*, 141–150, 1997.

Moore, W. S., The subterranean estuary: a reaction zone of ground water and sea water, *Marine Chemistry*, *65*, 111–125, 1999.

Moore, W. S., Determining coastal mixing rates using radium isotopes, *Continental Shelf Research*, *20*, 1993–2007, 2000.

Moore, W. S., and R. Arnold, Measurement of $^{223}\mathrm{Ra}$ and $^{224}\mathrm{Ra}$ in coastal waters using a delayed coincidence counter, *Journal of Geophysical Research*, *101*, 1321–1329, 1996.

Moore, W. S., H. Astwood, and C. Lindstrom, Radium isotopes in coastal waters on the amazon shelf, *Geochimica et Cosmochimica Acta*, *59*, 4285–4298, 1995.

National Atmospheric and Oceanic Administration, National Climate Data Center: Station COOPIDs 410805, 411651, 412015, 417170, 417677, 415661, 418354, and 419559, *http://www.ncdc.noaa.gov/oa/climate/stationlocator.html* , 2003.

Nowicki, B. L., E. Requintina, D. V. Keuren, and J. Portnoy, The role of sediment denitrification in reducing groundwater-derived nitrate inputs to Nauset Marsh estuary, *Estuaries*, *22*, 245–259, 1999.

Oberdorfer, J. A., Hydrogeologic modeling of submarine groundwater discharge: comparison to other quantitative methods, *Biogeochemistry*, *66*, 159–169, 2003.

Pennock, J. R., J. N. Boyer, J. A. Herrera-Silveira, R. L. Iverson, T. E. Whitledge, B. Mortazavi, and F. A. Comin, Nutrient behavior and phytoplankton production in Gulf of Mexico estuaries, In *Biogeochemistry of Gulf of Mexico Estuaries*, pp. 3–10, Wiley, 1999.

Pilson, M. E. Q., Salinity, Chlorinity, Conductivity, and Density, In *An Introduction to the Chemistry of the Sea*, pp. 41–57, Prentice-Hall, 1998.

Rama, and W. S. Moore, Using the radium quartet for evaluating groundwater input and water exchange in salt marshes, *Geochimica et Cosmochimica Acta*, *60*, 4645–4652, 1996.

Rutgers van der Loeff, M. M., and W. S. Moore, Determination of natural radioactive tracers, In *Methods of Seawater Analysis*, pp. 365–397, Wiley-VCH, Weinheim, Germany, 1999.

Rutkowski, C. M., W. C. Burnett, R. L. Iverson, and J. P. Chanton, The effect of groundwater seepage on nutrient delivery and seagrass distribution in the northeastern Gulf of Mexico, *Estuaries*, *22*, 1033–1040, 1999.

Ryder, P. D., Ground water atlas of the United States. Segment 4, Oklahoma, Texas, *HA-730E*, U.S. Geological Survey, 1996.

Sauer, V. B., and R. W. Meyer, Determination of error in individual discharge measurements, *Open File Report 92-144*, U. S. Geological Survey, 1992.

Schwartz, F. W., and H. Zhang, Regional Ground-Water Flow, In *Fundamentals of Ground Water*, pp. 183–218, John Wiley & Sons, 2003.

Schwartz, M. C., Significant groundwater input to a coastal plain estuary: assessment from excess radon, *Estuarine, Coastal and Shelf Science*, *56*, 31–42, 2003.

Scott, M. K., and S. B. Moran, Ground water input to coastal salt ponds of southern Rhode Island estimated using $^{226}\mathrm{Ra}$ as a tracer, *Journal of Environmental Radioactivity*, *54*, 163–174, 2001.

Sewell, P. L., Urban groundwater as a possible nutrient source for an estuarine benthic algal bloom, *Estuarine, Coastal and Shelf Science*, *13*, 569–576, 1982.

Shafer, G. H., Groundwater resources of Nueces and San Patricio counties, *Report 73*, Texas Water Development Board, 1968.

Sharma, P. V., Earth resistivity methods, In *Geophysical methods in geology*, Elsevier, Amsterdam, The Netherlands, 1976.

Simmons, C. T., T. R. Fenstemaker, and J. M. Sharp Jr., Variable-density groundwater flow and solute transport in heterogeneous porous media: approaches, resolutions and future challenges., *Journal of Contaminant Hydrology*, *52*, 245–275, 1991.

Smith, N. P., Numerical simulations of bay-shelf exchange with a one-dimensional model, *Contributions in Marine Science*, *28*, 1:13, 1985.

Solis, R. S., and G. L. Powell, Hydrography, Mixing Characteristics, and Residence Times of Gulf of Mexico Estuaries, In *Biogeochemistry of Gulf of Mexico Estuaries*, pp. 29–61, Wiley, 1999.

Stieglitz, T., Submarine groundwater discharge into the near-shore zone of the Great Barrier Reef, Australia, *Marine Pollution Bulletin*, pp. 51–59, 2005.

Swarzenski, P. W., C. D. Reich, R. M. Spechler, J. L. Kindinger, and W. S. Moore, Using multiple geochemical tracers to characterize the hydrogeology of the submarine spring off Crescent Beach, Florida, *Chemical Geology*, *179*, 187–202, 2001.

Texas Water Development Board, Groundwater records, *http://www.twdb.state.tx.us/DATA/waterwell/well_info.asp*, Texas Water Development Board, 2005.

Texas Water Development Board, Evaporation/precipitation data for Texas, *http://hyper20.twdb.state.tx.us/Evaporation/evap.html*, Texas Water Development Board, 2005.

Texas Railroad Commission, Public GIS viewer, *http://gis2.rrc.state.tx.us/public/*, Texas Railroad Commission, 2005.

Tunnel, J. W. J., Origin, Development, and Geology, In *The Laguna Madre of Texas and Tamaulipas*, pp. 28–37, Texas A&M University Press, College Station, Texas, 2002.

U.S. Geological Survey, GIRAS landuse/landcover data for the conterminous united states by quadrangles at scale 1:250,000, *http://www.epa.gov/OWOW/watershed/landcover* , 2005a.

U.S. Geological Survey, Surface water for Texas: Daily streamflow, *http://waterdata.usgs.gov/tx/nwis/discharge*, 2005b.

Valiela, I., et al., Coupling of watersheds and coastal waters: sources and consequences of nutrient enrichment in Waquiot Bay, Massechusetts, *Estuaries*, *15*, 443–457, 1992.

Veeh, H. H., W. S. Moore, and S. V. Smith, The behaviour of uranium and radium in an inverse estuary, *Continental Shelf Research*, *15*, 1569–1583, 1995.

Veil, J. A., T. A. Kimmell, and A. C. Rechner, Characteristics of produced water discharged to the Gulf of Mexico hypoxic zone, *ANL/EAD/05-3*, Argonne National Laboratory, 2005.

Webster, I. T., G. J. Hancock, and A. S. Murray, Modelling the effect of salinity on radium desorption from sediments, *Geochimica et Cosmochimica Acta*, *59*, 2469–2476, 1995.

Weight, W. D., and J. L. Sonderegger, *Manual of Applied Field Hydrogeology*, McGraw Hill, 2000.

Woodman, J. T., Availability of groundwater, Coastal Bend region, Texas, Ph.D. thesis, The University of Texas at Austin, 1975.

Yamane, T., and M. Asito, Simple approach for elimination of blank peak effects in flow injection analysis of samples containing trace analyte and excess of another solute, *Talanta*,*39*, 215–219, 1992.

Vita

John “Chip" Arthur Breier Jr. was born in Fort Benning, Georgia on December 19, 1972, the son of John A. Breier and Barbara E. Breier. He started university study in September 1991 at Texas A&M University in College Station, Texas where he received Bachelor of Science in Mechanical Engineering in May 1995. He served as an engineer in the U. S. Navy for 5 years and left the active service in June 2000. In August 2001, he entered the Graduate School of The University of Texas in the Marine Science Department.

Permanent Address: Apartment C2
551 Terminal Loop Road
McQueeney, TX 78373

This dissertation was typeset with LaTeX 2_ε[1] by the author.

[1]LaTeX 2_ε is an extension of LaTeX. LaTeX is a collection of macros for TeX. TeX is a trademark of the American Mathematical Society. The macros used in formatting this dissertation were written by Dinesh Das, Department of Computer Sciences, The University of Texas at Austin, and extended by Bert Kay, James A. Bednar, and Ayman El-Khashab.